EVALUATION OF THE SUITABILTY OF FISCHER-TROPSCH GAS-TO-LIQUID (GTL) PRIMARY COLUMN BOTTOMS AS PROCESS COOLING WATER: ANALYSIS OF MICROBIAL COMMUNITY DYNAMICS, FOULING, SCALING AND CORROSION

by

SAVIA SUSANNA SLABBERT

B.Sc. (PU for CHE)

Dissertation submitted in partial fulfilment of the requirement for the degree

MASTER OF ENVIRONMENTAL SCIENCE

in the

School for Environmental Sciences and Development: Microbiology
North-West University, Potchefstroom Campus
Potchefstroom, South Africa.

Supervisor: Mr. P.J. Jansen van Rensburg
Co-supervisors: Prof. C.C. Bezuidenhout
Mr. J.J. Bezuidenhout

January 2007

This work is dedicated to my sister, Mariëtte.

"Failure is only the opportunity to begin again more intelligently."

-Henry Ford-

ACKNOWLEDGEMENTS

I wish to convey my most sincere appreciation and gratitude to the following persons and institutions for their contribution to the successful completion of this study:

My superior, God, who makes all things possible, granting me the opportunity to perform this study.

Prof. C.C. Bezuidenhout, School for Environmental Sciences and Development: Microbiology, North-West University, Potchefstroom Campus.

Mr. P.J. Jansen van Rensburg, School for Environmental Sciences and Development: Microbiology, North-West University, Potchefstroom Campus.

Mr. J.J. Bezuidenhout, School for Environmental Sciences and Development: Microbiology, North-West University, Potchefstroom Campus.

Prof. K.J. Riedel, Sasol Technology Research and Development, Sasolburg,

Dr. L. Tiedt, Electron microscopy, North-West University, Potchefstroom Campus.

Mr. A. Palazzo, Buckman Laboratories, Hammarsdale, KwaZulu-Natal.

Mr. Don Watt Pringle, Improchem, Sasolburg.

NRF (National Research Foundation) and Sasol R&D (Sasolburg) for funding of this project.

Mr. P.C. Venter. For your appreciated help with the molecular techniques during the last few days.

My family and friends, particularly Coenraad, for your ongoing support and encouragement throughout this study.

DECLARATION

The experimental work conducted and discussed in this dissertation was carried out in the School of Environmental Sciences and Development: Microbiology, North West University, Potchefstroom Campus. This study was performed during the period of January 2004 to December 2006 under the supervision of Mr. P.J. Jansen van Rensburg, Prof. C.C. Bezuidenhout and Mr. J.J. Bezuidenhout.

This dissertation represents original work undertaken by the author and has not been previously submitted for degree purposes to any other university. Appropriate acknowledgements have been made in the text where the use of work conducted by other researchers has been included.

TABLE OF CONTENTS

The language and style used in this dissertation are in accordance with the requirements of the Journal - Water Research.

SUMMARY

Water in South Africa is becoming limiting due to economic growth, social development and the country's water demand that exceed its water availability. Water conservation in the industry can be accomplished by the reuse of process water instead of direct treatment and discharge. By reusing a process effluent as cooling water in cooling towers, the water requirements of an industry, such as Sasol, will be lower and a zero effluent discharge scenario could be achieved.

At Sasol, during the gas-to-liquid (GTL) conversion process, natural gas is converted to diesel and other products. During this process an aqueous effluent stream is produced in the Fischer-Tropsch (F-T) reactors known as Primary Column Bottoms. Primary Column Bottoms can be re-used as cooling water within cooling towers. Although this approach is technically feasible, the re-use of process water in cooling systems is characterised by major problems (fouling, scaling and corrosion) due to the complicated chemistry of the process water and the increased nutrient loads within the system.

The aim of this study was to evaluate the suitability of Fischer-Tropsch gas-to-liquid Primary Column Bottoms as process cooling water by analysing the microbial community dynamics, fouling, scaling and corrosion. Due to the corrosive nature of this process effluent, stabilisation of the water was essential. To determine whether efficient stabilisation was attained, an accelerated corrosion test was performed. Influence of the external operating parameters within the cooling tower on the rate of fouling, scaling and corrosion were also determined. Structural and functional diversity of planktonic and sessile communities were studied by making use of conventional microbiological techniques (plate counts, MPN technique) and molecular methods (PLFA, DGGE).

The accelerated corrosion test of 28 days conducted on mild steel and stainless steel (316L) corrosion coupons accelerated corrosion by immediately establishing the mature natural environment that causes corrosion. The test solution was stabilised as well as non-stabilised synthetic Primary Column Bottoms, in order to compare the effect of stabilisation. Scaling and corrosion indices were also calculated on stabilised and non-stabilised water to determine the scaling and corrosive tendencies of the water and how

this correlates with the actual corrosion results obtained. According to the Langelier Saturation Index (LSI), Ryznar Stability Index (RSI) and the Puckorius Scaling Index (PSI) the stabilised water was slightly scale forming with little corrosion and the non-stabilised water being more corrosive than scale forming. Average corrosion rate of the stabilised water was 0.032 mm/y and 0.049 mm/y for non-stabilised water. Average scaling rate was calculated as 7.269 mg/dm^2/d for stabilised water and 5.853 mg/dm^2/d for non-stabilised water. It can therefore be concluded that effective stabilisation was achieved since stabilised water was less corrosive than non-stabilised water which was also confirmed through experimental data (corrosion rates from accelerated corrosion test) and corresponded with the corrosive tendencies obtained form the scaling and corrosion indices.

A lab-scale cooling tower was operated with stabilised synthetic Primary Column Bottoms as cooling water. Five experiments were conducted under varying flow rates and cycles of concentration. Influence of the external operating parameters (linear flow velocity and cycles of concentration) on fouling, scaling and corrosion rates of mild steel and stainless steel (316L) corrosion coupons and heat exchanger tubes were determined through weight loss measurements. Routine physico-chemical analyses, EDS (energy dispersive spectrometry) microanalysis as well as scaling and corrosion indices of each experiment were also compared, in order to evaluate the influence of cycles of concentration and linear flow velocity. Based on the results obtained, it was evident that the variation in cycles of concentration and linear flow velocity had a significant effect ($p>0.05$) on the fouling, scaling and corrosion rates on the mild steel corrosion coupons and heat exchanger tubes. Experimental runs operated at low flow rates of 0.6m/s and 0.9 m/s resulted in relative high fouling, scaling and corrosion rates. Operation at 3 and 4 cycles of concentration had the highest scaling and corrosion rates. The COD within the cooling tower was not removed by the microorganisms within the planktonic and sessile communities and resulted in a build-up of COD in the sump. Thus, the cooling tower can not be used as a bioreactor to biologically degrade volatile organic acids and hydrocarbons.

To evaluate the structural and functional diversity of the bacterial and fungal communities, plate counts, most probable number technique, phospholipid fatty acid (PLFA) analysis as well as denaturing gradient gel electrophoresis (DGGE) was used.

According to PLFA profiles the community structure within the planktonic and biofilm samples of the experiments operated at low linear flow velocities were similar. The same percentages of Gram-positive, Gram-negative bacteria and fungi occurred.

The community structure composition of the planktonic and sessile phases in the experiments operated at higher linear flow velocities was also similar. PLFA analysis concluded that the highest estimated viable biomass was in experiment 1 which had a low linear flow velocity of 0.6 m/s. Shannon-Weaver index analysis of DGGE profiles (general structural diversity) indicated that the planktonic bacterial diversity of experiment 1 and 2 were the highest. Experiment 1 and 2 were operated at a linear flow velocity of 0.6 and 0.9 m/s respectively. The biofilm samples that had the highest Shannon-Weaver diversity index were experiment 1 and 5. Both experiment 1 and 5 were operated at a linear flow velocity of 0.6 m/s. Morphological changes between planktonic and sessile communities were monitored through scanning electron microscopy (SEM). SEM results illustrated that the planktonic and sessile microbial populations throughout the five experiments were similar, based on morphology. According to the results obtained from the MPN technique, the experiment operated at the lowest linear flow velocity had the highest numbers of sulphate reducing bacteria and also resulted in the highest corrosion rate. Both experiments that were operated at a low linear flow velocity of 0.6 m/s had the highest bacterial numbers and also resulted in high fouling rates. However, no relationship exists between the percentage increase in the numbers of aerobic bacteria and the cycles of concentration at which the cooling tower was operated. These observations are supported by results from PLFA profiles that showed that the community structure within the planktonic and sessile samples of the experiments operated at low linear flow velocities were similar. The planktonic and sessile phases of these two experiments had similar levels of Gram-positive-, Gram-negative- bacteria and fungi. The community structure composition of the planktonic and sessile phases in the experiments operated at high linear flow velocities was also similar. PLFA analysis further demonstrated that the highest estimated viable biomass was in the experiment operated at a low linear flow velocity of 0.6 m/s. Shannon-Weaver index analysis of DGGE profiles (general structural diversity) also indicated that the planktonic bacterial diversity during operation at low linear flow velocities were the highest. Although scanning electron microscopy results illustrated that the planktonic and sessile microbial populations throughout the five experiments were

generally similar, these results supported the observations of the other techniques. These techniques all supported the notion that corrosion rates may not be directly related to the total microbial biomass or the number of species on mild steel or stainless steel. Corrosion rates seem to be more profoundly affected by biofilm composition within the sessile phase.

Based on the results obtained when using Primary Column Bottoms as cooling water, it were evident that variation in cycles of concentration and linear flow velocity had a significant effect ($p>0.05$) on the fouling, scaling and corrosion rates on mild steel corrosion coupons and heat exchanger tubes. Low linear flow velocities resulted in high fouling rates, increased bacterial numbers as well as high bacterial and fungal diversities. High cycles of concentration resulted in high scaling and corrosion rates and also had the result of similar community structure profiles. This research study could facilitate the selection of optimised operational parameters for the re-use of industrial process water (such as Primary Column Bottoms) as cooling water to minimise fouling, scaling and corrosion.

OPSOMMING

Suid Afrika se water is besig om 'n beperkte bron te word weens ekonomiese groei, sosiale ontwikkeling en die aanvraag van water wat groter is as die watervoorraad beskikbaar. 'n Alternatiewe metode vir die direkte behandeling en terugplasing in die omgewing is om hierdie industriële water te hergebruik in die industrie. Daarom word die moontlike hergebruik van industriële water as verkoelingswater in koeltorings oorweeg om die aanvraag van water asook die terugplasing in die atmosfeer te verlaag.

Tydens die Sasol gas-na-vloeistof (GTL) omskakelingsproses sal natuurlike gas (hoofsaaklik metaan) omgeskakel word na 'n sintetiese petroleum eindproduk (diesel, petrol en naphta). Tydens hierdie proses word 'n uitvloeisel in die Fischer-Tropsch (F-T) reaksie geproduseer naamlik Primary Column Bottoms. Hierdie uitvloeisel kan hergebruik word as verkoelingswater in koeltorings. Alhoewel hierdie hergebruik moontlik is sal verskeie probleme met die verkoelingstelsel ondervind word (korrosie, bevuiling en chemiese deponering) weens die chemiese samestelling van die water asook 'n groot toename in voedingstowwe binne die verkoelingstelsel.

Die hoofdoel van hierdie studie is om te bepaal hoe geskik die gebruik van die Fischer-Tropsch GTL Primary Column Bottoms uitvloeisel is vir die gebruik as proses verkoelingswater. Dit sal bepaal word deur die mikrobiese gemeenskap, bevuiling, chemiese deponering asook die korrosie wat vorm, te analiseer. As gevolg van die korrosiewe aard van hierdie industriële uitvloeisel is dit noodsaaklik om hierdie water chemies te stabiliseer. Om te bepaal of effektiewe stabilisering bekom is, moes 'n versnelde korrosie toets uitgevoer word. Die invloed wat die eksterne parameters van die koeltoring op die bevuiling, chemiese presipitasie en korrosietempo het, is ook bepaal. Die strukturele en funksionele diversiteit van die planktoniese en sessiele mikrobiese gemeenskappe is ook bestudeer deur gebruik te maak van konvensionele mikrobiologiese tegnieke (plaattellings) asook molekulêre tegnieke (PLFA, DGGE).

Die versnelde korrosie toets van 28 dae op staal (mild steel, stainless steel) korrosie koeponne het korrosie versnel deur dadelik die natuurlike omgewing waarbinne korrosie vorm, te ontwikkel.

Die toetsmonsters was gestabiliseerde asook ongestabiliseerde sintetiese Primary Columns Bottoms uitvloeisel, om sodoende die effek van stabilisering te kan bepaal. 'n Chemiese deponering en korrosie indeks is gebruik vir die gestabiliseerde en ongestabiliseerde water om vas te stel wat die chemiese deponering en korrosiewe aard van die water was en hoe dit in verhouding tree met die eksperimentele korrosie resultate wat verkry is. Volgens die Langelier Saturation Index (LSI), Ryznar Stability Index (RSI) en die Puckorius Scaling Index (PSI) het die gestabiliseerde water min chemiese deponering asook min korrosie getoon. Die ongestabiliseerde water was meer korrosief as chemies deponerend. Die gestabiliseerde water het 'n gemiddelde korrosie tempo van 0.032 mm/a gehad en die ongestabiliseerde water 'n tempo van 0.049 mm/a. Die gemiddelde chemiese deponeringstempo van die gestabiliseerde water was 7.269 $mg/dm^2/d$ en 5.853 $mg/dm^2/d$ vir die ongestabiliseerde water. Dit kan opgesom word dat effektiewe stabilisering verkry is aangesien die gestabiliseerde water minder korrosief was as die ongestabiliseerde water.

Gestabiliseerde Primary Column Bottoms was gebruik in 'n laboratoriumskaal koeltoring. Vyf eksperimente is uitgevoer deur gebruik te maak van verskeie vloeitempo's en konsentrasiesiklusse. Die invloed van hierdie eksterne parameters op die bevuiling, presipitasie en korrosietempo's op staal (mild steel, stainless steel) korrosie koeponne asook hitte uitruilbuise is vasgestel deur gebruik te maak van gewigsverlieslesings. Roetine fisies-chemiese analises, EDS (energy dispersive spectrometry) mikro-analises asook chemiese deponering en korrosie indekse was vergelyk om sodoende die invloed van die konsentrasie siklusse en vloeitempo's te evalueer. Met vergelyking van resultate, was daar 'n betekenisvolle verskil ($p>0.05$) op die bevuiling, chemiese deponering en korrosietempo's op staal (mild steel, stainless steel). Die eksperimente wat uitgevoer is by lae vloeitempo's het hoë bevuiling, chemiese deponering en korrosietempo's tot gevolg gehad. Die eksperimente wat uitgevoer is by hoë konsentrasie siklusse het die hoogste chemiese deponering en korrosie tot gevolg gehad. Die COD binne die koeltoring is nie verwyder deur die mikroorganismes binne die planktoniese en sessiele fases nie en het 'n opbou van COD tot gevolg gehad. Daarom kan die koeltoring nie as 'n bioreaktor gebruik word om vlugtige organiese sure asook koolwaterstowwe biologies af te breek nie.

Om die strukturele en funksionele diversiteit van die bakteriese en fungiese gemeenskappe te bepaal was plaattellings asook mikrobiologiese tegnieke (PLFA en DGGE) gebruik. Soos die resultate vergelyk word van die konvensionele mikrobiologiese tegnieke, was die hoogste getalle sulfaat-reduserende bakterieë teenwoordig in die eksperimente wat by lae vloeitempo's uitgevoer was. Hierdie eksperimente het ook hoë bevuiling tot gevolg gehad. Die PLFA profiel dui aan dat die eksperimente wat by lae vloeitempo's uitgevoer is dieselfde gereageer het op die eksterne parameters. Die planktoniese en sessiele fases van hierdie eksperimente het dieselfde vlakke Gram-positiewe-, en Gram-negatiewe- bakterieë en fungi getoon. Die gemeenskapstruktuur komposisie van die planktoniese en sessiele fases van die eksperimente wat by hoë vloeitempo's uitgevoer is, het dieselfde gereageer. PLFA analises het verder gedemonstreer dat die eksperiment wat uitgevoer is by die laagste vloeitempo, die hoogste biomassa getoon het. Die Shannon-Weaver indeks wat uitgevoer is op die DGGE profiele (algemene strukturele diversiteit) het aangetoon dat die bakteriese diversiteit die hoogste was by die eksperimente uitgevoer by lae vloeitempo's. Alhoewel die skandeer elektron mikroskopie resultate geïllustreer het dat die planktoniese en sessiele fases in die vyf eksperimente deurlopend dieselfde was, het hierdie observasies die resultate van die ander tegnieke gesteun. Hierdie tegnieke het almal bewys dat korrosietempo's nie direk afhanklik is van die totale mikrobiese biomassa of die getal spesies teenwoordig op die staal nie. Korrosie word meer geaffekteer deur die samestelling van die biomassa.

Dit is duidelik dat konsentrasie siklusse en vloei tempo 'n betekenisvolle verskil ($p>0.05$) op bevuiling, chemiese deponering en die korrosietempo's op staal (mild steel, stainless steel) gehad het wanneer Primary Column Bottoms as verkoelingswater gebruik word. Die verskil in eksterne parameters het nie dieselfde uitwerking tot gevolg gehad op vlekvrye staal nie (stainless steel 316L). Lae vloeitempo's het hoë bevuiling, 'n toename in mikrobiese groei asook hoë bakteriese en fungiese diversiteit tot gevolg gehad. Hoë konsentrasie siklusse het hoë chemiese deponering en korrosie tot volg gehad.

Hierdie navorsingstudie kan van nut wees tydens die bepaling van geskikte sisteemparameters vir die hergebruik van industriële water (Primary Column Bottoms) as verkoelingswater om bevuiling, chemiese deponering en korrosie te beheer.

LIST OF FIGURES

LIST OF TABLES

ABBREVIATIONS

ANOVA: Analysis of variance

COC: Cycles of concentration

COD: Chemical oxygen demand

DGGE: Denaturing gradient gel electrophoresis

DO: Dissolved oxygen

DWAF: Department of water affairs and forestry

EDS: Energy dispersive spectrometry

EPS: Extracellular polymeric substances

FAME: Fatty acid methyl esters

F-T: Fischer-Tropsch

GC: Gas chromatogram

GTL: Gas-to-liquid

HSD: Honest significant difference

IRB: Iron reducing bacteria

LFV: Linear flow velocity

LSI: Langelier Stability Index

MIC: Microbiologically induced corrosion

MPN: Most probable number

PCA: Principal component analysis

PCR: Polimerase chain reaction

PLFA: Phospholipid fatty acids

PSI: Puckorius Scaling Index

PVC: Polyvinyl chloride

RDA: Redundancy analysis

RSI: Ryznar Stability Index

SEM: Scanning electron microscopy

SRB: Sulphate reducing bacteria

TDS: Total dissolved solids

TSS: Total suspended solids

ΔT: Temperature differential

CHAPTER 1

General introduction and problem statement

1.1 Introduction and problem statement

South Africa is a semi-arid region with minimal rainfall and has no large rivers compared to other countries (Basson *et al.*, 1997). Water in South Africa is becoming limiting because of the economic growth, social development and the country's water demand that exceed its water availability (Basson *et al.*, 1997). Many industries use water in their manufacturing operations and because some of this water is contaminated in the process it requires treatment before discharge (Alva-Argáez *et al.*, 1998; Bagajewicz, 2000). Industries also produce wastes that can affect the pH, colour, temperature of water and also the amount of nutrients, minerals and salts present in water (Anon, 2006c). Major water quality problems in South Africa include the contamination by acid water, bacteria, high salt and nutrient loads occurring in the water (DWAF, 2002). Furthermore, the cost of wastewater treatment to meet environmental standards has increased due to discharge regulations (Kim *et al.*, 2001). Therefore designing effluent treatment systems are necessary to reduce pollution and the effluent discharged (Kim *et al.*, 2001; Mohsen and Jaber, 2002).

Viessman and Hammer (1998) suggests that the wastewater treatment process must ensure the removal of residual pollutants to such a degree as to make the water acceptable for the specific re-use purposes. The Water Act (Act No 36 of 1998) is the controlling legislation regarding the use of water for industrial purposes and the discharge of effluents (Sampson, 2001).

Water conservation in the industry can be accomplished by the re-use of process water instead of direct treatment and discharge (Dry, 1999). Many industries are approaching the concept of zero liquid effluent discharge where the industry's water intake and discharge are reduced because of the usage of waste effluent in especially cooling towers (Buhrmann *et al.*, 1999). By re-using industrial water the water requirements of industries will be lower, discharge effluents will be less and this could also minimise pollution while saving water (You *et al.*, 1999).

At Sasol, during the gas-to-liquid (GTL) conversion process, natural gas is converted to diesel and other products (Collins *et al.*, 2006). During this process an aqueous effluent stream is produced in the Fischer-Tropsch (F-T) reactors known as Primary Column Bottoms, which requires treatment before discharge. Furthermore, this reaction water requires cooling before treatment. For this purpose cooling water towers are used in which the Primary Column Bottoms circulates. By re-using a process effluent as cooling water in cooling towers, the water requirements of an industry such as Sasol, will be lower and a zero liquid effluent discharge scenario could be achieved (Choudhary, 1998).

By making use of industrial effluents certain problems are associated with the operation of the cooling tower (Choudhary, 1998; Meesters *et al.*, 2003). Fouling, scaling and corrosion occur due to the complicated chemistry of the process water and the increased nutrient loads within the system (Videla, 2002; Ludensky, 2003). Both planktonic and sessile microorganisms have numerous adverse effects on industrial systems (Ludensky, 2003; Meyer, 2003). The uncontrolled growth of microorganisms in cooling water systems can be placed in three categories: biofilm formation, biofouling and microbiologically induced corrosion (Lutey, 1996). Impacts of biofilm formation include energy losses in cooling towers and heat exchangers, fluid frictional resistance as well as microbial induced corrosion (Ludensky, 2003). These factors contribute to the maintenance costs of any industrial system due to the loss of performance as well as the closure of systems for repair and maintenance (Choudhary, 1998; Yang *et al.*, 2006).

Extensive research has focussed on the prevention of microbiologically induced corrosion, biofouling, scaling and corrosion. However, hardly any research has focussed on the relationship between functional and structural microbial diversity in industrial cooling water systems.

1.2 Aim and objectives

The aim of this study was to evaluate the suitability of Fischer-Tropsch gas-to-liquid (GTL) Primary Column Bottoms as process cooling water by analysing fouling, scaling and corrosion potential of this water as well as microbial community dynamics. A lab-scale cooling tower was operated under different linear flow velocities and cycles of

concentration and also used as a bioreactor since microorganisms within a biofilm system can biologically degrade volatile organic hydrocarbons (Kolb and Wilderer, 1995). In the industry this biological degradation may result in the elimination of the water treatment step, before discharging or re-using this effluent. The objectives of this study were:

(i) to perform an accelerated corrosion test and using scaling and corrosion indices to optimise cooling tower performance.

(ii) to determine the influence of the external operating parameters (linear flow velocity and cycles of concentration) within the cooling tower on the rate of fouling, scaling and corrosion.

(iii) to evaluate the structural and functional diversity of planktonic and sessile community by making use of the following microbiological techniques; conventional microbiological techniques, scanning electron microscopy, phospholipid fatty acid (PLFA) analysis as well as denaturing gradient gel electrophoresis (DGGE).

This research study could facilitate the selection of optimised operational parameters for the re-use of industrial process water as cooling water to minimise fouling, scaling and corrosion (You *et al.*, 1999).

CHAPTER 2

Literature review

2.1 South Africa's water situation

South Africa is a semi-arid region where water is not available in sufficient quantities to meet human needs. It has an average rainfall of 500 mm per year, which is below the world average of about 860 mm per year (Basson *et al.*, 1997; Karlberg *et al.*, 2004). South Africa's rivers are small in comparison with neighboring countries and four of the major river systems in South Africa are shared with other countries (DWAF, 2002). More than half of the water management areas in South Africa indicates that the demand for water exceed its availability (DWAF, 2002). The total surface water available in South Africa averages 49 200 million cubic meters (m^3) per year. This includes about 4 800 million m^3 of water per year originating from Lesotho, and 700 million m^3 per year originating from Swaziland (DWAF, 2002). It has also been estimated that eleven of the nineteen water management areas in South Africa country are facing a water shortage (DWAF, 2002). Therefore half of these water management areas indicate that the demand for water exceeds its availability.

Basson *et al.* (1997) revealed that South Africa would reach the limits of its economically usable land based fresh water resources before the year 2025 since it is estimated that the total requirement for water will double over the next thirty years (Anon, 2006d). The water usage in South Africa is dominated by the agriculture and afforestation sectors, representing 62% of the total water use (Basson *et al.*, 1997). The domestic and urban use of water constitutes 4% and 25% respectively and large industries outside municipal areas have a requirement of 8% of the total water in the country (Basson *et al.*, 1997; Anon, 2005).

Due to discharge regulations the cost of wastewater treatment are increasing and alternative methods have to be implemented to reduce the effluent discharged (Kim *et al.*, 2001). Industries are turning more to recirculating systems and by re-using their process water for other industrial purposes they overcome their water needs (You *et al.*, 1999; Marcucci and Tognotti, 2002). This is an alternative approach to the direct

treatment and discharge of effluents, reducing their intake demand and effluent discharged. Therefore industries have an ongoing drive towards zero liquid effluent discharge (Bagajewicz, 2000). Some industries are using wastewater as cooling water within cooling towers (Buhrmann *et al.*, 1999; Mohsen, 2004) and in the process, removing unwanted heat from heat transfer surfaces (Choi *et al.*, 2002).

2.2 Wastewater management

The aim of wastewater treatment processes are: (i) the reduction of organic content of wastewater (COD) (Benzaoui and Bouabdallah, 2004), (ii) the removal of trace organics, toxic metals, pathogens and parasites (Salgot *et al.*, 2006), (iii) the reduction of nutrients (nitrogen and phosphorus) to reduce pollution of receiving surface waters or groundwater (Viessman and Hammer, 1998) and (iv) to meet environmental standards applied to wastewater discharge (Alva-Argáez *et al.*, 1998; Iojoiu *et al.*, 2006). Wastewater re-use appears to be more common in regions that experience low rainfall, high evaporation and a high demand of irrigation water (Viessman and Hammer, 1998).

2.3 Cooling towers

In many chemical and petrochemical industries cooling towers are used to remove heat from effluent streams before discharge by cooling the circulating water through evaporation (Kim *et al.*, 2001; Meesters *et al.*, 2003; Qi *et al.*, 2006). In an open recirculating system (Figure 2.1), water starts in the cooling tower basin and circulates in the cooling system through a heat exchanger (Ascolese and Douglas, 1998; Qureshi and Zubair, 2006). As illustrated in Figure 2.1, make-up water is added to the system as required, recirculates through the system passing through the corrosion coupons and heat exchanger tubes. Hot circulating water falls from the top of the tower, air enters the side of the tower and flows across the falling water (Beyer, 1993). This water meets the fanned rising air and loose heat through evaporation (Echols and Magne, 1990; Kim *et al.*, 2001; Meesters *et al.*, 2003). Cooled water falls down the tower filled with packing material and into the basin, situated at the bottom of the cooling tower (Figure 2.1). When air enters the cooling tower, it's moisture content is generally less than saturation. When air exits, it emerges at a higher temperature and with a moisture content at or near saturation (Kim *et al.*, 2001). Adding make-up water (Figure 2.1) to

the system will restore losses due to leaks in the system, evaporation and water lost through windage (caused by draught of air) (EPRI, 2003). For every 6°C decrease in temperature across the tower, approximately one percent of the recirculating water will be evaporated (Kim *et* al., 2001). Evaporation thus increases the dissolved salt content of water in the system (Kemmer and McCallion, 1979; Anon, 1994). As pure water evaporates all of the salt are left behind so they concentrate in the cooling tower water forming deposits on the heat exchangers, reducing flow and the heat transfer efficiency (Anon, 1994; Ascolese and Douglas, 1998; Choudhary, 1998).

The term that compares the dissolved salt concentration of the circulating water to that of the make-up water is called cycles of concentration (COC) (Anon, 1994; Ascolese and Douglas, 1998). The cycles of concentration are therefore an indication of the degree to which dissolved salt are being concentrated in the circulating water (Choudhary, 1998). When a cooling tower starts out with fresh water the tower has one cycle of concentration. When all the fresh (process) water is evaporated the tower refills itself with more fresh (make-up) water; the salt content is now twice as much and the system has two cycles of concentration. This process will proceed and scale will start forming at a certain point.

Increased cycles of concentration can reduce operating costs through water savings, reduction in the make-up water requirement and also reduction in water- and chemical discharges (You *et al.*, 1999). However, operation at high cycles of concentration in a cooling tower can increase the corrosion and scaling tendencies of the water, due to high salt concentrations (You *et al.*, 1999). Limiting the cycles of concentration by blow down in the circulated water, will lower the precipitation risks (Brás Pereira *et al.*, 1997). On the other hand, water with a high initial salt concentration can only be cycled a limited number of times before precipitation or scaling occurs.

Drift is the loss of small droplets of circulating water to the air flow and it contains some dissolved solids (Meroney, 2006). As drift exits the tower, it leaves chemical constituents and biological matter dispersed in the air flow as dry particulate matter (EPRI, 2003).

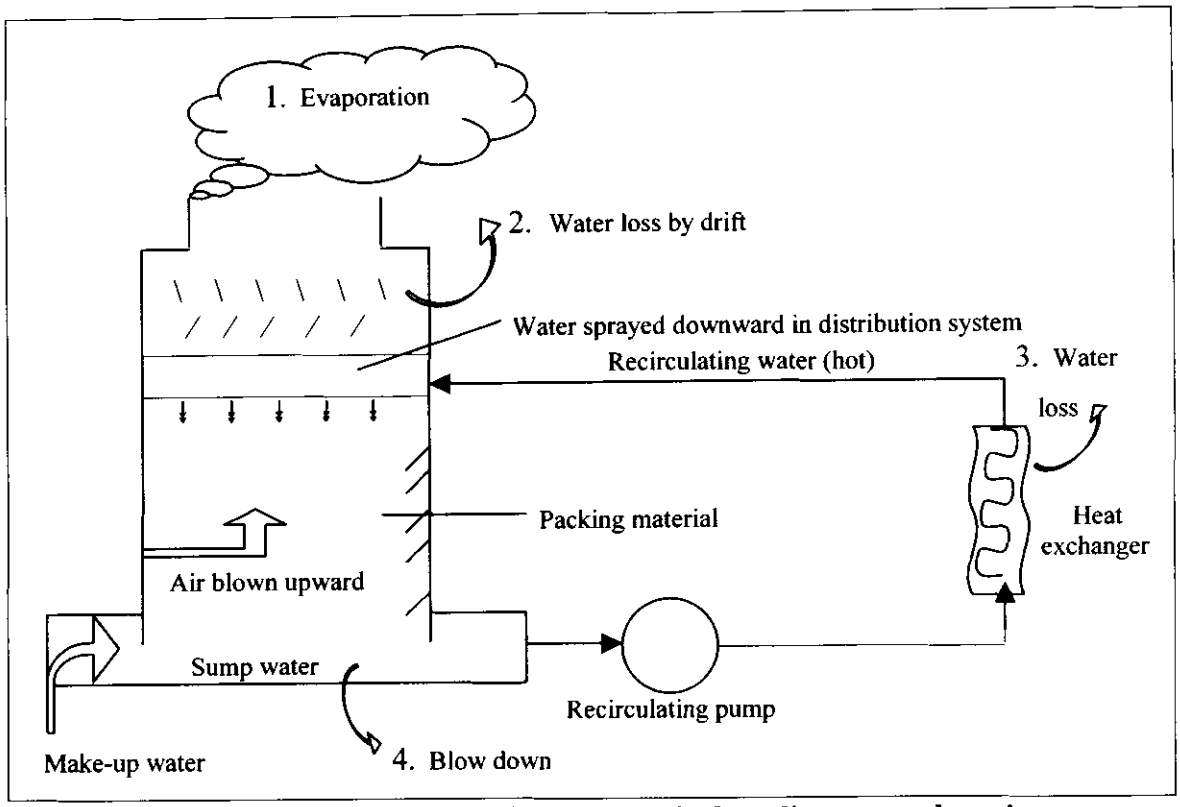

Figure 2.1: Schematic representation of a typical cooling tower loop in an open recirculating system with water loss areas indicated as 1 - 4.

Lithium chloride is used to determine cycles of concentration since lithium remains soluble even at high concentrations. The term cycles of concentration is thus best expressed as the ratio of lithium content of the circulating and make-up content.

The following equation can be used for this calculation: $COC = \frac{C_1}{C_0}$

Where C_1 is the final concentration of lithium in the sump water and blow down. C_0 is the initial concentration of lithium in the make-up water. Blow down is used to prevent the tower from reaching the point of scale formation and is an attempt to reduce the salt concentration in the circulation water (Choudhary, 1998). In figure 2.1 it is demonstrated that blow down removes a portion of the concentrated circulating water (to balance the incoming water solids), which is then replaced with fresh make-up water (Kemmer and McCallion, 1979; EPRI, 2003). By increasing the blowdown the cycles of concentration will decrease (Ascolese and Douglas, 1998). Linear flow velocity of water in a system affects the rate and amount of $CaCO_3$ deposition resulting in scaling (Viessman and Hammer, 1998; McLaughlan and Stuetz, 2004). Flow velocity also influences corrosion, where corrosion byproducts reduces the flow rate of water

(Kemmer and McCallion, 1979; Ramotlhola and Ringas, 2000). McLaughlan and Stuetz (2004) illustrates that a lower corrosion rate is associated with low flow velocities. Cycles of concnetration and linear flow velovity are thus two impotant operating parameters that needs optimisation.

2.4 Fischer-Tropsch reaction and effluent produced

The gas-to-liquid (GTL) process at Sasol comprises of three major process steps; synthesis gas production, Fischer-Tropsch synthesis and product work-up (Figure 2.2). Synthesis gas is a mixture of carbon monoxide and hydrogen produced through steam reforming natural gas (Knottenbelt, 2002; Demirbas, 2006). During the Fischer-Tropsch (F-T) reaction (Figure 2.3) hydrocarbons are produced from the gas mixture of carbon monoxide, hydrogen and oxygen (Dry, 1999; Tijmensen *et al.*, 2002). This process is commercially operated at Sasol plants in South Africa (Van Dyk *et al.*, 2006). In the GTL process natural gas is transported through pipelines from various natural gas reservoirs and converted into synthesis gas (Figure 2.2) in a high temperature process by means of reforming or partial oxidation (Thomas and Dawe, 2003; Olsen and Gobina, 2004; Collins *et al.*, 2006).

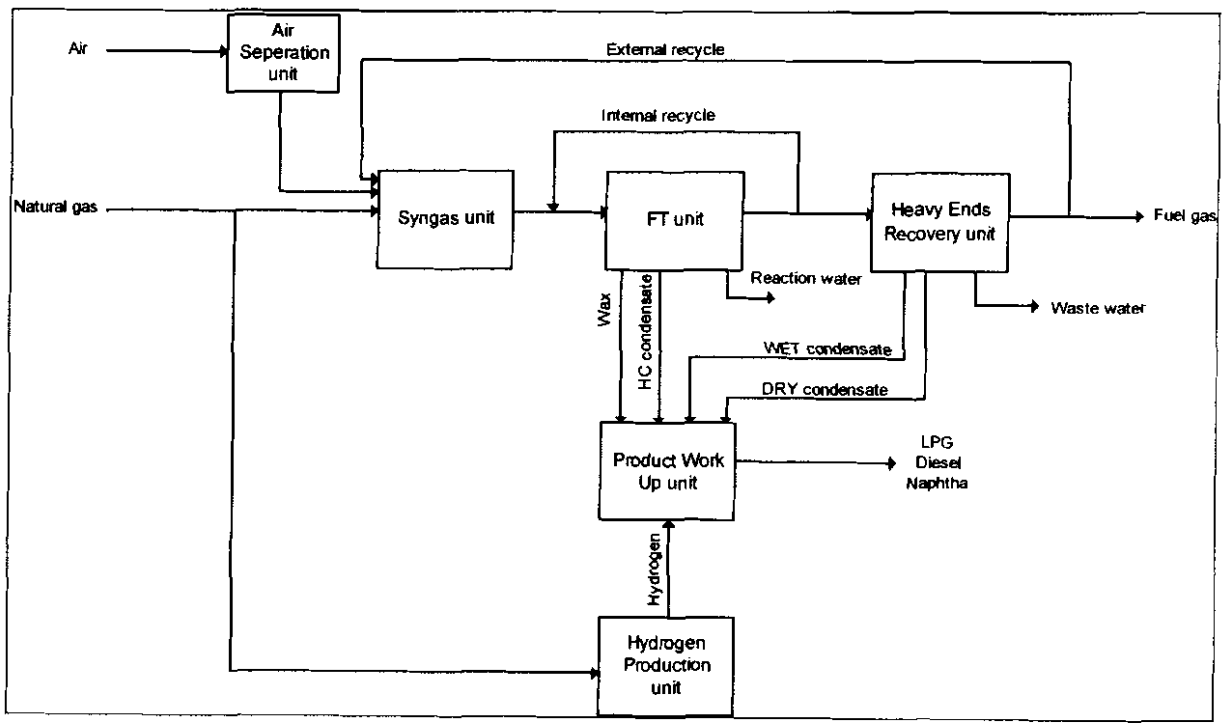

Figure 2.2: Typical stages in gas-to-liquid technology.

In the case where the F-T process is operated at high temperatures (HTFT) a light syncrude is produced (synthetic fuels which include petrol, naphta, kerosene and diesel) (Botha *et al.*, 1998; Van Dyk *et al.*, 2006). The CO, CO_2, H_2 and CH_4 gas mixture can be modified to the needs of the F-T process (Figure 2.3) by methane reforming, using an autothermal reformer (ATR) that converts CH_4 with steam to CO and H_2 (Tijmensen *et al.*, 2002; Aasberg-Petersen *et al.*, 2003).

The basic F-T reaction can be written as: $CO + 2H_2 \rightarrow CH_2 + H_2O$ Where CH_2 is the basic building block from which hydrocarbon molecules are synthesised by a chain growth process (Tijmensen *et al.*, 2002). For every bound carbon atom a molecule of water is produced (Dry, 1999). The F-T reaction therefore produces large amounts of water. Following primary column distillation for short chain alcohol (C_1-C_7) and carbonyl removal, an effluent stream known as Primary Column Bottoms is produced in the F-T reaction.

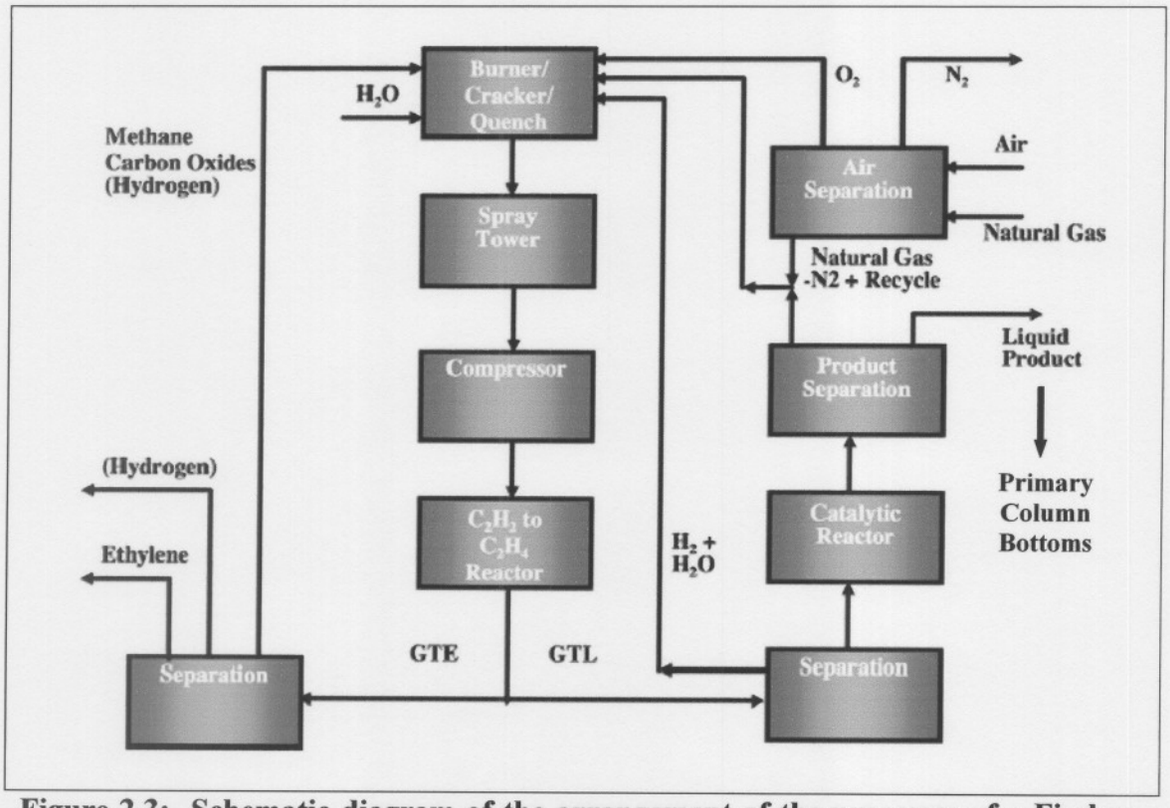

Figure 2.3: Schematic diagram of the arrangement of the processes of a Fischer-Tropsch synthesis plant (Hall, 2005).

Illustrated in Figure 2.3, the Primary Column Bottoms produced is indicated as the liquid product during product separation. This liquid water phase contains mainly formic and acetic acid, as well as methanol and has an average pH of 3.7. Usually, this effluent is treated in an aerobic bioworks where the organic material is oxidised biologically, the sludge produced is incinerated or landfilled and the treated water is used as cooling water (Dry, 1999).

The re-use of process effluents as cooling water in cooling towers is implemented at Sasol and the concept of zero liquid effluent discharge (the total re-use with no wastewater being released into the environment) is approached (Buhrmann *et al.*, 1999). One of these effluents is the Fischer-Tropsch gas-to-liquid Primary Column Bottoms. The main reason for using the F-T Primary Column Bottoms in an experimental setup as cooling water is to determine the suitability of this effluent as cooling water and also to use the cooling tower as a bioreactor (where microorganisms degrades the nutrients) in order to skip the biological water treatment process that normally follows the F-T reaction before discharge. By using the cooling tower as a bioreactor the microorganisms within the planktonic and sessile communities can biologically degrade volatile organic pollutants (volatile fatty acids and hydrocarbons) from the effluent (Aguilar *et al.*, 1995; Kolb and Wilderer, 1995).

2.5 Use of process water and problems associated with cooling towers

The cooling tower design and operation have a great impact on the chemistry of water as it influences fouling, scaling and corrosion in the system (Kim *et al.*, 2001; Videla 2002; Meesters *et al.*, 2003). Although it is possible to re-use industrial effluents in cooling towers certain problems (fouling, scaling and corrosion) are associated with the operation of the cooling tower (You *et al.*, 1999). These operational problems normally occur due to the complicated chemistry of the process water and increased nutrient loads within the system (Kemmer and McCallion, 1979; Martinez *et al.*, 2004). Scaling, corrosion and microbial fouling problems usually occur simultaneously (Allain *et al.*, 1998). These operational problems (fouling, scaling and corrosion) contribute to the maintenance costs of any industrial system due to the loss of performance as well as the closure of systems for repair and maintenance (Choudhary, 1998).

Therefore by operating the cooling water system under certain parameters (linear flow velocity, cycles of concentration and pH) operational problems can be reduced (Brás Pereira *et al.*, 1997; You *et al.*, 1999; Kim *et al.*, 2001).

2.6 Fouling

Fouling, scaling and corrosion are normally interrelated and do not occur independently of one another for a specific water type/ quality (Kemmer and McCallion, 1979; Allain *et al.*, 1998). Biofilm formation, corrosion products or the precipitation of inorganic and organic contaminants from the circulating water causes fouling (Brás Pereira *et al.*, 1997; You *et al.*, 1999). Low flow velocities may provide stagnant areas that will enhance the formation of deposits giving rise to microbiological activity and increased corrosion rates, leading to further decrease in efficiency of the cooling tower (Anon, 1994; Videla, 2002).

Environmental fouling (materials in make-up water quality) as well as operational fouling (caused by the system characteristics) are the cause of fouling (Anon, 1994). Biofouling reduces heat transfer efficiency on heat exchange surfaces, causes fluid frictional resistance or could result in microbial induced corrosion (Johansson and Saastomoinen, 1999; Videla, 2002; Ludensky, 2003). It is therefore necessary to do a microbial analysis on the water to eliminate biofouling (Abd El Aleem *et al.*, 1998). Controlling the operational conditions of the cooling system as well as the physico-chemical conditions could eliminate fouling (Brás Pereira *et al.*, 1997; Petrucci and Rosellini, 2005; You *et al.*, 1999). Chemical and microbiological analysis of the deposits could distinguish the origin of the fouling.

Extracellular polymeric substances (EPS) has also been identified as the main foulants in membrane bioreactors (Negaresh *et al.*, 2006). The continued growth of bacteria within a biofilm leads to an excessive excretion of EPS in which they are embedded and promote the formation of slime on the substratum surface (Vickery *et al.*, 2004). Microorganisms involved in biofilm formation that produces EPS are *Aerobacter*, *Arthrobacter*, *Proteus*, *Bacillus* and *Pseudomonas* (Choudhary, 1998). The biofilm structure of EPS causes high fluid frictional resistance in water systems and also stabilises microorganisms on the surface (Flemming *et al.*, 2001; Ludensky, 2003). EPS can be used to determine the biological and physico-chemical properties of

biofilms, since they are responsible for the structural and functional integrity of biofilms (Flemming *et al.*, 2001). It is therefore important to remove EPS to prevent new biofilm formation as the EPS matrix promotes the adhesion of microorganisms to a surface and each other (Flemming *et al.* 2001; Meyer, 2003; Cossart *et al.*, 2004).

2.7 Scaling

Scaling occurs in water that is supersaturated with scale forming salts (calcium carbonate, calcium sulphate or calcium hydroxide) and results in deposit formation on a metal surface (You *et al.*, 1999; Brink *et al.*, 2004; Macadam and Parsons, 2004). It occurs when solubilities are exceeded because of high concentrations or increased temperatures (Videla, 2002; Brink *et al.*, 2004; Hodgkiess, 2004). These dense crystal deposits reduce flow and heat transfer efficiency (Choudhary, 1998; You *et al.*, 1999). Scale build-up depends on temperature, pH, the chemical species involved in scale formation as well as water chemistry and flow rate (McLaughlan and Stuetz, 2004). The rate of scale formation is affected by the surface material on which it's forming (lowest $CaCO_3$ scaling rates on stainless steel), hydrodynamic conditions as well as supersaturation (Macadam and Parsons, 2004; Parsons and Doyle, 2004). When using water containing dissolved phosphates as make-up, the deposition of calcium phosphate will occur on the heat exchanger tubes (Anon, 1994).

Calcium phosphate normally precipitates as amorphous tri-calcium phosphate and is usually associated with a crystalline precipitate of calcium carbonate (Anon, 1994). The decomposition of calcium bicarbonate into calcium carbonate, carbon dioxide and water are shown in the following reaction: $Ca(HCO_3)_2 \rightarrow CaCO_3 + CO_2 + H_2O$ (Hamrouni and Dhahbi, 2002). Although a scale layer acts as a protective coating against corrosion (Hodgkiess, 2004), the occurrence of scale in process water causes operational problems (Ascolese and Douglas, 1998). Scaling increases the resistance to heat transfer, lowering the process performance and can also cause the blockage of pipes (Rafferty, 2000; Hodgkiess, 2004; Sheikholeslami, 2004).

2.8 Corrosion

Metal corrosion can be defined as the destruction of the metal through an electro-chemical reaction that involves the flow of electrons and ions (Maguire, 1980; Ramotlhola and Ringas, 2000). It results from oxidation and reduction reactions at sites on the metal-water interface (Mackintosh *et al.*, 1998). Corrosion is further accelerated by the removal of reduced products of the chemical reactions through bacterial activity (Brözel *et al.*, 1997). Corrosivity of water depends on the oxygen levels of the water carbonate balance and pH (Andijani and Turgoose, 2004). Thus corrosion requires an anode, a cathode, an electrolyte and a metallic path joining the anode and the cathode (Ramotlhola and Ringas, 2000). The three conditions required for the electrochemical corrosion process to occur are, a potential difference in the metal surface, a continuous conductive path and a mechanism for charge transfer between the conductors (Anon, 1994).

Biological factors influencing corrosion may be related to microbial community structure and function. It usually stems from the presence of biofilms at the metal surface and accelerate corrosion by changing the chemistry near the metal surface (Choudhary, 1998). Physical factors contributing to the corrosion process are temperature, water velocity and pH (Anon, 1994). Increase in temperature increases the rate of most chemical reactions and it is known that corrosion occurs at high temperatures (e.g. heat exchangers) (Anon, 1994). The deposits of corrosion products reduce both heat transfer and flow rates and can result in leaks and bursts within the industrial system (Kemmer and McCallion, 1979; Ramotlhola and Ringas, 2000).

Chemical factors that influence the tendency of cooling water to corrode are its mineral salt content (chlorides and sulphates) and dissolved gas content (oxygen and carbon dioxide) (Anon, 1994; Mackintosh *et al.*, 1998). Because oxygen plays a role in corrosion and acts as an oxidiser in pitting corrosion (Berdelle-Hilge, 1995), it is necessary to eliminate the presence of dissolved oxygen or hydrogen ions to prevent corrosion processes from occurring (Anon, 1994).

In aqueous systems the process of corrosion involves the electrochemical reaction, in which one section of the metal surface becomes corroding or anodic where oxidation occurs (Hey and Hollingshad, 1988). The anodic areas are where the metal atoms split

up to form a metal ion (ferrous iron) with the release of electrons e.g. $Fe \rightarrow Fe^{2+} + 2e^-$ (Iverson, 1987). This anodic reaction is an oxidative reaction, which causes the reaction to be shifted to the right, increasing the metal dissolution or corrosion, and is indicative of metal loss at the anodic sites (Iverson, 1987; Anon, 1994). This reaction is also known as the 'anodic half cell reaction' (Anon, 1994). For the dissolution of the metal to continue, electrons left behind on the metal surface have to be removed by two cathodic reactions (Iverson, 1987). In neutral or alkaline water conditions oxygen is reduced in the cathodic area by reacting with the electrons to form hydroxide ions $O_2 + 2H_2O + 4e^- \rightarrow OH^-$ (Anon, 1994). In an acidic solution the electrons react with the hydrogen ions to produce hydrogen gas $2H^+ + 2^{e-} \rightarrow H_2$ (Anon, 1994).

Cooling water provides the necessary link to allow the products of the anode and cathode processes to react, producing ferrous hydroxide (corrosion products) $Fe^{2+} + 2OH^- \rightarrow Fe(OH)_2$ (Iverson, 1987; Hey and Hollingshad, 1988). In the presence of additional oxygen, ferrous hydroxide is converted to ferric hydroxide ($Fe(OH)_3$), which precipitates as hydrous ferric oxide ($Fe_2O_3.H_2O$) a form of rust (Iverson, 1987; Hey and Hollingshad, 1988). The rate at which a corrosion process occurs is usually controlled by the rate at which dissolved oxygen or hydrogen ions become available at the cathodic areas (Anon, 1994).

2.8.1 Scaling and corrosion indices

Results from temperature regulated alkalinity and concentration of dissolved solids (Ryznar Stability Index and Langelier Saturation Index) as well as methods based on the determination of thermodynamic equilibrium of carbonic acid, can be used to prevent the build-up of calcium carbonate (scaling) in cooling systems (Videla, 2002). Calcium carbonate and magnesium hydroxide (alkaline scales) which have low solubilities that decrease with increasing temperature. They can be precipitated by process waters resulting in scaling (Brink *et al.*, 2004; Hodgkiess, 2004). Dissolved calcium carbonate in the condensate film that occurs due to improper venting of the gases, can lower the pH in the film and cause corrosion (Hodgkiess, 2004). Corrosion can be controlled by monitoring and controlling the pH (addition of caustic soda or acid dosing) (Anon,

1994). Without softening (soda ash and caustic soda) supersaturation will be high, resulting in high scaling rates (Brink *et al.*, 2004).

The Langelier Saturation Index can be used as a predictive tool to determine the tendency of a water to deposit or dissolve calcium carbonate (Kemmer and McCallion, 1979; Viessman and Hammer, 1998). This index can also be used to determine whether the water can be conditioned by chemical additives to deposit calcium carbonate (Hodgkiess, 2004). Caustic soda (NaOH) or soda ash ($NaCO_3$) can be used to increase the pH of the water or its alkalinity in order to produce water supersaturated with calcium carbonate ($CaCO_3$) (Hodgkiess, 2004). Acid dosing removes bicarbonate or carbonate ions by stripping the carbon dioxide out of the acidified water by passage through an aeration tower and therefore reducing the chance of alkaline scale precipitation from occurring (Hodgkiess, 2004). The Langelier Saturation Index can be interpreted as the pH change required to bring water to equilibrium and is therefore an accurate measure of determining the water balance (Anon, 2004a). It is purely an equilibrium index and provides no indication of how much scale or calcium carbonate will actually precipitate to bring water to equilibrium (Anon, 2004a). This index is used as a corrosivity index, but only measures the water stability in a system.

Table 2.1: The Langelier Saturation Index prediction (Anon, 2004a).

LSI	Likely behaviour of cooling water
+ 2	Severely scale forming (supersaturation)
+ 0.5	Scale forming/slightly corrosive (supersaturation)
0	Nominally balanced (saturation)
- 0.5	Non-scale forming/corrosive (undersaturation)
- 2.0	Severely corrosive (undersaturation)

The Langelier Saturation Index is defined as: $LSI = pH - pH_s$ where pH_s is the pH at saturation in calcite or calcium carbonate (Anon, 2004b). The LSI evaluates key variables (calcium hardness, M-alkalinity, temperature and TDS) and determines pH_s - the pH of $CaCO_3$ saturation (Rafferty, 2000; EPRI, 2003). A negative LSI value is indicative that the water is under-saturated and will dissolve calcium carbonate (Anon, 2004a). The behaviour of this type of cooling water is non-scale forming but corrosive

(Gebbie, 2000) (Table 2.1). A positive value refers that the water is oversaturated, calcium carbonate can precipitate and the tendency will be scaling (Nordell, 1961; Anon, 2004a) (Table 2.1). A Langelier Saturation Index value of zero indicates that the water is balanced (saturated) and no corrosion or scaling will occur (Gebbie, 2000; Anon, 2004a). It has been found that the maintenance of a positive index does not necessarily reduce the corrosivity of the water towards metal (Ramotlhola and Ringas, 2000).

The Ryznar Stability Index (RSI) is based on a study of actual operating results with waters having various saturation indices. It is used to quantify the relationship between the calcium carbonate saturation state and scale formation (Rafferty, 2000; Anon, 2004d). Both LSI and RSI are based on the saturation of calcium carbonate and is a better predictor of the degree of scaling than that of corrosion (Rafferty, 2000).

Water with a stability index of 6 or less, can have an increase in scaling and the tendency to corrode will decrease (Table 2.2). If the RSI value is above 7 no scaling should occur (Table 2.2) and the calcium carbonate formation probably does not lead to a protective corrosion inhibitor film (Anon, 2004d).

Table 2.2: The Ryznar Stability Index (Anon, 2004d).

RSI	Tendency of the water
4-5	Highly scale forming
5-6	Slightly scale forming
6-7	Slight scale formation or corrosion
7-7.5	Corrosive
7.5-9	Highly corrosive
>9	Very highly corrosive

The degree of corrosion towards mild steel is also described by the Larson Skold index and predicts the aggressiveness of water in once-through cooling systems (Anon, 2004b). Corrosivity increases with decreasing alkalinity and the aggressiveness of a water increases with increasing chloride or sulphate levels (Hodgkiess, 2004; Anon, 2006a). The index is the ratio of equivalents per million (epm) of sulphate (SO_4^{2-}) and

chloride (Cl^-) to epm of alkalinity in the form bicarbonate plus carbonate and is represented by the following equation:

$$LarsonSkold = \frac{(epmCl^- + epmSO_4^{2-})}{(epmHCO_3 + epmCO_3^{2-})}$$

If the index shows a value of less than 0.8, chlorides will not interfere with natural film formation and an index above 1.2 indicates the tendency towards high corrosion rates. An index between 0.8 and 1.2 is an indication that chlorides and sulphates may interfere with film formation, which may also lead to corrosion (Anon, 2004b).

The Puckorius Scaling Index is an indication of the relationship between saturation state and scale formation by incorporating the buffer capacity of the water in the index (Anon, 2004c). This index uses an equilibrium pH rather than the actual system pH to account for the buffer effects, since scale formation does not necessarily increase with pH (Anon, 2004c).

$$PSI = 2(pH_s) - pH_{eq}$$

Where: pH_s is the pH at saturation in calcite or calcium carbonate

$$pH_{eq} = 1.465 \times \log 10[Alkalinity] + 4.54$$

$$(Alkalinity) = (HCO_3^-) + 2(CO_3^{2-}) + (OH^-)$$

Calcium hardness can also be used as a key parameter in evaluating scale formation since scaling problems usually occur above levels of 100 ppm hardness (Rafferty, 2000).

2.8.2 Microbiologically induced corrosion and pitting corrosion

Microbiologically induced corrosion (MIC) occurs where the atoms on metal surfaces are exposed to an electron acceptor with a higher affinity than that of the potential donor. This results in a metal oxide or a salt that has little structural stability and the metal is rendered useless (Brözel *et al.*, 1997). In an aerobic environment metal oxides and hydroxides are formed with oxygen being the electron acceptor (Cord-Ruwisch, 2000). At low redox potentials, protons become the electron acceptor, yielding hydrogen gas and other highly reduced products (Keevil, 2004).

The process of corrosion is accelerated by the removal of the reduced products of the chemical reactions by bacterial activity (Brözel *et al.*, 1997). Generally, metabolic byproducts of biological activity react with the metal surface and can initiate a number of corrosion mechanisms. The pH can be changed into a range where general corrosion occurs due to the presence of metabolically produced acid (Angell, 1999). On the otherhand localised corrosion occur due to the increased sulphide content produced by sulphate reducing bacteria. The extracellular polymeric substances (EPS) of bacteria also contribute to the MIC mechanism by binding metal ions, resulting in the dissolution of metal (Flemming and Wingender, 2001a). EPS has also been identified as the main foulants in membrane bioreactors (Negaresh *et al.*, 2006). Microorganisms that are often involved in the MIC process which causes industrial problems are SRB, iron oxidizing bacteria, anaerobic acid or H_2 producing bacteria and slime forming bacteria (including acid or alkali producing bacteria), algae and fungi (Lutey, 1996; Choudhary, 1998).

According to Lutey (1996) the occurrence of MIC has become more severe and frequent and should be addressed in all process cooling water systems. The following observations can be used to confirm MIC existence which indicates that the corrosion is related to the uncontrolled growth of microorganisms (Lutey, 1996).

(i) pitting corrosion
(ii) microbiological biofilm on corroded surfaces
(iii) excessive bacterial populations in the planktonic phase
(iv) hydrogen sulphide (in anaerobic environments)
(v) metal sulphides or ferric hydroxide (in aerobic environments)
(vi) corrosion in systems with non-aggressive waters (e.g. high pH, alkalinity and low temperatures)
(vii) corrosion that occur in areas with a low flow velocity ("dead flow") areas.

Pitting corrosion is often seen in the presence of sulphate reducing bacteria (biological growths) (Anon, 1994), which enhances the formation of aeration cells in oxygen saturated cooling water (Brás Pereira *et al.*, 1997). The pitted type of corrosion is often the result of biological growths associated with SRB (Anon, 1994), by enhancing the formation of aeration cells in the oxygen saturated cooling water (Brás Pereira *et al.*, 1997). Common iron oxidising bacteria involved in MIC are *Gallionella*, *Sphaerotilus*,

Crenothrix, *Leptohtrix* as well as *Arthrobacter* species that oxidise ferrous ions to ferric ions to obtain their energy (Lutey, 1996). A low density hydrated iron oxide formed in the tubercles is the key factor for pitting corrosion of steel (Choudhary, 1998; Rao *et al.*, 2000).

Conflicting opinions exist whether there is a correlation between MIC failure and the number of SRB present in the planktonic or the sessile phase of operational systems (Angell and Urbanic, 2000). A previous study has shown that high numbers of sulphate reducing bacteria (SRB) from a nuclear power plant system was not associated with severe corrosion but was observed in the absence of SRB. In the latter case acid producing bacteria was the cause of MIC (Videla, 1994). Pit initiation can also occur where low numbers of SRB are present (Angell and Urbanic, 2000). High sulphate concentrations due to the presence of SRB have shown higher corrosion rates of steel coupons than those in a low sulphate concentration (Peng and Park, 1994). When the SRB mortality increases the corrosion rate drops due to the absence of a source of sulphide which act as a pitting activator (Angell and Urbanic, 2000). Experimental evidence has shown that SRB activity is the key parameter influencing localised corrosion of stainless alloys (Angell and Urbanic, 2000).

2.9 Sessile and planktonic community influence on sclaing, fouling and corrosion

The bacterial count of the bulk water reflects only planktonic microorganisms and not the type and number of organisms living in biofilms, which may give indirect hints on the biofilm formation (Videla, 2002; Meyer, 2003). Planktonic organisms are not representative of the bacteria causing corrosion and only represents a small proportion of the active sessile population of corrosion causing bacteria, which may have detached from the biofilm (Costerton, 1984; Videla, 2002). It is also becoming clearer that biofilms rather than planktonic microorganisms causes damage to water based technological processes since biocides are less effective against sessile microorganisms than planktonic microorganisms (Ludensky, 2003; Meyer, 2003). Biofilms also have not completely been associated as a source of microbiological problems but is rather seen as fouling or scaling in the industry (Ludensky, 2003).

2.10 Conventional methods to monitor bacteria in industrial effluents

Environmental bacteria and biofilms have traditionally been studied by culture dependent methods which are simple and inexpensive methods used for the enumeration and identification of cell viability (Camper *et al.*, 1999; Sartory and Watkins, 1999). Conventional microbial analysis of the planktonic phase can be used for the analysis of biofouling, this can also be an indicator of MIC. Conclusions made solely on the basis of planktonic microbial counts may be incorrect and the planktonic population does not reflect the total number and type of organisms living in the biofilm (Videla, 2002; Meyer, 2003). Thus, the microorganisms within the biofilm should be studied by making use of conventional methods.

2.10.1 Plate count method (Spread plate technique)

Due to the technical difficulties of examining biofilms *in situ* in industrial cooling and process water, most conventional microbiological studies have focussed on the analysis of the planktonic phase for monitoring microbial populations by culturing microorganisms using the spread plate technique. The spread plate technique involves the streaking of a known volume of the water sample over an agar (semi-solid) surface. Nutrients can be added to the agar culture medium to stimulate the growth of the microorganisms that are to be quantified. If it is desired to determine the number of iron reducing bacteria (IRB), ferric ammonium citrate may be included in the medium and the IRB will utilise the citrate as a source of organic carbon while the ferric ion stimulates the bacteria to initiate the reduction oxidation (ferrous/ferric) cycle. The success of growth depends on media, conditions (pH, moisture and oxygen) and ability of the microbe to adapt to major environmental changes (Csuros and Csuros, 1999 *et al.*, 1999). The clusters of microbes or colonies can be counted as being representative of the population size and only plates with 30 to 300 colonies are counted (Csuros and Csuros, 1999).

An advantage of the plate count method (done by a pour plate or a spread plate technique) is that the number of viable cells is measured, which allows quantitative values of bacterial activity (Csuros and Csuros, 1999; Palazzo and Allison, 2004). The heterotrophic plate count method uses media that supports the growth of most

heterotrophic bacteria and is a direct quantitative measurement of the viable aerobic and facultative anaerobic bacteria in water (Csuros and Csuros, 1999).

A disadvantage of the pour plate method (standard plate count method) is that the medium at 44° to 46°C may cause heat shock to stressed bacteria and the nutritionally rich medium may decrease recovery of starved bacteria (APHA *et al.*, 1985). An alternative technique is the spread plate method that eliminates heat shock caused by tempered agar and all colonies will be on the agar surface where they can be seen, counted and easily distinguished from particles or air bubbles (APHA *et al.*, 1985). This technique also requires less time and space than the pour plate method. Unfortunately, the agar spreadplate technique has a tendency to underestimate the population since either the microorganisms will not all grow under the conditions presented, or they become competitive for space and food. Bacterial cells may be overcrowded and won't develop if too many colonies are present (Csuros and Csuros, 1999).

2.10.2 Most probable number technique (MPN)

MPN usually gives viable counts that are ten times higher than plate counts. This is usually attributed to:

- Liquid medium less harsh than agar surface (e.g. low water activity)
- Consortia can persist better in liquid
- Lower O_2 concentration in liquid

In the MPN method the greater the number of bacteria in a sample, the more dilution is needed to reduce the density of the bacteria to reach a point of extinction (Csuros and Csuros, 1999). Therefore replicate dilutions needs to be made to obtain the most probable number of viable organisms.

A positive MPN test can be indicated by growth and fermentative gas production and bacterial densities are based on positive and negative tube results obtained from an MPN table (Csuros and Csuros, 1999). This method is most useful when the microbes being counted will not grow on solid media such as sulphate reducing bacteria, iron reducing bacteria as well as aerobic bacteria (Csuros and Csuros, 1999).

2.11 Culture independent methods for microbial community dynamics

Despite the fact that the functionality, structure and genetic diversity of microbial communities influence the overall performance of the biological system, the influence of external parameters on the microbial community are poorly understood nor has it been successfully characterised. Since conventional methods (heterotrophic plate counts) only detects a portion of the total microbial population and therefore underestimating the numbers and diversity of environmental bacteria, alternative culture independent techniques have been developed to perform qualitative analyses without cultivation (Camper *et al.*, 1999; Wobus *et al.*, 2003; Van der Kooij *et al.*, 2003). The development of alternative approaches includes molecular techniques which allow the successful *in situ* analysis of the functional, structural and genetic diversity of a microbial community, resulting in distinguishable fingerprints (Wuertz *et al.*, 2003). The molecular techniques in this study that are considered are denaturing gradient gel electrophoresis (DGGE) as well as phospholipid fatty acid (PLFA) analyses to determine the structural diversity of microbial communities (Kozdrój and Van Elsas, 2001). This approach would yield data that could be used to assist in the control of biofouling and MIC of industrial systems. Such results would be useful to optimise operational conditions for systems such as cooling towers in which process waters are re-used.

2.11.1 Structural diversity: denaturing gradient gel electrophoresis

The objective of DNA profiling techniques is to give an overall pattern of the structural changes within the microbial community (Cocolin *et al.*, 2003). DNA profiles of whole microbial communities are generated in single electrophoretic tracks and can be analysed using indexes adapted from phylogenetic and ecological studies (Ampe and Miambi, 2000). The dynamics of individual bands on a DGGE gel are units (melting types) that are used to monitor these microbial community structural changes. These melting types could be indicative of species diversity within the microbial population and the bands can be reanalysed and sequenced to determine the identity of the organisms it represents (Kisand and Wikner, 2003).

2.11.2 Functional diversity: signature lipid biomarker analysis

By making use of signature lipid biomarkers the structural diversity of microbial communities can be determined (Kehrmeyer *et al.*, 1996). Phospholipid fatty acids (PLFA) are a unique class of lipids that can be used as signature lipid biomarker to determine microbial community structure. Community structure and biomass can be determined through PLFA without relying on the cultivation of microorganisms (Kozdrój and Van Elsas, 2001; Ibekwe *et al.*, 2002). This technique is not capable of identifying microorganisms at the species or strain level but is able to produce descriptions of microbial communities based on functional groupings of fatty acid profiles indicative of prokaryotic and eukaryotic taxa (Ibekwe *et al.*, 2002). PLFA can also indicate microbial physiological status by analysing stress indicators that represents the microbial biomass, indicating active living microbial components (Ibekwe *et al.*, 2002).

2.11.3 Microscopy

Qualitative information can be obtained on the morphological structure of a biofilm by making use of scanning electron microscopy (SEM) (Wobus *et al.*, 2003). It provides fast and accurate images of biofilms (Ray and Little, 2003). Before quantification the biofilm must be coated with a conductive film of metal to prevent the build up of local electrons that prevents the formation of usable images (Ray and Little, 2003). The SEM technique can be used for visual impressions of bacteria as a (semi) quantitative technique (Hilbert *et al.*, 2003).

2.11.4 Summary

The literature review in this chapter demonstrated that by re-using process effluents (Primary Column Bottoms) within cooling towers in an industry, such as Sasol, water requirement as well as the volume of effluent discharged may be reduced, but it will still be contaminated. Although it is technically feasible to re-use these effluents, operational problems such as fouling, scaling and corrosion are likely to occur. Certain techniques can be used to obtain data useful for predicting operating parameters as well as predictions on the fouling, scaling and corrosion phenomenon. These techniques that could optimise cooling tower performance and minimise fouling, scaling and corrosion

includes, microbiological techniques (conventional and culture independent), scaling and corrosion indices as well as microscopy.

CHAPTER 3

Accelerated scaling and corrosion tests to optimise cooling tower performance

3.1 Introduction

Accelerated corrosion tests accelerate corrosion by immediately establishing the mature natural environment that causes corrosion (Angell and Urbanic, 2000). This test is also conducted to understand the factors that will influence long term corrosion rates, test specific metals or a certain test solution (McLaughlan and Stuetz, 2004). Coupon corrosion testing is designed to investigate general corrosion by using weight loss during the test period as a principal measure of corrosion (ASTM, 1999a). The corrosion rate implies that all weight loss has been due to general corrosion and not to pitting corrosion (localised corrosion) (ASTM, 1999b). This assumption is based on the notion that weight loss measurements delivers no insight on the size or depth of pitting corrosion and pitting may occur even when there is only a slight weight loss (Anon, 1994).

The chemical characterisation of the water as well as the various scaling and corrosion indices on the stabilised and non-stabilised water are performed to evaluate the scaling properties of the water (Brink *et al.*, 2004). If the water has a tendency to be scale forming, fouling may occur on the heat exchanger surface resulting in reduced heat exchange efficiency and performance (Rafferty, 2000). Increasing values of pH, total alkalinity and total hardness indicates that the water has a tendency to dissolve $CaCO_3$ (Hamrouni and Dhahbi, 2002). The heating of water usually results in water that is supersaturated with $CaCO_3$ (Videla, 2002; Brink *et al.*, 2004; Hodgkiess, 2004). This will result in calcium carbonate precipitating on the heated wall (Hamrouni and Dhahbi, 2002; Brink *et al.*, 2004).

The equilibrium condition occurs when water is saturated with calcium carbonate which neither dissolves, nor precipitates calcium carbonate scale (Hamrouni and Dhahbi, 2002). To bring the water to calco-carbonic equilibrium, NaOH is added to the feed

water raising the pH to 8.0 - 8.3, producing water that is supersaturated with $CaCO_3$ (Mackintosh *et al.*, 1998; Hodgkiess, 2004). This water is known as the stabilised water. Another reason for stabilising the water is to produce water that will avoid scale deposition but more importantly, result in minimal corrosion formation (Gebbie, 2000). The original make-up water has a pH of 3.7 and low pH conditions are corrosive to metals (Echols and Magne, 1990; Hodgkiess, 2004).

It is therefore important to determine the aggressiveness of water by determining the mineral dissolving potential (saturation state) (Mackintosh *et al.*, 1998). The general character (scale formability or corrosiveness) of a water sample is thus determined by analysing the total dissolved solids (TDS), temperature, pH, calcium hardnes, alkalinity as well as the presence of Cl, SO_4 and Fe (Rafferty, 2000).

A study done by Hodgkiess (2004) showed that a reduction in the corrosion rate over time was associated with the build up of a calcerous scale layer, protecting against corrosion. However, scale formation results in reduced heat exchange. Olesen *et al.* (2004) showed that besides pH, carbonate balance and oxygen levels, bacterial activity as well as deposits also influence the rate of corrosion. The corrosion rate reduces with time due to the reduction of the oxygen concentration since the corrosion process consumes oxygen (Andijani and Turgoose, 2004). According to Olesen *et al.* (2004) corrosion of 316 stainless steel under neutral or alkaline conditions is related to temperature and the presence of halides (e.g chloride and fluoride). The cathodic reaction on the stainless steel is the oxygen-reduction reaction and this promotes scale deposition on the surface of the stainless steel (Hodgkiess, 2004). High concentrations of salt carbonates and sulphates of calcium and magnesium as well as barium salts, silicates and phosphates can result in scaling or corrosion (You *et al.*, 1999; Hamrouni and Dhahbi, 2002; Macadam and Parsons, 2004).

The Langelier Saturation Index (LSI) expresses the effects of pH, calcium hardness, total alkalinity, dissolved solids and temperature (Hamrouni and Dhahbi, 2002), in relation to the solubility of calcium carbonate for waters in the 6.5 to 9.5 pH range (Nordell, 1961; Anon, 2004). The Ryznar Stability Index on the otherhand is used to quantify the relationship between the calcium carbonate saturation state and scale formation (Anon, 2004d). It is thus a better predictor of scaling than of corrosion

(Rafferty, 2000; Anon, 2006a). Both the LSI and Ryznar indices offer qualitative information about the scaling tendencies of water (Rafferty, 2000). LSI and Puckorius Scaling Index (PSI) are usually used for water with a pH of above 8.0 (Rafferty, 2000).

The Puckorius Scaling Index is an indication of the relationship between saturation state and scale formation by incorporating the buffering capacity of the water in the index. This index uses an equilibrium pH rather than the actual system pH to account for the buffering effects (Anon, 2004c). The corrosivity of water towards mild steel is described by the Larson Skold index and predicts the aggressiveness of water in once-through cooling systems (Anon, 2004b). The objective of using these indices are to adjust the cooling water to a non-scaling condition and also to predict if a water will precipitate a layer of $CaCO_3$, as in the case of the LSI (Hodgkiess, 2004). The accepted values for LSI to prevent corrosion are between –0.5 and +0.5 (Brink *et al.*, 2004). Values higher than +0.5 are indicative of scale forming water and values below -0.5 indicate that the water has a tendency to be corrosive (Anon, 2004). According to Gebbie (2000) the acceptable values for a stable, non-corrosive water is an LSI >-1.5 and RSI value <10.

Cooling towers are designed to evaporate water by contact of water with air (Kim *et al.*, 2001). Even though evaporation water is pure, some droplets escape as mist through the evaporation equipment. Drift is the loss of small droplets of circulating water to air flow and it contains some dissolved solids (EPRI, 2003; Meroncy, 2006). As drift exits the tower, it evaporates and leaves chemical constituents, suspended material (e.g scale and corrosion byproducts) and biological matter (planktonic, sessile bacteria or metabolic byproducts) dispersed in the air flow as dry particulate matter (EPRI, 2003). Drift establishes the maximum concentration ratio in the absence of controlled blow down, by controlling the chemical character of the recirculating water. It can travel large distances from the cooling tower. These distances are dependent on ambient conditions such as wind direction, wind speed, air temperature, and relative humidity. Drift can also be the cause of salt deposition in the area surrounding the cooling tower (EPRI, 2003). In order to reduce the loss of mist, drift eliminators are placed in the cooling towers (Anon, 1994).

The aim of this chapter was to perform accelerated scaling and corrosion tests using scaling and corrosion indices to optimise cooling tower performance. The objectives were to:

(i) prepare and stabilise acid water similar to the composition of Primary Column Bottoms as produced at Sasol's Fischer-Tropsch GTL process.

(ii) analyse the physical and chemical characteristics of the stabilised and non-stabilised synthetic Primary Column Bottoms.

(iii) perfom accelerated corrosion tests on mild steel and stainless steel corrosion coupons.

(iv) determine the drift loss within the cooling tower.

3.2 Materials and methods

3.2.1 Acid water preparation, stabilising the water and pH control

An acid water (average pH 3.7) similar with the same composition as the Primary Column Bottoms produced at Sasol's Fischer-Tropsch gas-to-liquid conversion process was synthetically prepared. Acetic acid was the major component at 43% of the total acids. Formic acid contributed 23%, methanol and hydrocarbons each contributed 8%, butyric and pentanoic acid each contributed 7% and propionic acid 4%. All these were added in the proportions indicated to make 100 liters and were mixed well,

Primary Column Bottoms primarily consists of fatty acids in the make-up water and with its low pH was expected to be very corrosive (Hodgkiess, 2004; Echols and Magne, 1990). The water had to be chemically corrected before used as cooling water. The water was stabilised by adding sodium hydroxide to the recirculating water within the cooling tower to increase the pH of the water to pH 8.0 - 8.3 (Mackintosh *et al.*, 1998). Water that was in equilibrium or supersaturated with calcium carbonate was then produced (Hamrouni and Dhahbi, 2002; Hodgkiess, 2004). A pH probe (HI 1006-32) was installed in the sump of the cooling tower, connected to a pH controller (Hanna HI 504, USA) as well as two peristaltic pumps (Watson Marlow 101U/R, England). The pH was continuously monitored and corrected through the pH controller using HCl (2N) and NaOH (2N) respectively. The pH probe continuously measures the pH of the circulating water. When the pH increases or decreases between the two set points (8.0

and 8.3) the acid or sodium hydroxide pump was energised, maintaining the pH between these two values.

3.2.2 Physico-chemical analyses of the process water

Both total dissolved and suspended solids were determined gravimetrically on the test solution (ASTM, 1999b). A Whatman GF/A filter paper (110 mm diameter) was inserted in the filtration apparatus. A vacuum was applied and the paper washed with three successive portions of distilled water. The filter paper was then dried in a drying oven (104 °C) for 1 hour and cooled in a desiccator to room temperature. The GF/A filter paper were weighed to the nearest 0.0001 g before returned to the filtration apparatus. A sample (100 ml) was measured where after the suction began in the filtering apparatus. The filtrate was removed and kept to determine the total dissolved solids at a later stage. The filter paper was then dried in a drying oven (104 °C) for 1 hour, cooled in a desiccator and weighed to determine the total suspended solids.

An evaporating dish was dried in an oven (104 °C), cooled in a desiccator and weighed. A known volume (100ml) of the filtrate that was put aside was transferred into the evaporating dish, dried in an oven (104°C), cooled in a desiccator and weighed. The weights of each method (TSS and TDS) were subtracted from each other and divided by the volume of sample used to determine the total dissolved and total suspended solids in mg/L.

Dissolved oxygen and pH which are two of the main factors influencing corrosion, redox potential as well as conductivity were also evaluated during the accelerated corrosion test (Mackintosh *et al.*, 1998; Andijani and Turgoose, 2004). Dissolved oxygen, conductivity and pH were measured daily using a portable ion meter (WTW, Germany). Redox potential was measured by making use of a Metrohm 704 meter (Hanna, USA).

3.2.3 Accelerated corrosion test

Before any of the later experimental runs were performed on the cooling towers, accelerated corrosion tests were done to compare the corrosion rates of the stabilised and non-stabilised feed water and to conclude whether the stabilisation of the water was efficient. To obtain the water required for the accelerated corrosion test, make-up water was stabilised, recirculated in the cooling tower until the various cycles of concentration (2, 4 and 6) were obtained. The pH of the stabilised water at each cycle of concentration was monitored on-line with two set points (8.0 and 8.3) and automatically dosed with NaOH (2N) and HCl (2N). In the case of the non-stabilised water, the pH was maintained between 6.0 and 6.5. These feed waters (stabilised and non-stabilised) at the various cycles of concentration (2, 4, 6) were collected from the cooling towers and stored until used in the accelerated test described below.

The corrosion coupons were rinsed with acetone to remove any oil and grease from the surface, dried at 104°C and weighed before using them in the test experiment (weight 1) (McLaughlan and Stuetz, 2004). Each stainless steel and mild steel corrosion coupon were hung in a 250 ml glass beaker and placed in a water bath at 60°C. This was the maximum temperature at which the block temperature within the cooling tower were operated at. The accelerated corrosion tests were done over a period of 28 days since short-time tests performed on alloys such as stainless steel can give inaccurate results due to the formation of passive films (ASTM, 1999a). Only one type of metal (either stainless steel or mild steel) was exposed in a given test due to the fact that corrosion products from the coupons may influence the corrosion rate of the metal itself or the different metals exposed at the same time (ASTM, 1999a) and can also accelerate the corrosion attack on one metal (Hodgkiess, 2004).

In some cases of accelerated tests, the composition of the test solution may change as a result of catalytic decomposition or by reaction with the test coupons and it is therefore allowable to add the exhausted constituents to the coupons during the course of the accelerated test (ASTM, 1999a). The loss of feed water due to evaporation was frequently added (every third day) with the appropriate test liquid, at the various cycles of concentration and pH values to ensure reproducible results (ASTM, 1999a). The test solution was not aerated since it is stated that the corrosion test related to the process

equipment (cooling tower) should be run with the same natural atmosphere inherent in the process (ASTM a, 1999). In this accelerated corrosion test experiment that was done below boiling point, the only source of liquid velocity was thermal convection (ASTM, 1999a).

After the 28 days, a mechanical (scrubbing, brushing) and chemical cleaning (NaOH, inhibited HCl, citric acid) procedure were performed on the coupons (ASTM, 1999c). The coupons were then dried at 104°C for 2h and cooled in a desiccator for 2h. After each cleaning, drying and cooling procedure the coupons were weighed in a weighing boat. The corrosion rate (mm/y) was then calculated based on weight loss measurements (Videla, 2002; McLaughlan and Stuetz, 2004).

3.2.4 Scaling and corrosion indices

Langelier Saturation Index is defined as: $LSI = pH - pH_s$

where pH_s is the pH at saturation in calcite or calcium carbonate (Anon, 2004a).

$pH_s = (9.3 + A + B) - (C + D)$ (Rafferty, 2000)

$$A = \frac{\log(TDS) - 1}{10}$$

$B = [-13.12 \times \log(°C + 273)] + 34.55$

$C = \log(CalciumHardness) - 0.4$

$D = \log(Alkalinity)$

$RSI = 2pH_s - pH$ (Gebbie, 2000; Anon, 2004d)

$Puckorius\ Scaling\ Index\ (PSI) = 2(pH_s - pH_{eq})$

$pH_{eq} = 1.465 + \log(Alkalinity) + 4.54$

$[Alkalinity] = [HCO_3^-] + 2[CO_3^{2-}] + [OH^-]$ (Anon, 2004c)

The Larson Skold index is the ratio of equivalents per million (epm) of sulphate (SO_4^{2-}) and chloride (Cl^-) to the epm of alkalinity in the form bicarbonate plus carbonate:

$$LarsonSkold = \frac{\left(epmCl^{-} + epmSO_4^{2-}\right)}{\left(epmHCO_3^{-} + epmCO_3^{2-}\right)}$$ (Anon, 2004b)

3.2.5 Determination of drift loss

A measured quantity of TRASAR product was added to the circulating water within the cooling system. The fluorometer was calibrated and a 10 ml sample from the cooling tower sump was placed into a cuvette and measured. The analyses were done immediately after sampling and the sample was placed back into the cooling tower. These samples were taken approximately every 6 to 8 hours over a period of 3 days. The percentage drift loss was then calculated by dividing the drift loss (L/hr) through the recirculation flow rate (L/hr) and multiplied by 100.

3.3 Results and discussion

The results of the chemical analyses that were done on the make-up, stabilised and non-stabilised water are presented in Table 3.1. Although a low pH (pH 3.7) has an important inhibition effect on scaling, the make-up water water with its low pH (Table 3.1) resulted in high corrosion rates (Table 3.2). The stabilised water has a higher total alkalinity than the non-stabilised water (Table 3.1). Alkalinity has an important effect on scaling but an inhibitory effect on corrosion (You *et al.*, 1999). This is confirmed when comparing the scaling and corrosion rates of the stabilised and non-stabilised water in Table 3.2. Scaling is higher in the stabilised water and the non-stabilised water resulted in higher corrosion rates (Table 3.2). The high chlorides and SO_4 values, as well as dissolved oxygen (Table 3.1) could eplain the occurrence of corrosion in the stabilised water (You *et al.*, 1999).

The various indices that were calculated as explained in Section 3.2.4, indicated that the make-up water is very corrosive and mild steel corrosion may be problematic (Anon, 2004d). This high corrosion may be due to the low pH (3.68) of the make-up water (You *et al.*, 1999). The accepted limits for the LSI to prevent corrosion are between an LSI value of –0.5 and +0.5 (Brink *et al.*, 2004). The neutral point of RSI and PSI is a value of 6.0 which is indicative of stable water with minimal scaling or corrosion (You *et al.*, 1999; Anon, 2004b). The Sasol guidelines are the optimal values for fouling,

scaling and corrosion on mild steel and stainless steel. According to the Sasol guidelines for corrosion coupons, the fouling and scaling rate of this water are within the acceptable values of 20 mg/dm^2/d and 2 mg/dm^2/d respectively. Since scaling protects against corrosion a higher scaling rate can be associated with a low corrosion rate (Hodgkiess, 2004).

Table 3.1: Water chemistry of the Primary Column Bottoms, chemically stabilised and non-stabilised water used in the accelerated *corrosion* test.

Variable	Unit	Primary Column Bottoms	Range of values of Stabilised water	Range of values of Non-stabilised water
pH		3.68	8.0 - 8.3	6.0 - 6.5
Electrical conductivity	mS/cm	0.84	1.96 - 5.81	1.96 - 3.14
Total alkalinity	mg $CaCO_3$/L	0	270 - 650	90 - 290
Total hardness	mg $CaCO_3$/L	335	459 - 1516	567 - 1069
Total iron	mg Fe/L	4.181	1.90 - 2.8	2.3 - 5.3
Chloride	mg Cl/L	45	79 - 384	93 - 296
Sulphate	mg SO_4	123	142 - 507	155 - 276
Total dissolved solids	mg/L	3185	1400 - 3400	1200 - 2000
Total suspended solids	mg/L	100	13 - 63	36 -75
Dissolved oxygen	mg/L	3	1.9 - 2.5	1.2 - 2.8

At 4 and 6 cycles of concentration the water becomes more scale forming and has a higher tendency towards $CaCO_3$ precipitation (Table 3.2). However, the values of the LSI indicate that the 2, 4 and 6 cycles of concentration the water is corrosive and the corrosion rate increases as the index increases (Anon, 2004b).

Table 3.2: Fouling, scaling and corrosion results of corrosion coupons after accelerated corrosion test.

	Fouling ($mg/dm^2/d$)	Scaling ($mg/dm^2/d$)	Corrosion (mm/y)
Sasol guideline (Anon, 2007)	**20**	**2**	**0.2**
2COC, S, ss	0	0	0
2COC, S, ms	15.017	8.521	0.036
4COC, S, ss	0.258	0.218	0
4COC, S, ms	14.619	7.508	0.033
6COC, S, ss	0.139	0	0
6COC, S, ms	9.574	5.78	0.029
2COC, N, ss	0.02	0.02	0
2COC, N, ms	15.056	9.157	0.047
4COC, N, ss	0.02	0.02	0
4COC, N, ms	9.872	6.912	0.037
6COC, N, ss	0.06	0.04	0
6COC, N, ms	3.953	1.49	0.063
COC = cycles of concentration, S = stabilised water, N = non-stabilised water, ms = mild steel, ss = stainless steel			

The stabilised water at 2 cycles of concentration was more corrosive than the 4 and 6 concentrated water (Table 3.2). This could be due to the chemical properties of this water such as Fe, Cl and SO_4 (Table 3.1). The LSI of the 4 cycles of concentration stabilised water indicated that the water is more scale forming than corrosive (Anon, 2004a) which also corresponds with the scaling and corrosion results (Table 3.2) obtained from the accelerated corrosion test. The accelerated corrosion test on this water was run under alkaline operating conditions (pH >7.8) which reduces cooling water corrosivity (Ascolese and Douglas, 1998). The stabilised water at 6 cycles of concentration resulted in the smallest corrosion rate.

The non-stabilised water at 2 cycles of concentration had a pH of 6.86 which can be seen as a neutral system that provide a certain level of protection against scaling (Ascolese and Douglas, 1998). This water therefore had a high corrosion rate (0.047 mm/y) which was also predicted by all 4 of the scaling indices (Table 3.3).

Table 3.3: The various scaling and corrosion indices as well as the pH of the make-up, stabilised and non-stabilised water after the accelerated corrosion test was conducted.

	RSI	LSI	PSI	LS	pH
Make-up water	16.39	-6.35	13.2	-	3.7
2COC, S	6.92	0.46	6.3	0.97	7.85
4COC, S	5.59	0.46	4.86	1.64	8.01
6COC, S	5.46	1.19	4.49	1.37	7.85
2COC, N	7.93	-0.53	6.54	1.66	6.86
4COC, N	6.71	0.19	5.29	1.56	7.06
6COC, N	10.76	-3.12	7.31	6.83	4.51

RSI = Ryznar Stability Index, LSI = Langelier Saturation Index, PSI = Puckorius Scaling Index, LS = Larson Skold index, COC = cycles of concentration, S = stabilised water,
N = non-stabilised water

According to the LSI, RSI as well as PSI (Table 3.3) the stabilised water at 2 cycles of concentration is more stable and has a tendency of being slightly scale forming (Rafferty, 2000). Water with high values of calcium hardness may precipitate calcium carbonate forming a barrier film at the cathode to protect against general corrosion (Ascolese and Douglas, 1998; Hodgkiess, 2004). The LSI of this water indicates that the water is under-saturated with a tendency to dissolve $CaCO_3$ and is slightly corrosive but non-scale forming (Rafferty, 2000; Anon, 2004a). The RSI, PSI as well as the LS index also predicts that this water will be corrosive (Table 3.3).

The indices performed on the 4 cycle of concentration non-stabilised water indicate that the water is slightly scale forming and little corrosion should occur (Rafferty, 2000). This water had a pH of 7.06 (Table 3.3). The corrosivity of water is thus reduced as predicted by the indices in Table 3.3, that indicated that this water had the lowest corrosion potential (Ascolese and Douglas, 1998) .

From Table 3.3 the non-stabilised water at 6 cycles of concentration had an RSI value of 10.76, which predicts that mild steel corrosion may become a problem (Anon, 2004d). The mild steel corrosion coupon tested in this water had the highest corrosion rate (Table 3.2). This high corrosion rate was also correctly predicted by the high LS

value (Table 3.3). The high corrosivity of this water may be due to the low pH (4.51) of this water (Hodgkiess, 2004). Stainless steel corrosion coupons usually attain low $CaCO_3$ scaling rates (Macadam and Parsons, 2004). Stainless steel is resistant to localised corrosion in low chloride flowing water (<1000 ppm) (Angell and Urbanic, 2000). According to Choudhary (1998) a corrosion rate of 2.53 mm/y was calculated on a 16mm mild steel corrosion coupon and 1.3 – 5.07 mm/y on stainless steel coupons. Mild steel coupons exposed in sterile conditions (no bacterial growth) showed corrosion rates in the range 0.015 - 0.044 mm/y (Rao *et al.*, 2000). In the presence of *Leptothrix* sp. (iron reducing bacteria) and *Desulfovibrio* sp. (SRB) corrosion rates on carbon steel ranged from 0.076 - 0.33 mm/y (Rao *et al.*, 2000). From Table 3.2 it can be seen that the corrosion rates of the stabilised water are lower than those of the non-stabilised water and are within within the Sasol guideline.

The average fouling and corrosion rates of the mild steel and stainless steel corrosion coupons from the stabilised water were within the Sasol guidelines. The scaling rates of the mild steel coupons from the stabilised water (5.7, 7.5 and 8.5 $mg/dm^2/d$) were not within the Sasol guideline of 2 $mg/dm^2/d$ (Table 3.2).

The composition of the test solution (stabilised and non-stabilised water at the various cycles of concentration) changed due to catalytic decomposition or by the reaction of the test coupon (ASTM, 1999a). Electrical conductivity was kept constant throughout the test period by adding new test solution to the accelerated corrosion test. Dissolved oxygen, pH as well as redox potential reduced with time until fresh test solution was added. Since the corrosion process consumes oxygen, the corrosion rate also reduces due to the reduction of oxygen concentration (Berdelle-Hilge, 1995; Andijani and Turgoose, 2004). The decrease in the dissolved oxygen levels could be due to respiratory activity of microbial species (Keevil, 2004).

Although the pH was monitored between two set points the peristaltic pumps occasionally overdosed and therefore the blow down that was used as the test water in the accelerated corrosion test were not always in the precise pH range of 6.0 - 6.5 or 8.0 - 8.3. The pH of the test water also varied during the accelerated corrosion test possibly due to microbial activity (Angell, 1999). Calcium precipitation of microbiological processes might also have been responsible for the decrease in pH (Slaats *et al.*, 2004).

When the water quality parameters were measured (pH, conductivity, dissolved oxygen, redox potential) the test solution was removed from the water bath and afterwards put back into the 60°C bath. This could have had and influence the redissolving potential of the calcium carbonate since supersaturated water was formed resulting in precipitation and leading to the high scaling rates found on each corrosion coupon, Table 3.2 (You *et al.*, 1999; Hamrouni and Dhahbi, 2002). Calcium carbonate solubility decreases as temperatures increases (Anon, 1994; Brink *et al.*, 2004).

The loss of water from the beakers was replaced with the various test liquids and not distilled water. This resulted in minimal increase in electrical conductivity (Appendix A Figure A1 – A4). It is thus evident that during this accelerated corrosion study the addition of test liquid did not dilute the test liquied and affect the end cycles of concnetration.

Neutral pH systems provide a certain level of protection against scaling. Alkaline operating conditions (pH >7.8) on the other hand reduces cooling water corrosivity (Ascolese and Douglas, 1998). Water with high values of calcium hardness may precipitate calcium carbonate forming a barrier film at the cathode to protect against general corrosion (Ascolese and Douglas, 1998; Hodgkiess, 2004; Macadam and Parsons, 2004). In the present accelerated corrosion test the coupon was rotated, once a day in the test solution. The only form of liquid flow velocity was thermal convection. This minimal flow velocity could explain the high scaling rates obtained from the corrosion coupons (Table 3.2).

The results of the TRASAR readings as well as the drift of the cooling tower are presented in Table 3.4. The percentage drift loss was calculated as 0.039, 0.026 and 0.019 at the various flow rates (0.6, 0.9 and 1.2 m/s) and at 0.6 and 0.9 m/s is somewhat higher than the drift loss found at Sasol (0.022). The calculated drift loss is still within the limits of normal operation, where 2% of recirculation is considered to be the limit. According to Kemmer (quoted by Kim *et al.*, 2001) the drift loss in conventional cooling towers is not more than 0.2% of the inlet cooling water.

Table 3.4: Table showing TRASAR data obtained, the drift of the cooling tower was calculated as 0.043 L/h.

Calculated Volume (liter)	9.93
Initial Trasar Reading	6.15
Final Trasar Reading	4.13
Drift (L/h)	0.043
Variance over 53 hours	1.1
T0 = 0 hr	6.15
T1 = 8 hr	5.23
T2 = 16 hr	4.9
T3 = 24 hr	4.62
T4 = 32 hr	4.52
T5 = 40 hr	4.23
T6 = 48 hr	4.13

3.4 Conclusion

The corrosiveness of the stabilised and non-stabilised water Primary Column Bottoms were evaluated by determining the corrosiveness of the water through experimental data (accelerated corrosion test) and also comparing these results with various scaling and corrosion indices. Both LSI and RSI are based on the saturation of calcium carbonate, but do not calculate the amount of precipitation that will occur and is a better predictor of scaling than of corrosion (Rafferty, 2000; Brink *et al.*, 2004). According to the LSI, RSI and the PSI the stabilised water was slightly scale forming with little corrosion and the non-stabilised water being more corrosive than scale forming. The LS index predicted that all 6 test solutions (stabilised and non-stabilised) were corrosive. This predictions were not accurate when the corrosion rates of the various corrosion coupons were analysed. The main reason for this might be due to the high alkalinity, chloride and sulphate levels that are used to calculate the LS index. According to Asano *et al.*, 1988; Crook *et al.*, 1994; Hwang *et al.*, 1995, (quoted by You *et al.*, 1999) when using water within cooling towers the make-up water quality should be of a certain standard or within a certain range. Chlorides should not exceed 500 mg/L, SO_4 200 mg/L, pH

6.9 – 9.0, dissolved solids 500 mg/L, suspended solids 100 mg/L, Fe 0.5 mg/L, alkalinity 350 mg/L as $CaCO_3$ and the hardness 650 mg/l as CaCO3 (You *et al.*, 1999). According to the result from Table 3.1 the total dissolved solids (3185 mg/L) and Fe (4.181 mg/L) of the make-up water exceeded these quality standards.

The corrosion rate of the unstabilised Primary Column Bottoms is much higher than the stabilised water since pH and carbonate balance influences the corrosion rate (Mackintosh *et al.*, 1998). All 4 indices indicated that the stabilised water, at the different cycles of concentration was more scale forming than corrosive. This also corresponds to the scaling and corrosion results obtained from the accelerated corrosion test. It can also be concluded that the fouling and scaling rates of the stabilised water were higher than the fouling and scaling rates of the non-stabilised water. This could have been due to the fact that the corrosion rate of the non-stabilised water was higher than the corrosion of the stabilised water.

When comparing the scaling and corrosion results obtained through the weight loss measurement, the scaling results corresponded more to what the LSI, RSI and PSI predicted than the corrosion results. In this study no corrosion occurred on the 316 stainless steel coupons. A study done by Macadam and Parsons (2004) concluded that stainless steel attains a very low scaling rate which is also confirmed during this experiment on the corrosion coupons. When corrosion occurs under neutral or alkaline conditions it could be related to the temperature and the presence of halides such as chloride and fluoride (Olesen *et al.*, 2004). Scaling causes cathodic polarisation by reducing the rate of electrochemical reactions between the environment and the metal surface (McLaughlan and Stuetz., 2004). Therefore corrosion decreases with time due to scale formation (precipitates or insoluble corrosion products). The non-stabilised water at 6 cycles of concentration was the only test solution that attained a high corrosion rate and a very low scaling rate. Five of the test solutions attained high scaling rates as well as fairly high corrosion rates. The corrosion coupons were only removed after 28 days and the effect that the scale formation had on the corrosion rate over time are not fully known. However, scale formation does not only depend on water chemistry but also flow rate within the system (McLaughlan and Stuetz, 2004; Olesen *et al.*, 2004).

During the accelerated scaling and corrosion test, the fouling, scaling and corrosion rates of the stabilised water decrease as the cycles of concentration increases. From this accelerated corrosion experiment it can be concluded that the stabilisation of the make-up water was effective since the stabilised water resulted in less fouling, scaling and corrosion. By controlling the pH of cooling water the expected corrosion, microbiological fouling as well as chemical deposits could be minimised to obtain optimal operating conditions and minimal operational problems (Brás Pereira *et al.*, 1997; Ascolese and Douglas, 1998; You *et al.*, 1999). The accelerated corrosion test was done in beakers and does not consider linear flow velocity. Thus, in the following chapter the cooling tower will be operated at various linear flow velocities and cycles of concentration using stabilised Primary Column Bottoms. The Primary Column Bottoms will therefore be chemically stabilised by adding a NaOH solution to the circulating water, to obtain a pH of 8.0 to 8.3 since this reduces corrosion.

Although this accelerated corrosion experiment was performed on synthetic Primary Column Bottoms at 2, 4 and 6 cycles of concentration the actual cooling tower experiment will be operated at 2, 3 and 4 cycles of concentration. This change in operating parameters was due Sasol's commissioning requirements at the time.

CHAPTER 4

Influence of the external operating parameters within the cooling tower on the rate of fouling, scaling and corrosion

4.1 Introduction

In cooling towers water is distributed uniformly over the top of the tower and permitted to drop through the air (Figure 2.1). In an open recirculating system water is pumped from the cooling tower basin and is circulated in the system through a heat exchanger (Mcesters *et al.*, 2003). The two operational characteristics that control the conductive heat transfer in the heat exchanger are temperature difference of the cooling water within the heat exchanger as well as fouling and scaling deposits on the heat exchanger tubes (Kemmer and McCallion, 1979). The temperature differential (ΔT) refers to the difference between the average water temperature returning to the tower from the heat exchanger and the average water temperature flowing from the tower basin towards the heat exchanger (Kemmer and McCallion, 1979). Packing material can be used in the tower to increase the contact of water and air and acts as the media of heat and mass transfer (Beyer, 1993; Qi *et al.*, 2006). The perforated bars or holes within the packing material enhance thermal performance, if the holes become plugged thermal capacity of the cooling tower will be reduced (Beyer, 1993; Qi *et al.*, 2006).

A mechanical draft tower uses a motor driven fan to move air into the tower through the circulating water, unlike natural draft towers depending on air or wind (Kemmer and McCallion, 1979; Echols and Magne, 1990). This fan increases the air velocity over the droplets of water, increasing the contact time between the water and the air and therefore maximizing the heat transfer (Qureshi and Zubair, 2006). The fan is located at the base or the side of the tower to force (forced-draft tower) air into the tower horizontally and then up to meet the falling water droplets (Kemmer and McCallion, 1979; Qureshi and Zubair, 2006). Because the fans are not within the air-water contact zone, they are sheltered from corrosion and scale deposition.

The breaking of water into droplets and moving air across the water droplets causes the evaporative cooling of the water (Echols and Magne, 1990). When air enters the cooling tower, its moisture content is generally less than saturation. When air exits, it emerges at a higher temperature and with a moisture content at or near saturation (Makkinejad, 2001). Cooling towers are therefore used to bring warm water into contact with cooler air to evaporate some portion of the water and to release the latent heat of evaporation in order to lower the water temperature (Meesters *et al.*, 2003; Qureshi and Zubair, 2006). Heat rejection is accomplished primarily by evaporation of a portion of the cooling water and cooling towers are designed to optimise air-water contact (Choi *et al.*, 2002; Qureshi and Zubair, 2006).

The tower can be a crossflow design so that air and water is mixed at a 90° angle or a counterflow design tower that allows vertically falling water to mix with vertically rising cooling air at an angle of 180° (Beyer, 1993). Drift eliminators at the top minimize the amount of water loss (called drift) with the existing air stream. Generally crossflow and counterflow cooling towers have a similar drift loss. Return water goes past a blow down valve, which allows water to be taken out of cooling system as required or is sent to the heat exchanger. Water recirculates to the top of the tower to meet fanned rising air and loose heat by evaporation. The circulated water falls down into the basin, situated at the bottom of the cooling tower (Makkinejad, 2001). The term cycles of concentration and implications in cooling tower operation is explained in section 2.3 (page 6).

The aim of this chapter was to determine the influence of the external operating parameters within a lab-scale cooling tower, by using synthetic Primary Column Bottoms effluent as cooling water. The objectives were to:

(i) determine physico-chemical characteristics of the cooling water and determine the COD removal.

(ii) determine the fouling, scaling and corrosion rates of mild steel and stainless steel corrosion coupons and heat exchanger tubes.

(iii) determine the effects of the operational conditions (cycles of concentration and linear flow velocity) on the parameters mentioned in ii.

4.2 Materials and methods

4.2.1 Cooling tower design and operation

A lab-scale mini cooling tower test rig (Nucleus Engineering, Durban, South Africa) were operated while being fed with synthetic Primary Column Bottoms (Figure 4.1). The purpose of the test rig is to simulate, as closely as possible, a full size factory heating and cooling system under the following operational conditions: linear flow velocities of 0.6, 0.9, 1.2 m/s and 2, 3 and 4 cycles of concentration. The pH was kept at 8.0 - 8.3. These parameters were commisioned by Sasol.

By using the lab-scale mini cooling tower test rig experimental design (PVC tubing with an internal diameter of 18cm), process water starts in a basin next to the cooling system. The water is pumped through a heat exchanger, recirculates through the system passing the corrosion coupons and biocells, falling down the plastic tower filled with packing material and onto the glass microscope slides.

The lab-scale cooling tower contains 2 coupon racks each containing 3 mild steel and 3 stainless steel corrosion coupons of 74.0mm x 11.5mm x 1.6mm. Four mild steel and 4 stainless steel heat exchanger tubes (length: 750mm, outer diameter: 10mm, wall thickness: 1mm) were fitted within the heat exchanger. The biocell is a 30cm PVC (polyvinyl chloride) pipe with an internal diameter of 12mm. The first 4cm of the biocell is the stagnant area and is used to establish linear flow, the rest (26cm) thereafter is pre-scored in units of 2cm each which are the biocell test units used for the conventional microbiological techniques. The cooling tower has a total volume of 11.5L and a sump volume of 9.5L.

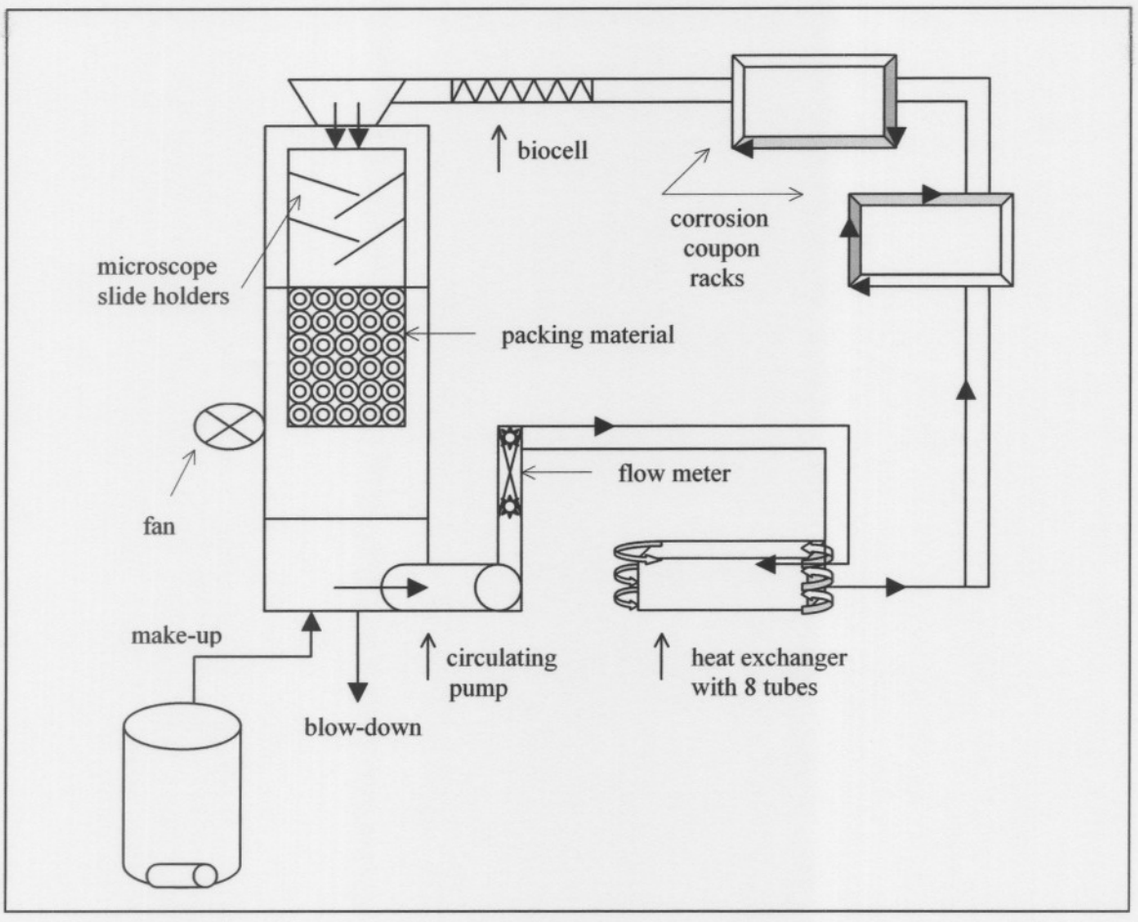

Figure 4.1: Schematic representation of the lab-scale cooling tower.

Operation of the cooling tower lasted several months which included experimental runs of 5 weeks each where the biocells, corrosion coupons and heat exchanger tubes were analysed for fouling, scaling and corrosion. The lab-scale cooling tower were operated at a ΔT of 10°C, heat exchanger block temperature <60°C and a sump temperature not exceeding 35°C. The aluminium block temperature was controlled by trial and error until the correct outlet temperature was reached. The PVC biocells, 8 heat exchanger tubes as well as 6 corrosion coupons were cleaned, weighed, and inserted.

The PVC cooling tower was filled with packing material and glass microscope slides were installed above the packing material (Figure 4.1). The packing material was 25mm Pall V-rings made of polypropylene with a surface area of $1m^3$ each (Mass and Heat Transfer Technology (Pty) Ltd, Roodepoort, South Africa). A fan situated on the side of the cooling tower sump supplied the cooling air. The sump level is maintained

by a floating level switch, installed on the inside of the sump. For the completion of a single experimental run, the cooling tower was operated continuously for 5 weeks.
After completion of the experimental run, the biocells, mild steel and stainless steel (316L) corrosion coupons as well as heat exchanger tubes (10mm OD, mild steel and stainless steel) were removed and studied. Biofilm obtained from the biocells were analysed by PLFA and DGGE techniques. Conventional microbial techniques and routine analyses on the blow down and make-up water were also performed. Heat exchanger tubes were cleaned and re-weighed. Community morphology of microbial growth on the microscope slides (scanning electron microscopy) was studied. The functional and structural diversity of the planktonic phase, as well as the biofilm obtained from the biocells were studied accordingly.

4.2.2 Acid water preparation, stabilising the water and pH control

Synthetic make-up water similar to the Primary Column Bottoms produced at Sasol's Fischer-Tropsch gas-to-liquid conversion process was prepared, with an average pH of 3.7. Due to the fact that the Primary Column Bottoms primarily consists of fatty acids, the make-up water will be very corrosive. Therefore the water has to be chemically corrected before used as make-up water, by making use of a 'water cycle' computer model (Buckman Laboratories). The water was stabilised by adding sodium hydroxide as the cooling water within the cooling recirculates. A pH probe was installed in the sump of the cooling tower that is connected to the pH controller as well as two peristaltic pumps. The pH probe continuously measures the pH of the sump water. When the pH increases or decreases between the two set points (8.0 and 8.3) the acid (10% H_2SO_4) or the caustic (10% NaOH) pump is energized, maintaining the pH between the two set points

4.2.3 Routine analyses on the make-up and blow down water: COD, total suspended and dissolved solids

Water quality parameters that were measured daily include pH, conductivity, dissolved oxygen and redox potential as well as cycles of concentration. The chemical oxygen demand (COD), total suspended solids (TSS) and total dissolved solids (TDS) were analysed twice a week. The COD was determined spectrophotometrically using the 100

- 1500 mg/L method (APHA *et al.*, 1985). It is a parameter that encourages biological activity and increases the demand for biological control chemicals (e.g. chlorination) (EPRI, 2003). The COD can also be seen as the extent to which a substance or mixture serves as a nutrient to bacteria in the water that will cause depletion of the oxygen in the water (DWAF, 2003). The make-up and blow down water were analysed after each experimental run for dissolved Fe, Na, Ca, Mg, PO_4, SO_4, NO_3, NH_4, F, NO_2 and Cl.

Total suspended solids and total dissolved solids were determined gravimetrically according to Standard Methods (APHA *et al.*, 1985). Dissolved oxygen and conductivity were measured once a day in the make-up water as well as in the sump, using a multimeter (WTW, Germany) and various probes. Redox potential was also measured daily by making use of a Metrohm 704 meter (Hanna, USA).

Carbon acts as an energy source as well as a source for cell growth (Schröder and De Haast, 1988; Angell and Urbanic, 2000). In the lab-scale cooling towers the microorganisms use the various short chain fatty acids from the circulating water as a source of carbon for growth and energy. Nitrogen within the system is important for incorporating into growing cells in the formation of proteins, and as a component for nucleic acids (Schröder and De Haast, 1988). Although the Fischer-Tropsch Primary Column Bottoms effluent contains no nitrogen or phosphorous, the C:N:P ratio were not corrected. The reason for not correcting the C:N:P ratio is to use this study as a control study.

4.2.4.1 COD (Chemical oxygen demand) Speqtroquant 100 – 1500 mg/L method

To a clean cell was added 3 ml of solution A and 2.3 ml of solution B. This reaction cell was then filled with 3.0 ml of the sample solution and heated in a thermoreactor (CR300, WTW, Labotec) at 148 °C for 2 hours. The cell was then removed from the heating block and placed in a rack to cool, shaken after 10 minutes, placed back in the rack to cool to 20 ^{0}C - 40 ^{0}C. The COD was then measured spectrophotometrically using Spectroquant, Nova 60 (Merck, Darmstadt, Germany). Potassium hydrogen phthalate (KHP) was used as the COD standard and theoretically has a COD value of 500 mg/L (APHA *et al.*, 1985).

4.2.4.2 Total dissolved solids and total suspended solids

Total dissolved (TDS) and suspended solids (TSS) were determined gravimetrically twice a week (APHA *et al.*, 1985). TDS were used to determine the Langelier Saturation Index of each water sample. TDS is an indication of water quality. As the TDS increases water quality is more likely to decrease (Rafferty, 2000). A Whatman GF/A filter paper (110 mm diameter) was inserted in the filtration apparatus. A vacuum was applied and the paper washed with three successive portions of distilled water. The filter paper was then dried in a drying oven (104 °C) for 1 hour and cooled in a desiccator to room temperature. The GF/A filter paper was weighed to the nearest 0.0001 g before use. A sample (100 ml) was measured where after the suction began in the filtering apparatus. The filtrate was removed and kept to determine the total dissolved solids at a later stage. The filter paper was then dried in a drying oven (104 °C), cooled in a desiccator and weighed to determine the total suspended solids.

An evaporating dish was dried in an oven, cooled in a desiccator and weighed. A suitable volume of the filtrate that was put aside was transferred into the evaporating dish, dried in an oven (104°C), cooled in a desiccator and weighed. Calculation of TSS can be seen in Appendix A1.

4.2.5 Cleaning of corrosion coupons, heat exchanger tubes and u-bends

The fouling, scaling and corrosion rates of the corrosion coupons and heat exchanger tubes were determined using a modified NACE and ASTM method, optimised by Sasol Research and Development, Sasolburg (ASTM, 1999c). The heat exchanger tubes, corrosion coupons and u-bends were rinsed with acetone to remove any oil and grease from the surface and then weighed (weight 1) before using them in the cooling tower. Dry lubricant (Teflon) was sprayed to the outer surface of the mild steel and stainless steel heat exchanger tubes to allow easy removal after each experimental run. After each experimental run of 30 days the coupons were dried at 104°C for 2 hours, the tubes for 24 hours at 104°C and weighed (weight 2) to determine the fouling rate. Mild steel and stainless steel coupons and tubes were then washed in 10% sodium hydroxide for 3 minutes and rinsed under running tap water. The coupons (mild steel and stainless steel) were dried for 2 hours and weighed (weight 3) to determine the scaling rate. Mild

steel and stainless steel tubes were dried for 24 hours and weighed (weight 3) to determine the scaling rate. The corrosion coupons and tubes (mild steel) were then washed with an inhibited hydrochloric acid solution for 25 minutes, dried and weighed (weight 4) to determine the corrosion rate. Stainless steel coupons and tubes were washed with 15% citric acid for 2 hours, dried and weighed (weight 4) to determine the corrosion rate.

4.2.6 EDS (Energy dispersive spectrometry) microanalysis

Oven dried corrosion byproducts found on the corrosion coupons were scraped off and analysed to obtain compositional and chemical information about the sample. A powder specimen was fixed onto conductive tape, mounted directly onto the sample stub and coated with a conductive layer of gold/palladium (Tiedt and Pretorius, 2006). The sample was then analysed under a scanning electron microscope, resulting in structural, compositional and chemical information about the sample.

4.2.7 Staistical analyses

Parametric and non-parametric statistical analyses will be performed on all data obtained using Statistica 6 (Stasoft, Inc.). One-way ANOVA, Tukey's honest significant difference test (HSD), Kruskal-Wallis ANOVA and Median test will be used on the parametric or non-parametric data to determine statistical significance between the various samples. Multivariate statistical analyses (principal component analysis and redundancy analysis using Canoco for Windows 4.0, GLW-CPRO) will be used to determine the influence of the operational conditions on the functional, structural and genetic diversity of the planktonic and sessile microbial communities as well as the fouling, scaling and corrosion. This multidisciplinary approach could facilitate the selection and implementation of operational parameters to minimise biofouling, scaling and corrosion during the reuse of process water as industrial cooling water.

4.3 Results and discussion

Table 4.1 indicates the chemical characteristics of the stabilised water used in these experiments, when the experiments were started. The same water was then used as make-up water throughout the 5 week period. Results in Table 4.1 are thus the averages of all the various variables. The calcium and magnesium values in Table 4.1 were used to determine the hardness of the water. According to You *et al.* (1999), calcium and magnesium has an important inhibition effect on corrosion and also an important effect in scale formation. Predictions of fouling, scaling and corrosion rates are made based on the various scaling and corrosion indices. According to the indices (Table 4.3) the make-up water has a tendency to be very corrosive. This is probably due to the low pH of this water (Hodgkiess, 2004).

Table 4.2 indicates the characteristics of the sump water after operating the cooling tower for 5 weeks under the specific COC (cycles of concentration) and linear flow velocity. From Table 4.2 the total alkalinity of the sump water (490.0 mg/l - 1294.50 mg/l) is relative high according to a suggested cooling water standard (You *et al.*, 1999). Changes in ability of the water for fouling, scaling and corrosion is also determined. Thus, scaling and corrosion indices were calculated on the sump water (Table 4.3). Actual fouling, scaling and corrosion rates were measured and then compared to the scaling and corrosion predictions.

Table 4.1: Make-up water sample analysis results.

Parameter	Values				
	Exp 1 2 COC 0.6 m/s	**Exp 2** 3 COC 0.9 m/s	**Exp 3** 2 COC 1.2 m/s	**Exp 4** 4 COC 1,2 m/s	**Exp5** 4 COC 0.6m/s
Hardness, total as $CaCO_3$ mg/l	290.55	311.22	379.32	349.30	332.60
Hardness, calcium as $CaCO_3$ mg/l	99.48	146.09	154.11	123.10	130.70
Hardness, magnesium as $CaCO_3$ mg/l	191.07	165.13	225.21	226.20	201.90
Alkalinity, M as $CaCO_3$ mg/l	0.00	72.00	89.00	74.00	85.00
Alkalinity, Total as $CaCO_3$ mg/l	0.00	112.00	124.50	115.00	124.50
Conductivity, mS/cm at 25°C	0.73	0.72	0.72	0.75	0.71
pH	4.48	5.11	5.47	5.13	5.10
Phosphate, ortho as PO_4 mg/l	0.23	<0.01	<0.01	<0.01	<0.01
Ammonia as NH_4 mg/l	0.07	0.41	0.36	0.18	0.70
Nitrates as NO_3 mg/l	0.04	0.38	2.00	1.14	0.07
Nitrites as NO_2 mg/l	0.01	<0.01	0.87	<0.01	<0.01
Sulfate as SO_4 mg/l	103.55	104.40	106.51	88.81	106.06
Chloride as Cl mg/l	45.38	38.55	37.02	36.96	37.22
Fluoride as F mg/l	8.80	1.06	2.22	0.24	0.86
Iron as Fe mg/l	2.30	1.40	1.80	1.10	8.20

Table 4.2: Cooling tower recirculation water analysis results.

Parameter	Values				
	Exp 1 2 COC 0.6 m/s	**Exp 2** 3 COC 0.9 m/s	**Exp 3** 2 COC 1.2 m/s	**Exp 4** 4 COC 1.2 m/s	**Exp5** 4 COC 0.6m/s
Hardness, total as $CaCO_3$ mg/l	1034.06	1098.89	973.79	1122.93	804.92
Hardness, calcium as $CaCO_3$ mg/l	616.50	399.29	300.21	365.26	420.32
Hardness, magnesium as $CaCO_3$ mg/l	417.56	699.60	673.58	757.67	637.10
Alkalinity, M as $CaCO_3$ mg/l	404.50	415.00	381.50	1020.00	435.00
Alkalinity, Total as $CaCO_3$ mg/l	514.50	526.00	490.00	1294.50	535.00
Conductivity, mS/cm at 25°C	15.50	9.29	2.82	8.36	2.14
PH	10.35	7.54	7.83	8.00	7.23
Phosphate, ortho as PO_4 mg/l	<0.01	<0.01	<0.01	<0.01	<0.01
Ammonia as NH_4 mg/l	0.11	0.32	0.90	0.13	2.67
Nitrates as NO_3 mg/l	8.98	0.60	3.79	<0.10	1.79
Nitrites as NO_2 mg/l	<0.01	<0.01	<0.01	<0.01	<0.01
Sulfate as SO_4 mg/l	10234.58	4814.00	615.98	3046.37	311.62
Chloride as Cl mg/l	114.26	92.60	97.71	258.27	111.16
Fluoride as F mg/l	9.60	4.40	5.84	4.25	4.53
Iron as Fe mg/l	4.10	5.40	6.60	8.50	12.0

The high chlorides (92.60 mg/l - 258.27 mg/l) and SO_4 (311.62 mg/l - 3046.37 mg/l) values within the sump (Table 4.2) could explain the high corrosion rates on the corrosion coupons and heat exchanger tubes (You *et al.*, 1999). The scaling rates of the mild steel corrosion coupons and tubes (Table 4.4) may be due to alkalinity, since alkalinity is the main cause for this operational problem (You *et al.*, 1999). According to the LS index, the sump water from all five experiments had a tendency to be corrosive (Table 4.3). This can be explained by the high alkalinity, chloride and sulphate values that were used to determine the LS value (calculation in Chapter 3).

Table 4.3: The various scaling and corrosion indices of the make-up and sump water after each experimental run.

	RSI	LSI	PSI	LS
Value	**<6 scaling >6 corrosive**	**<0 corrosive >0 scaling**	**<6 scaling >6 corrosive**	**>1.2 pitting**
Exp 1, Make-up	14.65	-5.09	-	-
Exp 1, Sump	1.81	4.27	3.44	0.33
Exp 2, Make-up	9.22	-2.05	6.27	1.46
Exp 2, Sump	5.31	1.11	4.23	2.70
Exp 3, Make-up	8.67	-1.60	6.04	4.00
Exp 3, Sump	4.83	1.50	3.97	4.00
Exp 4, Make-up	9.41	-2.14	6.47	1.26
Exp 4, Sump	3.77	2.11	2.66	3.56
Exp 5, Make-up	9.23	-2.06	6.23	1.31
Exp 5, Sump	5.00	1.12	3.49	0.90

RSI = Ryznar Stability Index, LSI = Langelier Saturation Index,
PSI = Puckorius Scaling Index, LS = Larson Skold index,
Exp 1 = 2 COC, 0.6 m/s, Exp 2 = 3 COC, 0.9 m/s,
Exp 3 = 2 COC, 1.2 m/s, Exp 4 = 4 COC 1.2 m/s,
Exp 5 = 4 COC 0.6 m/s

All four indices indicated the sump water from experiment 1 had a tendency to be more scale forming than corrosive (Table 4.3). This was evident when comparing the scaling

and corrosion rates obtained from the corrosion coupons and heat exchanger tubes (Table 4.4). The water from experiment 2 is light scale forming as well as corrosive (Table 4.3). Experiment 2 had the second highest scaling and corrosion rates (Table 4.4). According to the indices the sump water of experiment 3 is highly corrosive, when in fact this experiment had the least amount of scaling and corrosion (Table 4.4). The same trend occurred in experiment 4, where three of the four indices indicated the water has a tendency to be scale forming (Table 4.3). However, when the scaling and corrosion rates where compared, the corrosion formation on mild steel tubes was 149.48 $mg/dm^2/d$ (Table 4.4). From the indices in Table 4.3 can be concluded that the water from experiment 5 is not only scale forming but also corrosive. This is evident from Table 4.4, where the mild steel tubes from experiment 5 delivered the higest rate of scaling (196.61 $mg/dm^2/d$) and corrosion (0.96 mm/y).

4.3.1 Statistical analyses

When descriptive statistics (Shapiro Wilk's test) were done on the fouling, scaling and corrosion rates, the data appeared to be non-parametric and not normally distributed (Normal–probability plot) (also see Appendix B Figure B1). When both parametric and non-parametric analyses were conducted on these data the results appeared to be similar. Therefore it can be concluded that the data are parametric and normally distributed. Tukey honest significant difference (HSD) was performed on these results to determine the statistical difference between the various samples, indicated by ^{a}, ^{b}, ^{c}, or ^{d}. E.g. coupons that reacted the same, based on their fouling rates, are indicated with an ^{a}. All coupons indicated with e.g. ^{a,b} statistically reacted the same, based on their fouling, scaling or corrosion results. A breakdown and one-way Anova were also conducted on the fouling, scaling and corrosion results to determine the average and standard error values (Table 4.4).

Table 4.4: Average fouling, scaling and corrosion rates of the corrosion coupons and heat exchanger tubes at different COC and linear flow velocities.

	Fouling ($mg/dm^2/d$)	Scaling ($mg/dm^2/d$)	Corrosion (mm/y)
Sasol guideline (Anon, 2007)	**20**	**2**	**0.2**
Exp 1 ssc	1.698 ± 0.806^{a}	0.452 ± 0.136^{a}	$0 \pm 0^{a,b}$
Exp 1 msc	$19.697 \pm 4.260^{a,b}$	1.464 ± 0.175^{a}	$0.104 \pm 0.008^{a,b,c,d}$
Exp 2 ssc	2.458 ± 0.278^{a}	0.079 ± 0.020^{a}	$0 \pm 0^{a,b}$
Exp 2 msc	77.732 ± 3.986^{c}	6.406 ± 0.065^{a}	$0.230 \pm 0.016^{a,b,c,d}$
Exp 3 ssc	1.623 ± 0.429^{a}	0.077 ± 0.043^{a}	$0 \pm 0^{a,b}$
Exp 3 msc	$63.646 \pm 5.140^{b,c}$	10.370 ± 1.397^{a}	$0.201 \pm 0.030^{a,b,c,d}$
Exp 4 ssc	1.855 ± 0.445^{a}	0 ± 0^{a}	$0 \pm 0^{a,b}$
Exp 4 msc	77.976 ± 0.652^{c}	8.067 ± 0.604^{a}	$0.185 \pm 0.002^{a,b,c,d}$
Exp 5 ssc	1.774 ± 0.393^{a}	0.104 ± 0.104^{a}	$0 \pm 0^{a,b}$
Exp 5 msc	86.846 ± 12.144^{c}	5.765 ± 0.314^{a}	$0.252 \pm 0.036^{a,b,c,d}$
Exp 1 sst	0.245 ± 0.211^{a}	1.434 ± 1.045^{a}	0 ± 0^{a}
Exp 1 mst	163.326 ± 17.421^{d}	160.768 ± 19.651^{c}	$0.655 \pm 0.159^{c,d,e}$
Exp 2 sst	3.236 ± 0.851^{a}	1.348 ± 0.369^{a}	0 ± 0^{a}
Exp 2 mst	215.79 ± 20.04^{d}	164.335 ± 24.742^{c}	0.923 ± 0.222^{e}
Exp 3 sst	0.237 ± 0.085^{a}	0.159 ± 0.067^{a}	0 ± 0^{a}
Exp 3 mst	78.412 ± 12.820^{c}	73.020 ± 13.850^{c}	$0.590 \pm 0.145^{b,c,d,e}$
Exp 4 sst	4.676 ± 0.647^{a}	3.143 ± 0.601^{a}	0 ± 0^{a}
Exp 4 mst	149.481 ± 13.120^{d}	150.364 ± 11.613^{c}	$0.727 \pm 0.213^{d,e}$
Exp 5 sst	1.568 ± 0.200^{a}	1.952 ± 0.261^{a}	0.002 ± 0^{a}
Exp 5 mst	$196.048 \pm 16.909^{d,e}$	196.606 ± 16.517^{c}	0.962 ± 0.202^{e}

Exp 1 = 2 COC, 0.6 m/s, Exp 2 = 3 COC, 0.9 m/s, Exp 3 = 2 COC, 1.2 m/s
Exp 4 = 4 COC, 1.2 m/s, Exp 5 = 4 COC, 0.6 m/s, ssc = stainless steel coupon, msc = mild steel coupon, sst = stainless steel heat exchanger tube,
mst = mild steel heat exchanger tube

± Standard error as well as the statistical difference between the various samples, as indicated by [a], [b], [c].

4.3.2 Fouling results

From Table 4.4 it is evident that in all 5 experiments the stainless steel coupons and stainless steel tubes statistically reacted the same when comparing the fouling data (indicated with [a]). The mild steel coupons from experiment 2, 4 and 5 statistically reacted the same (indicated with [c]). Thus experiment 2, 4 and 5 that were operated at higher cycles of concentration (3 and 4 COC) reacted the same to this operating parameter (cycles of concentration). As the linear flow velocity changed during the different experiments, the fouling results also differed from each other when comparing the statistical significance. Operating the cooling tower at low linear flow velocities

(0.6 m/s and 0.9 m/s) during experiment 2 and 5, resulted in high fouling rates (77.732 $mg/dm^2/d$ and 86.846 $mg/dm^2/d$) on the mild steel coupons (Table 4.4). High fouling rates also occurred on stainless steel coupons during experiment 2 and 5 (2.458 $mg/dm^2/d$ and 1.744 $mg/dm^2/d$). However, these fouling rates on stainless steel coupons are within the Sasol guideline (Table 4.4). Thus, by operating a cooling tower at lower water velocities reduces the water quality and therefore enhances the fouling rate (Webb and Wei, 2000). Fouling rates of the stainless steel heat exchanger tubes are within the Sasol guideline during all 5 experiments (Table 4.4).

From Table 4.4 it is evident that experiments 1 and 3 had low fouling rates on their stainless steel coupons (1.698 $mg/dm^2/d$ and 1.623 $mg/dm^2/d$) as well as low values on stainless steel tubes (0.245 $mg/dm^2/d$ and 0.237 $mg/dm^2/d$). Thus operating the cooling tower at lower cycles of concentration (2 COC), results in lower fouling rates (Table 4.4). When comparing the fouling results of the stainless steel coupons from experiment 2, 4 and 5 (operated at higher COC), the fouling rates were significantly higher (Table 4.4). The various fouling rates of the mild steel coupons and tubes are not within the Sasol guideline (Table 4.4).

4.3.3 Scaling results

Mild steel and stainless coupons statistically reacted the same (Table 4.4), when comparing the scaling results (indicated with ^{a}). Scaling rates on the mild steel tubes statistically reacted the same (indicated with ^{c}), during all 5 experiments (Table 4.4). Stainless steel tubes also statistically reacted the same (indicated with ^{a}), based on their scaling results. From Table 4.4 it is evident that the stainless steel corrosion coupons from experiment 3 and 4 attained the lowest scaling rates (0.077 $mg/dm^2/d$ and 0 $mg/dm^2/d$). Therefore, by operating a cooling tower at a high linear flow velocity results in minimal scaling (Videla, 2000). Experiment 1 and 3 had the lowest scaling rates (1.434 $mg/dm^2/d$ and 0.159) on stainless steel tubes (Table 4.4). Scaling rate of the stainless steel tubes operated at high cycles of concentration (4 COC) resulted in the highest scaling rate (3.143 $mg/dm^2/d$). It can therefore be concluded that high cycles of concentration results in increased scaling rates (You *et al.*, 1999; EPRI, 2003). Scaling results of both mild steel coupons and tubes are not within the Sasol guideline (Table 4.4). Stainless steel tubes from experiment 4, were the only tubes that were not within

the Sasol guideline for scaling. This could be due to operation at high cycles of concentration.

4.3.4 Corrosion results

From Table 4.4 it is evident that the mild steel coupons from all 5 experiments statistically reacted the same when comparing their corrosion results (indicated with [a],[b],[c],[d]). Corrosion rates of the stainless steel coupons also reacted similar during this study (indicated with [a],[b]). Experiment 1, 2 and 5 were operated at low linear flow and resulted in high corrosion rates when studying the mild steel tubes (Table 4.4). Low flow velocities enhance the formation of deposits and therefore increase corrosion rates (Anon, 1994; Videla, 2002).

Relative low corrosion rates (0.104 mg/dm^2/d and 0.201 mg/dm^2/d) occurred on mild steel coupons during experiment 1 and 3 (Table 4.4). Therefore by operating the cooling tower at low cycles of concentration (2 COC) results in minimal corrosion (You *et al.*, 1999; EPRI, 2003). Corrosion rates of stainless steel coupons and tubes were within the Sasol guideline (Table 4.4).

From Table 4.4 it is evident that the worst corrosion rates from the mild steel coupons and tubes were from experiment 2 (3 COC and 0.9 m/s) and experiment 5 (4 COC and 0.6 m/s). Fouling, scaling and corrosion are normally interrelated and do not occur independently of one another (Allain *et al.*, 1998). Therefore, fouling rates on mild steel coupons of experiment 2 and 5 were also exceptionally high (77.732 mg/dm^2/d and 86.846 mg/dm^2/d).

4.3.5 COD in the cooling system

From Table 4.5 it is evident that the COD of the make-up water was kept constant throughout the experiments. The COD values of the make-up ranged between 300.13 mg/L and 441.11 mg/L. The COD values of the sump water were between 596.56 mg/L and 1042 mg/L (Table 4.5) and concentrated when make-up water was added to the cooling system.

Table 4.5: Average COD in make-up, COD in sump and % COD removal.

	COD in make-up (mg/L O_2)	COD in sump (mg/L O_2)	% COD removal
Exp 1	441.11 ± 52.01^{a}	596.56 ± 43.61^{a}	-50.01 ± 21.27^{a}
Exp 2	407.00 ± 46.10^{a}	$790.22 \pm 57.97^{b,c}$	-111.03 ± 24.20^{a}
Exp 3	406.75 ± 23.86^{a}	632.88 ± 32.53^{a}	-58.01 ± 9.74^{a}
Exp 4	351.50 ± 33.57^{a}	1042.0 ± 64.04^{c}	-216.39 ± 33.57^{b}
Exp 5	300.13 ± 9.75^{a}	$898.87 \pm 75.31^{b,c}$	-198.65 ± 22.14^{b}

± Standard error as well as the statistical difference between the various samples, as indicated by ^{a}, ^{b}, ^{c}.

This phenomenon could not be explained. However COD was not removed and therefore the cooling tower can not be used as a bioreactor. Further investigation is needed to resolve the issues surrounding this aspect. use the cooling tower as a bioreactor COD was not removed and therefore the cooling tower can not be used as a bioreactor to remove organic carbon since the bacterial growth weren't capable of utilising the make-up water as nutrients.

4.3.6 Analysis of corrosion products

X-ray microanalysis specifically gives information about the elemental composition of a specimen, in terms of quantity and distribution (Tiedt and Pretorius, 2006) as well as qualitative and semi-quantitative information on the nature of byproducts accumulated on a metal surface (Beech, 2004). EDS analysis was performed on the byproducts obtained from the corrosion coupons and identified the various elements present in each sample at the different operating parameters (linear flow velocity and cycles of concentration). More or less the same elements were found in all five experiments except for Al or Mg that were absent in some experiments (Table 4.6). The composition of each sample was determined through a quantitative analysis and used to compare the amount of iron found in that sample. Iron was present in all five experiments, with experiment 1, 2 and 5 having slightly higher iron content. In a study done on SRB induced corrosion (Abedi *et al.*, 2006), the main elements found in the corrosion product was C, O, Si, S and Al which was also observed through EDS-SEM analysis. The same elements are recongnised in the different corrosion product samples (Table 4.6) except for S content that differs and is probably related to SRB activity (Abedi *et al.*, 2006).

Table 4.6: EDS elemental analysis of the corrosion products on the external surface of the mild steel corrosion coupons.

	Elements present	% FeO
Exp 1	C, Al, Na, Si, S, Ca, Fe, O	56.15
Exp 2	C, Mg, Na, Si, S, Ca, Fe, O	54.87
Exp 3	C, Al, Mg, Na, Si, S, Ca, Fe, O	42.33
Exp 4	C, Mg, Na, Si, S, Ca, Fe, O	29.12
Exp 5	C, Mg, Na, Si, S, Ca, Fe, O	45.62

The EDS analysis conducted on the microscope slides from the cooling tower during experiment 2 and 3 (Appendix A Table A1) showed that the crystal formation was possibly $CaCO_3$ scaling (Casademont *et al.*, 2006; Li *et al.*, 2006). Precipitation of scale forming salts (calcium carbonate or calcium sulphate) occurs when solubilities are exceeded because of high concentrations or increased temperatures (Videla, 2002; Brink *et al.*, 2004; Hodgkiess, 2004). One of the corrosion products is $FeCO_3$ and is attended by a suitable alkaline pH (8.0 - 8.3) for the absorption of CO_2. The circulating water within the cooling tower contained various compounds such as hydroxide, carbonate and bicarbonate (Table 4.2). The recognition of $FeCO_3$ and iron oxide (Table 4.6) on the external surface of the corrosion coupons also indicates the existence of carbonate and bicarbonate environment (Abedi *et al.*, 2006).

4.3.7 Redundancy analysis

A RDA (redundancy analysis) graph (Figure 4.2) indicates the similarity between samples, variation in data as well as the correlation between different variables. The clustering effect or distance between the samples indicates similarity. Variables or species are represented by arrows. The shorter the arrow the smaller the variation. Long arrows tend to matter most since the length of the arrow also indicates the slope of response. Direction of the arrow indicatices the direction of maximum change. Angles between arrows indicate correlation, acute angles indicate high positive correlation. Angle of $\pm$ 180° is indicative of a negative correlation and an angle $\geq$ 90° is indicative of no correlation. An angle smaller than 90° indicates a positive correlation between variables. Relation between samples and variables shows the relative ranking of each sample to each variable.

From the redundancy analysis (Figure 4.2) the variables corresponding to the respective axes, as well as correlations between the species and environmental variables can be made. Environmental variables are corrosion rate, imbalance, redox, conductivity and dissolved oxygen of the make-up (m) and sump (s) water. Fouling, scaling and corrosion rates of the mild steel and stainless steel corrosion coupons and heat exchanger tubes were used as species data in the redundancy analysis (Figure 4.2).

According to the statistical summary of this RDA, the cycles of concentration and linear flow velocity are the environmental variables that correspond the most with the respective axes (Figure 4.2). Cycles of concentration is the first axis and have the biggest influence, followed by linear flow velocity being the second axis. The x-axis represented cycles of concentration and linear flow velocity was represented by the y-axis. This is clearly seen when comparing the positions where the various experiments are situated (Figure 4.2). Experiment 1 and 3 (low COC) are situaded on the left half (Figure 4.2) and experiment 2, 4 and 5 (operated at high COC) are situated on the right half. Operation at low linear flow velocities (experiment 1 and 5) are postioned in the upper half in Figure 4.2, with the higher flow velocities (experiment 4 and 5) situated at the bottom.

When correlations between the species and environmental variables are compared, the species data that have the biggest influence is conductivity of the sump water (Figure 4.2). It can also be seen that cycles of concentration have a positive correlation on dissolved oxygen and conductivity (indicated by an angle $< 90°$). Linear flow velocity affects dissolved oxygen, corrosion rate and as well as conductivity (Figure 4.2). From Figure 4.2 can be seen that cycles of concentration has a positive correlation ($< 90°$) on the tubes of mild steel and stainless steel fouling, scaling and corrosion rates. Thus, increased cycles of concentration will result in high fouling, scaling and corrosion rates. Cycles of concentration has no correlatation on corrosion of stainless steel coupons but do affect the fouling and scaling rate of stainless steel coupons (Figure 4.2). Figure 4.2 indicates that linear flow velocity has a positive correlation on mild steel fouling, scaling and corrosion coupon results. Thus, as linear flow velocity decreases, fouling, scaling and corrosion rates on mild steel tubes will increase (indicated by the direction of the arrows). However, no correlation exists between linear flow velocity and fouling,

scaling and corrosion rates of stainless steel coupons or stainless steel tubes (angle $\geq$ 90°).

According to the eigenvalues from the RDA log file, 40.5% of the variance was due to cycles of concentration and 26% due to linear flow velocity. Thus, the cumulative percentage variance of the species data being 66.5%. Meaning that fouling, scaling and corrosion caused the high variation in the data. The statistical summary indicates that the inflation factor of this analysis is <6 and should normally be kept below 20 to ensure that the variables aren't to closely plotted to each other. According to the Monte Carlo test, the test of significance of first the canonical axis has a p-value of 0.002 and the test of significance of all canonical axes has a p-value of 0.002. This summarises that there is a statistical significance ($p \leq 0.05$) between the various environmental variables and species data.

In Figure 4.2 groupings of the various experiments were also observed. Experiments operated at high cycles of concentrations (3 and 4) grouped together and experiments operated at high linear flow velocities (1.2 m/s) had similar locations. Cycles of concentration had a positive correlation on the fouling, scaling and corrosion rates of mild steel and stainless steel tubes. Thus further increase of cycles of concentration will result in higher fouling, scaling and corrosion rates. Cycles of concentration had no effect on corrosion of stainless steel coupons but did affect the fouling and scaling rate of stainless steel coupons. Linear flow velocity had a positive effect on mild steel fouling, scaling and corrosion coupon results. Thus a decrease in linear flow velocity will cause an increase in fouling, scaling and corrosion rates on mild steel tubes. However, no correlation existed between linear flow velocity and fouling, scaling and corrosion rates of stainless steel coupons or stainless steel tubes.

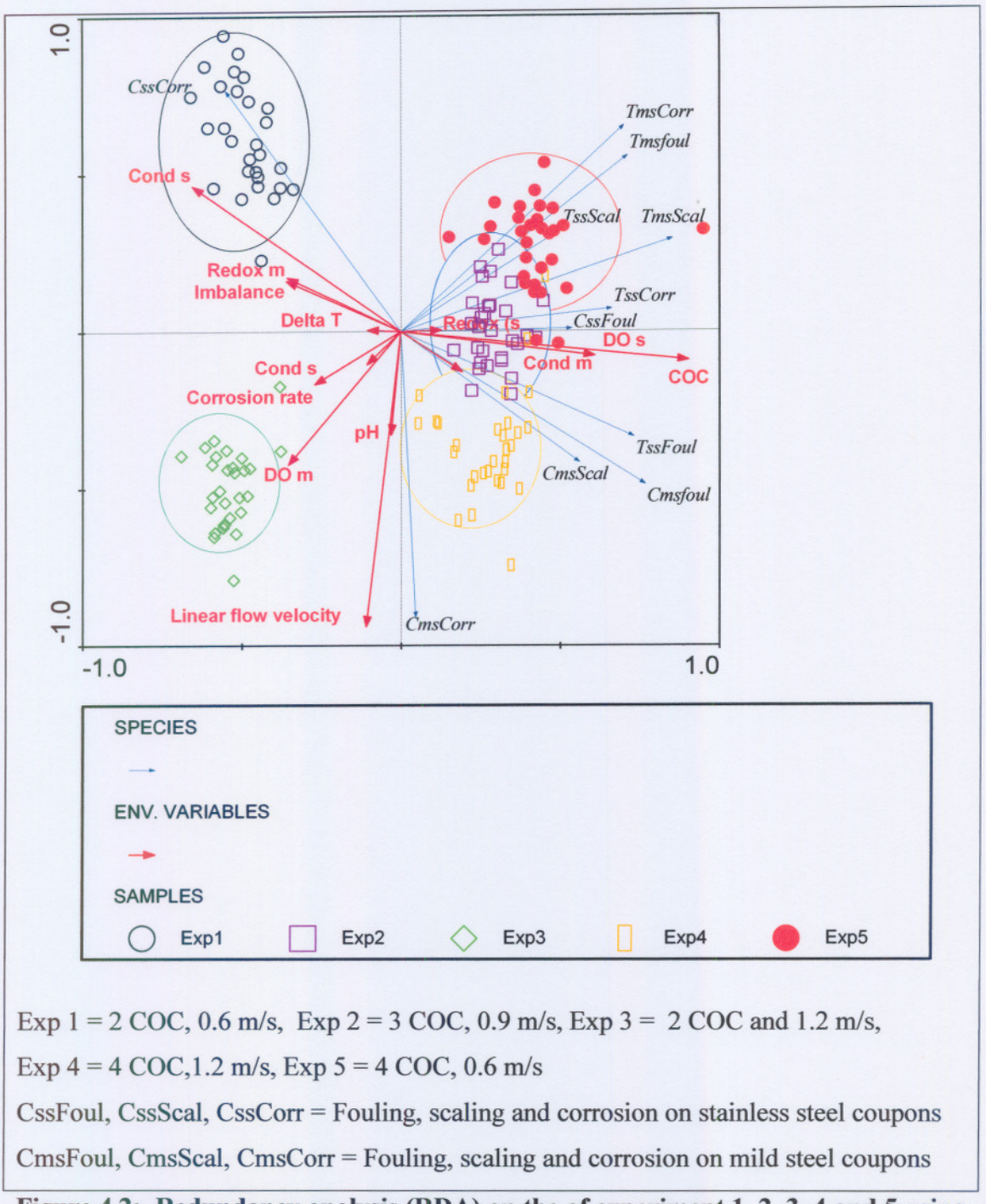

Exp 1 = 2 COC, 0.6 m/s, Exp 2 = 3 COC, 0.9 m/s, Exp 3 = 2 COC and 1.2 m/s,

Exp 4 = 4 COC,1.2 m/s, Exp 5 = 4 COC, 0.6 m/s

CssFoul, CssScal, CssCorr = Fouling, scaling and corrosion on stainless steel coupons

CmsFoul, CmsScal, CmsCorr = Fouling, scaling and corrosion on mild steel coupons

Figure 4.2: Redundancy analysis (RDA) on the of experiment 1, 2, 3, 4 and 5 using external operating parameters.

4.4 Conclusion

Chemical characteristics of the make-up as well as stabilised sump water were analysed. These analyses were used to make predictions of fouling, scaling and corrosion rates by using various scaling and corrosion indices. Actual fouling, scaling and corrosion rates were measured and then compared to the original predictions. Predictions made by scaling and corrosion indices indicated that the sump water was in general less corrosive and scale forming when compared to predictions made on the make-up water. This was evident when comparing the corrosion rates to the scaling rates obtained during the 5 experiments. Actual scaling rates were much higher than corrosion results. It can therefore be concluded that by stabilising the circulating water within the cooling tower less corrosion occured (Gebbie, 2000).

Operating the cooling tower at low linear flow velocities (0.6 m/s and 0.9 m/) resulted in high fouling rates on the mild steel as well as stainless steel corrosion coupons. These fouling rates on stainless steel coupons and tubes are within the Sasol guideline, not exceeding the recommended 20 $mg/dm^2/d$. Experiments operated at high cycles of concentration resulted in high fouling rates. Fouling affects thermal performance, which reduces cooling tower effectiveness and tower capability with time (Qureshi and Zubair, 2006). This was observed during the operation of the lab-scale cooling tower when the ΔT and the heat transfer within the cooling tower decreased. Operating the cooling tower at high linear flow velocity results in minimal scaling. High cycles of concentration resulted in increased scaling rates. Stainless steel tubes from experiment 4, being the only tubes not within the Sasol guideline for scaling, due to operation at high cycles of concentration.

Experiments operated at low linear flow resulted in high corrosion rates on mild steel tubes. Operation at low cycles of concentration resulted in minimal corrosion. Corrosion rates of stainless steel coupons and tubes are within the Sasol guideline. Limiting the cycles of concentration in the circulated water will lower the precipitation risks (scaling), while water with a high initial solids can only be cycled a limited amount before precipitation or scaling occurs (Brás Pereira *et al.*, 1997).

Percentage COD removal in all five experiments had negative values, as the COD in the sump water concentrated. Thus, COD was not removed and the cooling tower can not be used as a bioreactor.

RDA analyses illustrated that cycles of concentration and linear flow velocity as operating parameter had a significant effect ($p>0.05$) on fouling, scaling and corrosion rates where positive and negative correlations observed. When using corrosion coupons and heat exchanger tubes, the cooling tower should be operated at low cycles of concentration and a high linear flow velocity in order to minimise fouling, scaling and corrosion.

CHAPTER 5

Structural and functional diversity of planktonic and sessile community: conventional methods, microscopy, PLFA and DGGE

5.1 Introduction

The application of conventional microbiological techniques for the characterisation of microbial communities is limited. Only one percent of microorganisms are culturable using conventional microbiological techniques (Ward *et al.*, 1990; Amann *et al.*, 1995; Hugenholtz *et al.*, 1998). Pre-culture isolation and enumeration techniques such as heterotrophic plate counts only detect an unknown fraction of the culturable microorganisms (Sartory and Watkins, 1999; Van der Kooij *et al.*, 2003). These methods are therefore not well suited for the estimation of the total viable biomass of the microbial community structure in industrial and environmental samples. Most of the classical techniques are dependent on the growth of the microbial population, selection occurs against many environmental organisms. Conclusions made solely on the basis of planktonic microbial counts may be incorrect as the planktonic population does not reflect the total number and type of organisms living in the biofilm (Videla, 2002; Meyer, 2003).

Development of these alternative approaches includes molecular techniques which allow the successful *in situ* analysis of the functional, structural and genetic diversity of the microbial community in environmental samples resulting in distinguishable fingerprints (Wuertz *et al.*, 2003). Molecular methods are more progressively being used for the identification of environmental organisms (Camper *et al.*, 1999) without relying on cultivation on selective or non-selective media (Wobus *et al.*, 2003). These methods could thus be used to study the diversity and structure of microbial communities in the planktonic and sessile phases of cooling tower waters.

5.1.1 Conventional methods

The plate count and most probable number (MPN) technique are two techniques used as a direct analysis for the determination of viable counts in industrial water systems (Sartory and Watkins, 1999). Total plate counts have traditionally been used for

determining planktonic counts in the bulk phase with the advantage of obtaining quantitative values of bacterial activity (Palazzo and Allison, 2004). A culture media that is selective for the certain physiological groups found in the wastewater system should be used to favour the growth of the desired microorganisms (Stams and Oude Elferink, 1997). Culture conditions similar to the environmental conditions of the cooling system should also be accounted for (e.g. temperature, pH and oxygen and nutrients), which could influence the numbers and type of microorganisms that will grow on the culture media. The plate count method is based on the assumption that the original inoculum is homogeneous and that each bacterium grows and divides to produce a single colony (Csuros and Csuros, 1999 *et al.*, 1999). Saboraud media are used for plating and enumeration of yeast and fungi. *Pseudomonas* sp. are enumerated on King's B and Cetrimide agar and total aerobic heterotrophic bacteria on R2A-agar (Lutterbach and De França, 1997). MPN method gives quantitative insight and uses dilution and statistical analyses for the determination of the viable microorganisms found in the waste water (Stams and Oude Elferink, 1997). Rao *et al.* (2000) monitored iron reducing bacteria, sulphate reducing bacteria (SRB) as well as anaerobic bacteria within cooling water using the MPN technique. SRB are normally assayed using Postgate's medium (Jain, 1995; Rao *et al.*, 2000; Stilinovic and Hrenovic, 2004). For quantification of anaerobic bacteria, thioglycollate culture medium are used (Lutterbach and De França, 1997). B10 nutrient broth are used as culture medium for quantification of iron reducing bacteria (Csuros and Csuros, 1999).

5.1.2 Scanning electron microscopy

Other than conventional methods, direct microscopy is traditionally used to study biofilms as well as environmental bacteria *in situ* (Camper *et al.*, 1999). By making use of a scanning electron microscope, biofilm can be studied as a three-dimensional specimen that provides information on the existence of extracellular polymers, development of the biofilm as well as their spatial relationship to substrata (Ray and Little, 2003; Wobus *et al.*, 2003). SEM can be used as a semi quantitative technique to provide visual impressions of bacteria on a surface (Hilbert *et al.*, 2003). Microscopy techniques can be used to study the development, organisation and structure of biofilms that gave detailed images of the biofilm (Hidalgo and García-Encina, 2002). Biofilms are non-conducting samples and must therefore be dehydrated, by coating with a

conductive film of metal before viewing the specimen (Ray and Little, 2003; Tiedt and Pretorius, 2006). Industrial ecosystems that were examined by microscopic methods have shown that most of the bacteria in aquatic systems grow in biofilms attached to available surfaces (Ray and Little, 2003).

5.1.3 Phospholipid fatty acids

Community structure and biomass can be quantified by making use of phospholipid fatty acid (PLFA) analyses (Ibekwe *et al.*, 2002). Direct lipid extracts through PLFA analysis from a biofilm sample may detect changes in microbial community structure (Kozdrój and Van Elsas, 2001). PLFA analyses are not capable of identifying microorganisms at species or strain level but are able to produce descriptions of microbial communities based on functional groupings of fatty acid profiles (Ibekwe *et al.*, 2002). These fatty acid profiles are indicative of prokaryotic and eukaryotic taxa (Ibekwe *et al.*, 2002). PLFA analysis can also indicate microbial physiological status by analysis of stress indicators and represents all microbial biomass, indicating active living microbial components (Kehrmeyer *et al.*, 1996; Ibekwe *et al.*, 2002).

5.1.4 Denaturing gradient gel electrophoresis

DGGE is a culture independent method used to study the diversity of natural microbial populations by separating fragments of DNA which have the same size but different sequences (Ranjard *et al.*, 2000; Kisand and Wikner, 2003). Differences in melting behaviour are also associated with differences in nucleotide composition of the fragments (Muyzer *et al.*, 1993; Teske *et al.*, 1996). The strategy for genetic fingerprinting using this technique consists of the extraction of nucleic acids (DNA and RNA), followed by the amplification of the genes encoding the 16S rRNA and 18S rRNA as well as the analysis of the PCR products using the DGGE technique (Muyzer, 1999). Amplified samples with different sequences are separated during electrophoretic migration and DGGE profiles provide the comparison of the diversity of the microbial community and also for the monitoring of population dynamics (Brandt *et al.*, 2004).

The objective of a DNA profiling technique is to give an overall pattern of the structural changes within the microbial community (Cocolin *et al.*, 2003). DNA profiles of whole microbial communities are generated in single electrophoretic tracks and can be analysed using indexes adapted from phylogenetic and ecological studies (Ampe and Miambi, 2000). The dynamics of individual bands on a DGGE gel are units (melting types) that are used to monitor these microbial community structural changes. These melting types could be indicative of species diversity within the microbial population and the bands could be reanalysed and sequenced to determine the identity of the organisms it represents (Kisand and Wikner, 2003). Information obtained from this fingerprint includes interspecies relationship as well as abundance (based on band intensity variation over time).

5.1.5 Aim and objectives

The aim of this chapter was to evaluate the structural and functional diversity of planktonic and sessile (biofilm) communities by using culture independent methods. The objectives were to:

(i) use selective plating and MPN methods to determine the levels of heterotrophic plate counts, *Pseudomonas*, yeast and fungi, SRB, IRB and anaerobic bacteria.

(ii) observe the morphological changes within the microbial community using SEM.

(iii) use PLFA in order to quantify community structure and biomass.

(iv) use DGGE to compare the diversity of the microbial community and to monitor population dynamics.

5.2 Materials and methods

5.2.1 Conventional microbiological techniques

5.2.1.1 Spread plate technique

Various agar media were prepared and used as the culture media for the microorganisms from the cooling system. The agar media were melted in an autoclave at 121 °C for 15 minutes and cooled to 45 to 47 °C (to prevent condensation in the petriplates). The

sessile phase represents the biofilm found in the biocells and the planktonic phase represents the microorganisms in the circulating water. The biocell sections assigned for the conventional technique were aseptically scrapped off using a sterile spatula and transferred into a sterile saline solution to prepare a dilution series. An inoculum of 0.1 ml was added to the surface of the agar and spread uniformly. An incubation period for at least 24 hours was allowed for growth of the colonies. Only the plates with 30 to 300 colonies were counted. The original inoculum was diluted to ensure that the counts are within this range (Csuros and Csuros, 1999).

Plate count methods were used to determine counts of *Pseudomonas*, yeast and fungi as well as total aerobic heterotrophic bacteria. King's B medium as well as Cetrimide agar were used for culturing of *Pseudomonas* and were incubated at 37°C for 5 days (Lutterbach and De França, 1997). Yeast and fungi were grown on Saboraud medium and incubated at 25°C for 7 days (Lutterbach and De França, 1997). Total aerobic heterotrophic bacteria were cultured on R2A-agar (Lutterbach and De França, 1997).

5.2.1.2 Most probable number (MPN) method

In this statistical estimating method the greater the number of bacteria in a sample, the more dilution is needed to reduce the density of the bacteria to reach a point of extinction (Csuros and Csuros, 1999). Therefore, replicate dilutions were made to obtain the most probable number of viable organisms. The microorganisms attached to the biocells were aseptically scrapped off using a sterile spatula and transferred into a sterile saline solution to prepare a dilution series. The dilutions of the samples were inoculated into liquid tube media. A positive MPN test can be indicated by growth and fermentative gas production and bacterial densities are based on positive and negative tube results obtained from an MPN table (Csuros and Csuros, 1999). The MPN method was used to culture the sulphate reducing bacteria (SRB), iron reducing bacteria as well as the total anaerobic bacteria on different growth media (broth) (Lutterbach and De França, 1997). Modified Postgate medium B was used for SRB growth, B10 broth for the iron reducing bacteria and Thioglycolate medium (Difco) for cultivation of the total anaerobic bacteria (Jain, 1995; Lutterbach and De França, 1997). All growth media were incubated at 37°C for 5 days, except for the Thioglycolate media that was

incubated at 32°C for 28 days under anaerobic conditions (Lutterbach and De França, 1997).

5.2.2 Scanning electron microscopy (SEM)

The microscope slides from the tower (planktonic phase) as well as the biocells (sessile phase) were analysed through SEM (Tiedt and Pretorius, 2006). The microscope slides and biocells were fixed (70% ethanol) and dehydrated through a graded series of acetone solutions (70%, 80%, 90% and 100% x 2) at intervals of 15 minutes each. The samples were then critical point dried and coated with gold/palladium (Ray and Little, 2003). The SEM micrographs were then taken with a scanning electron microscope.

5.2.3 Phospholipid fatty acids (PLFA)

5.2.3.1 Sample preparation of PLFA

Biofilm was scraped with a sterile spatula from the biocells and transferred to a sterile Falcon tube. In the case of the planktonic samples, 50 ml from the sump water of the lab scale cooling tower were transferred to 50 ml sterile Falcon tubes. These biofilm and planktonic samples were then frozen and stored at -60°C until lyophilisation.

5.2.3.2 Lipid extraction

Extraction was performed using a Bligh and Dyer (1959) lipid extraction method as modified by White and Ringelberg, (1998). After lyophilisation the dry mass of the samples was determined and transferred to 50 ml red-capped test tubes. Four millimeter of phosphate buffer (50mM, pH 7.5), 10 ml methanol and 5 ml chloroform were added to the lyophilised samples in the centrifuge tubes. The samples were then sonicated for 2 minutes and vortexed for 30 seconds. After 2 hours each sample were centrifuged at 1800 rpm for 15 minutes. The liquid phase (top layer) was then decanted into a 50 ml red-capped centrifuge tube. Chloroform (5 ml) was added to the original tube and vortexed for 30 seconds and centrifuged at 1800 rpm for 15 minutes. The chloroform was then pooled into the (second) centrifuge tube. Nano-pure water, 5 ml, was added to the decanted liquid, shaken and left for 18 hours or until the aqueous (upper) phase was no longer cloudy. After the phases had separated, the samples were centrifuged at 1800 rpm for 15 minutes. A Pasteur pipette was used to transfer the bottom phase into a 15

ml Kimax tube. The samples were then dried under a stream of nitrogen with a very low flow and stored at -20°C until further use.

5.2.3.3 Selective extraction of hydrocarbons

Hexane:chloroform (4:1) and 2 ml nano-pure water were added to the glass tubes with the dried samples from the lipid extraction stage. The samples were then vortexed and centrifuged at 2000 rpm for 5 minutes. The organic upper phase was then transferred to another Kimax tube. These steps for the selective extraction of hydrocarbons were repeated to recover a volume of 6 ml. These samples were then dried under a gentle stream of nitrogen and stored at -20 °C until silicic acid fractionation (White and Ringelberg, 1998).

5.2.3.4 Lipid fractionation

Kimax tubes containing 0.5 g silicic acid were dried at105°C (2h) and allowed to cool in a desiccator. Five milliliter chloroform was added to the silicic acid tube. A fractionation column with a glass wool plug was packed with the activated silicic acid and chloroform using a Pasteur pipette. The silicic acid column was then flushed with 5 ml acetone and 5 ml chloroform, respectively. The lipid sample was then re-dissolved in 100 µl chloroform and transferred to the silicic acid column using a solvent rinsed glass syringe. This step was repeated three times to ensure that the entire lipid sample was transferred into the silicic acid column (White and Ringelberg, 1998). The neutral fatty acid fraction, glycolipids and the phospholipids were eluted into 15 ml glass screw-cap tubes with 5ml chloroform, 5 ml acetone and 10 ml methanol. These samples containing the lipid fractions were then dried under a gentle stream of nitrogen and stored at -20 °C.

5.2.3.5 Fatty acid methyl ester (FAME) preparation

Chloroform and methanol (0.5 ml each) as well as 1 ml methonolic KOH (0.28 g KOH in 20 ml methanol) were added to the 15 ml Kimax tubes containing the lipid fractions. The sample was then vortexed for 30 seconds, incubated at 60 °C for 30 minutes and allowed to cool. Hexane (2 ml), 200 µl glacial acetic acid (1N) and 2 ml nano-pure

water were added to the sample. Samples were then vortexed for 30 seconds and centrifuged at 2000 rpm for 5 minutes. Upper organic phase was transferred to another Kimax tube. Bottom phase was further extracted by adding 2 ml hexane, vortexing for 30 seconds and centrifuging at 2000 rpm for 5 minutes. This step was repeated three times (White and Ringelberg, 1998). The top phase was transferred into the Kimax tube with the organic phase, dried under a gentle stream of nitrogen and stored at -20°C.

5.2.3.6 GC conditions

Methylated samples were analysed using a Hewlett Packard 6890 II Plus gas chromatograph equipped with a Hewlett Packard 7683 injector, a Hewlett Packard 7683 auto sampler, a flame ionization detector and a SPB-1 column (60 m x 0.25 mm x 25 μm). Temperature was then ramped up to 230°C at 7°C per minute and kept constant at 230°C for 2 minutes. Temperature was again ramped up to 300°C at 10°C per minute and kept constant at 300°C for 3 minutes (Van der Merwe *et al.*, 2002). Inlet and detector temperatures were 230°C and 250°C, respectively. Data were integrated using the HP Chem Station Rev. A.07.02 (682) software.

5.2.3.7 *PLFA data analysis*

The lipid profile data were entered into an Excel spreadsheet and lipid group structure profiles based on the different lipid classes were created. Lipid profiles of the different experiments were represented as bargraphs (Perkiömäki *et al.*, 2003). The fouling, scaling and corrosion data were combined with the lipid data in order to draw a redundancy analysis (RDA) ordination diagram using Canoco. The different samples were compared to each other, based on lipid classes using the Tukey test in Statistica (Stasoft, Inc., Tulsa, OK). The arcsine square root transformation was applied to the mole percent PLFA data. Three different classification algorithms (cluster analysis and two variations of factor analysis) were applied to the data, to ensure the stability of the groups obtained. Hierarchical cluster analysis was performed from the transformed mole percent PLFA using Ward's method. Factor analysis was used as a data reduction method in conjunction with hierarchical cluster analyses to access changes in the community structure. A one way ANOVA was performed on the factor scores and Tukey's honest significant difference test (HSD) was used to identify significant

differences between plots, with the within-experiment family-wise error rate set at p = 0.05 (Araya *et al.*, 2003). The box and whisker plots of the results were generated with a 95% confidence limit. A dendrogram (UPGA with Euclidian distances) was also constructed using the lipid grouping data.

5.2.4 Denaturing gradient gel electrophoresis (DGGE)

5.2.4.1 Sample collection for DGGE

For experiments reported here duplicate samples (50 ml) were collected from the sump of the cooling tower representing the planktonic phase. For the sessile microbial communities biofilm from the biocells within the cooling tower was scraped off with a sterile spatula and dissolved in 10 ml of water. Both the planktonic and the sessile samples were then freeze-dried.

5.2.4.2 DNA extraction (estimation yield and quality of DNA)

A CTAB-PVP DNA, hot phenol-chloroform-isoamyl alcohol (25:24:1) and salt-ethanol precipitation treatment was used to extract the DNA from the sessile and planktonic phases. Quality and quantity of the extracted DNA were assessed by spectrophotometry. The 260nm reading was used to determine the quantity of DNA using the constant $1A_{260}$ = 50 µg/ml ds DNA (Maniatis *et al.*, 1989; Kozdrój and Van Elsas, 2001). The DNA quality was determined using the A_{260}/A_{280} ratio. A ratio of 1.8 is regarded as pure DNA (Maniatis *et al.*, 1989; Kozdrój and Van Elsas, 2001). The integrity of the DNA was determined using agarose gel electrophoresis.

5.2.4.3 Agarose electrophoresis

Each agarose gel (1 % w/v) contains a DNA molecular weight standard (Molecular Weight Marker XIV; Roche diagnostics, Germany) to which the intensities of the genomic DNA bands were compared (Toffin *et al.*, 2004). Electrophoresis were conducted in a IBI electrophoresis system model MP 1015 (Shelton Scientific, USA) for 2.0 hours at 80 V using 1 x TAE (40mM Tris, 1mM EDTA and 20mM glacial acetic acid, pH 8.0). A Gene Genius Bio Imaging System (Syngene, Synoptics UK) was used to capture the image using GeneSnap (version 6.00.22) software. Images were analyzed

using GeneTools (version 3.00.22) software (Syngene, Synoptics, UK) to determine the relative intensities of the bands in each lane. Also see section 5.2.4.6 for statistical analysis of DGGE profiles.

5.2.4.4 PCR amplification

Community 16S ribosomal DNA was amplified using the universal eubacterial primer combination GM5F and 907R (Nakagawa *et al.*, 2002). The sequence of forward primer (GM5F) is 5'-GCC CGC CGC GCC CCG CGC CCG TCC CGC CGC CCC CGC CCG CCT ACG GGA GGC AGC AG-3' (GC –clamp is underlined) and the reverse primer (907R) 5'-CCG TCA ATT CCT TTG AGT TT-3' (synthesized by Inqaba BioTech, South Africa). PCR conditions for each of the 35 cycles consisted of an annealing temperature of 65 °C for 30 seconds, primer extension temperature at 72 °C for 1 minute and denaturing at 94 °C for 30 seconds. An additional initial denaturation step of 95°C for 300 seconds and a final extension of 72 °C for 300 seconds were also introduced.

Nested PCR was used to amplify the 18S fragments. The first fungal primer combination that was used included nu-SSU-0017FGC (forward primer) and nu-SSU-1196R (reverse primer). The sequence for the forward primer was 5'-CGC CCG CCG CGC GCG GCG GGC GGG GCG GGG GCA CGG GGG GCC AGT CAT ATG CTT GTC-3' and the reverse primer 5'-TCT GGA CCT GGT GAG TTT CC-3'. This amplified a 1200 bp fragment. One microliter of this PCR amplicon was then used as a template for the next PCR in which the above-mentioned forward primer and the nu-SSU-0583R reverse primer was used. The sequence for the reverse primer was 5'-GAA TTA CCG CGG CTG CTG GC-3'. This PCR yielded fragments of 500 bp that could be used for DGGE analyis. All primers were synthesized by Inqaba BioTech, South Africa. PCR conditions consisted of an annealing temperature of 60 °C for 30 seconds, primer extension temperature at 95 °C for 30 seconds and denaturing at 60 °C for 30 seconds. An additional initial denaturation step of 72 °C for 60 seconds and a final extension of 72 °C for 5 minutes were also introduced.

A thermal cycler (I-Cycler, BioRad, UK) was used for PCR's. The double concentrated PCR master mix contained: 2.5 U *Taq* DNA polymerase in 20 mM Tris-HCl, 100 mM KCl, 3.0 mM $MgCl_2$, Brij 35, 0.01% (v/v), dNTP mix (dATP, dCTP, dGTP, dTTP each 0.4 mM), final pH 8.3 (20°C) (PCR Master; Roche, Germany). Additionally, Supertherm *Taq* polymerase (1 U; JM Holdings, UK), $MgCl_2$ (4mM final) and BSA (50ng) were added to the 25µl PCR mixture. One hundred nanogram of template DNA was used in each reaction.

5.2.4.5 DGGE analysis

DGGE was performed using D-Code universal mutation detection system and electrophoresis agents from BioRad (UK). The conditions of the DGGE were: 1-mm-thick 6.0 % (w/v) polyacrylamide gels and a denaturant gradient ranging from 30 to 60% for 16S and 20 to 50% for 18S (100 % denaturant contains 7M urea and 40% formamide). Electrophoresis was conducted at 60°C, electrophoresis buffer was 1x TAE and a constant voltage (100V) for 16 hours (Muyzer *et al.*, 1997a). Gels were stained with ethidium bromide (0.0001%) for 15 minutes and destained in 1x TAE buffer for 25 minutes (BioRad D-Code manual).

5.2.4.6 Statistical analysis of DGGE profiles

The DGGE fingerprints obtained were analysed according to the quantity of each diagnostic band using Gene Tools (version 3.00.22, Syngene, UK). To determine the community structure, a single band in the gel was selected as reference band and given an arbitrary quantity value and the relative quantities of the other bands were normalised in relation to the quantity of the band chosen as reference. The quantities of the DNA in the specific bands were plotted in relation to their Rf distances along the DGGE gel to determine the microbial community structure.

For the structural diversity of the bacterial and fungal communities, the Shannon-Weaver index of general structural diversity was calculated according to Ampe and Miambi (2000) using the following function:

$$H = -\sum P_i \log P_i$$

Where P_i is the relative probability of the bands in a lane. H was calculated on the basis of the bands on the gel lane by using the relative quantities of the bands.
The relative probability, P_i was calculated as:

$$P_i = \frac{n_i}{N}$$

Where n_i is the relative quantity of a band and N is the sum of all the relative quantities in a lane. Relative intensities of the bands were normalised in relation to the quantitiy of the band chosen as reference. The present, absent and relative intensity data were used to construct a matrix using Microsoft Excel.

5.3 Results and discussion

5.3.1 Conventional methods: Plate counts and most probable number technique

Problematic organisms found in industrial process cooling water systems are bacteria, algae and fungi, causing fouling, biofilm formation as well as microbiological induced corrosion (Anon, 1994; Lutey, 1996). Iron oxidizing bacteria, sulphate reducing bacteria, anaerobic acid or H_2 producing bacteria as well as slime forming bacteria are often the cause of industrial problems (Choudhary, 1998) until recently the trend was to use culture techniques in an attempt to culture these physiological groups (Little *et al.*, 1998).

Plate counts were used as a direct analysis for the determination of viable counts within the planktonic and sessile (biofilm) phases (Figure 5.1 and 5.2). Different culture media that is selective for certain physiological groups were used to favour the growth of the desired microorganisms. Quantitative insight was given by the most probable number (MPN) method where dilution and statistical analyses were used for the determination of viable numbers of selected physiological groups in the planktonic and sessile phases (Figure 5.1 and 5.2).

Conflicting opinions exist whether there is a correlation between MIC failure and the number of SRB that are present in the planktonic or the sessile phase of operational systems (Angell and Urbanic, 2000). However, high sulphate concentrations due to the presence of SRB have shown higher corrosion rates of steel coupons than those in a low sulphate concentration (Peng and Park, 1994). According to the results obtained from

the MPN technique (Figure 5.2), the highest numbers of SRB were from experiment 5 which also resulted in the highest corrosion rate (Chapter 4, Table 4.4). SRB numbers within the biofilm were also higher than in the planktonic phase during each of the 5 experiments (Figure 5.2). According to Costerton *et al.* (1984) bacterial corrosion is caused by sessile bacteria within a biofilm and not planktonic bacteria. A study conducted by Angell *et al.* (2000) illustrated that as SRB mortality increases, the corrosion rate drops due to the absence of a source of sulphide which act as a pitting activator.

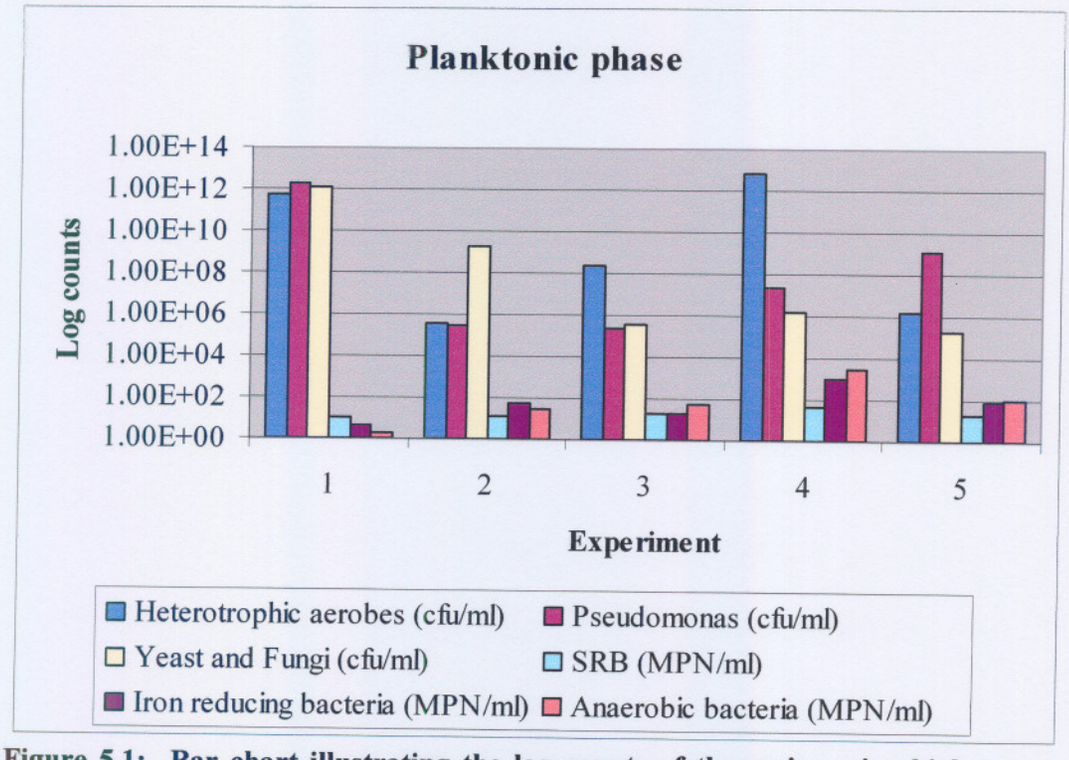

Figure 5.1: Bar chart illustrating the log counts of the major microbial groups enumerated from the planktonic phase.

Iron oxidising bacteria are normally *Gallionella*, *Sphaerotilus*, *Crenothrix*, and *Leptohtrix* species that oxidise ferrous ions to ferric ions to obtain their energy (Rao *et al.*, 2000). From Figure 5.2 it is evident that the highest number of iron reducing bacteria (IRB) were present in the biofilm. High counts of IRB were also present in experiment 2 and 5 in the planktonic as well as in the sessile phase (Figure 5.1 and 5.2). It is also evident that experiment 2 and 5 had the highest corrosion rate (Chapter 4, Table 4.4). These iron reducing bacteria enzymatically catalyse the oxidation of iron and produces treadlike slime and ferric hydroxide that causes plugging and fouling and also increases corrosion (Choudhary, 1998; Csuros and Csuros, 1999 *et al.*, 1999). Experiment 4 (Figure 5.1) had the highest number of IRB in the planktonic phase and the lowest counts of ferric oxide (Chapter 4, Table 4.6). From Figure 5.1 can be seen that the smallest counts of IRB was also present where the ferric oxide concentration were the highest (Chapter 4).

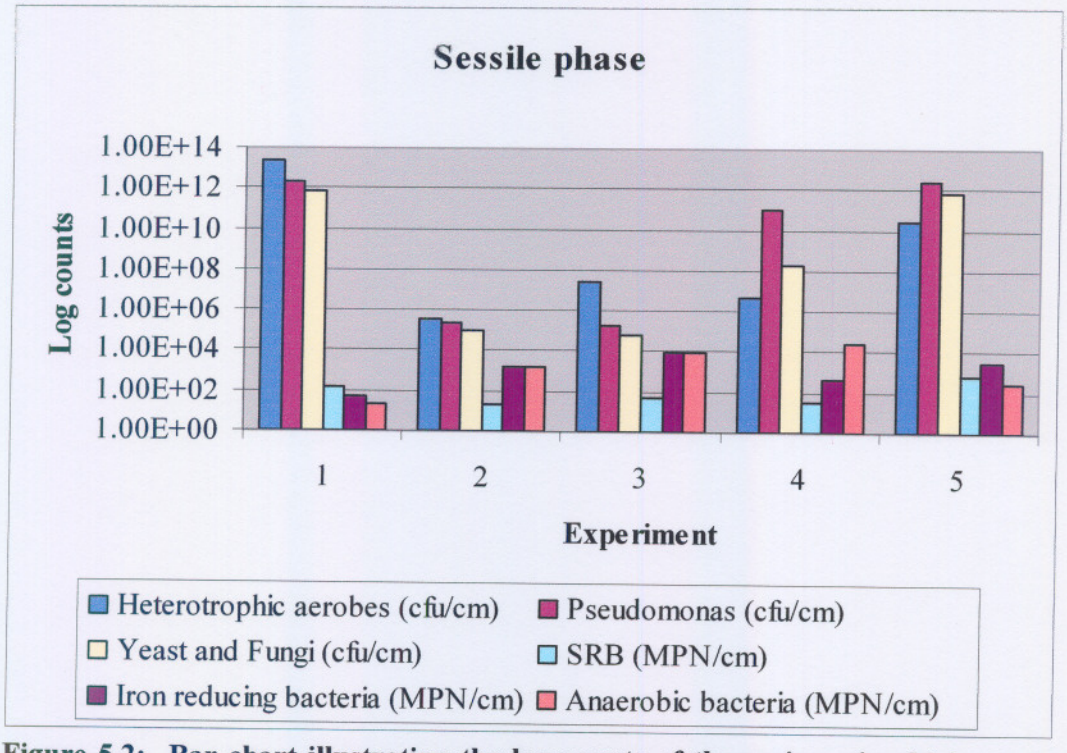

Figure 5.2: Bar chart illustrating the log counts of the major microbial groups enumerated from the sessile phase.

Common slime forming bacteria normally found in cooling water systems are species of *Pseudomonas, Aeromonas, Enterobacter, Bacillus, Aerobacter, Arthrobacter* and *Proteus* (Choudhary, 1998; Palazzo and Allison, 2004). Slime forming bacteria and iron-utilizing organisms produce slime or massive quantities of polysaccharide-based material, which support many other bacteria. Heat transfer efficiency begins to drop as soon as the slime layers form and drops at a more rapid rate as slime build-up continue and will also result in blockages (Choudhary, 1998). This is because fouling of the surface occurs slowly at first, since only a few organisms can attach, survive, grow and multiply. Experiment 1 and 5 which were both operated at a low linear flow velocity of 0.6 m/s had the highest bacterial numbers (Figure 5.1 and 5.2) and also resulted in high fouling rates (Chapter 4, Table 4.4). Increased bacterial activity had been associated with slow flowing water areas (Bondonno *et al.*, 1999). No relationship existed between the percentage increase in the numbers of aerobic bacteria (heterotrophic aerobes and *Pseudomonas*) and the cycles of concentration at which the cooling tower was operated (Figure 5.1 and 5.2).

Majority of microorganisms present in the planktonic phase were heterotrophic aerobes (Figure 5.1). From Figure 5.1 and 5.2 it is evident that *Pseudomonas* dominated the planktonic as well as the sessile phase. More than 50% of fouling in cooling towers is usually caused by *Pseudomonas* and *Aerobacter* (Choudhary, 1998). Aerobic bacteria on the surface of tubercles may play a role in the corrosion process directly by oxidation or reduction activities or indirectly by the formation of slimy biofilm that then harbours SRB (Bondonno *et al.*, 1999). Aerobic bacteria have higher growth rates than anaerobes and that their metabolic activity is much higher and therefore leading to much higher corrosion rates (Brözel *et al.*, 1997). This is evident when comparing the high corrosion rates of experiment 1 and 5 (Chapter 4, Table 4.4) with the high bacterial numbers from experiment 1 and 5 (Figure 5.1 and 5.2).

5.3.2 SEM results

SEM graphs provided a visual impression of bacteria on the glass microscope slides and biocells and can be used as a (semi) quantitative technique when bacteria are not clumped together or positioned in layers (Hilbert *et al.*, 2003). Cell morphologies that were observed were more or less the same during each of the 5 experiments. Cell morphologies observed were bacilli-, cocci- and vibrio-shaped cells.

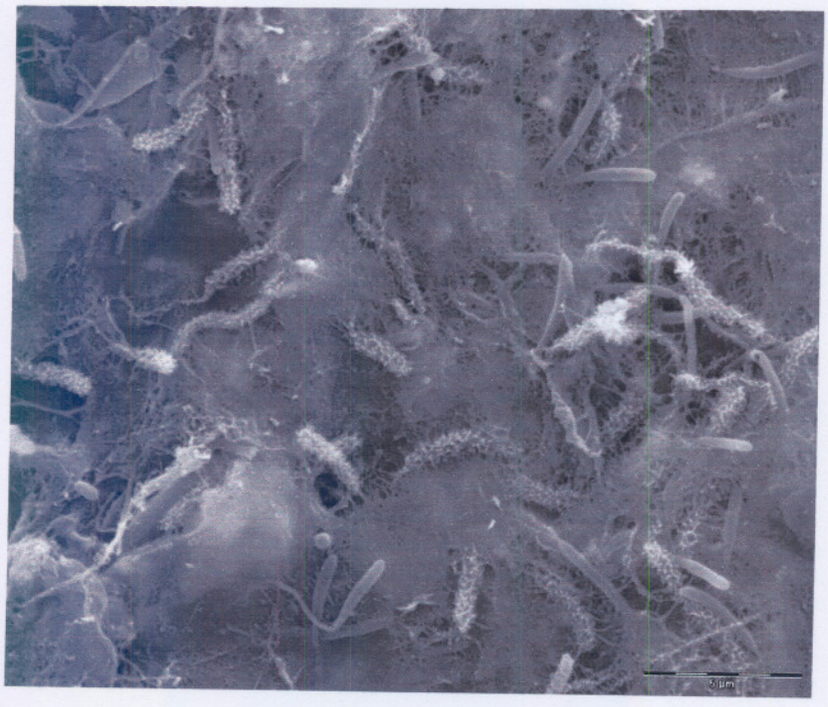

Figure 5.3: Scanning electron micrograph (magnification 10 000x) of the microscope slide, representing the planktonic community from experiment 2.

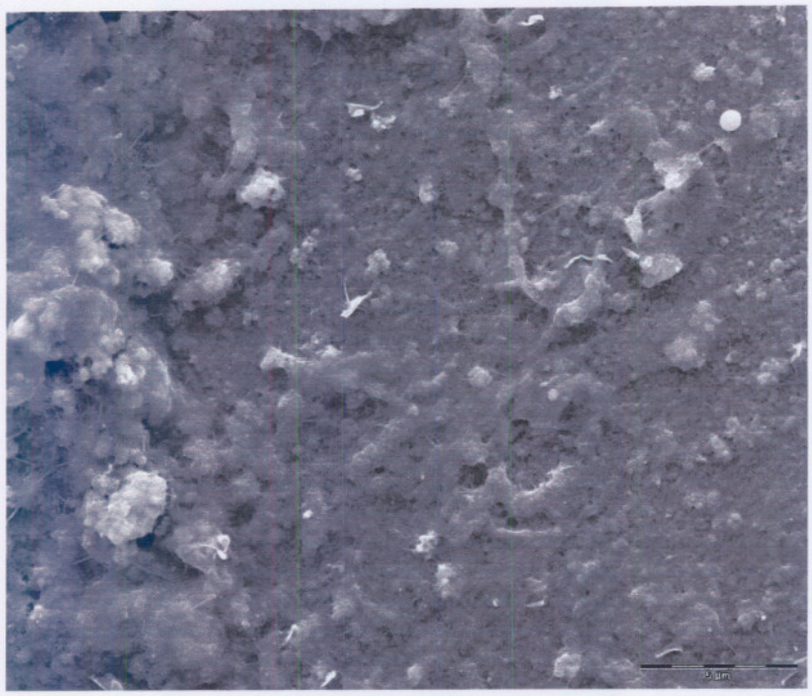

Figure 5.4: Scanning electron micrograph (magnification 10 000x) of the microscope slide, representing the planktonic community from experiment 3.

During each of the 5 experiments it were evident that the planktonic phase (microscope slides) had higher microbial diversity than the biofilm phase (biocells) (Figure 5.5 and 5.8). Although the microbial numbers of the bacteria present within the planktonic and sessile phases differed, their physiological compositon were more or less the same based on morphology (Figure 5.3 and 5.5) as well as conventional microbiological techniques (Figure 5.1 and 5.2). In the planktonic phase (Figure 5.3 - 5.5) single cells as well as small microcolonies were observed.

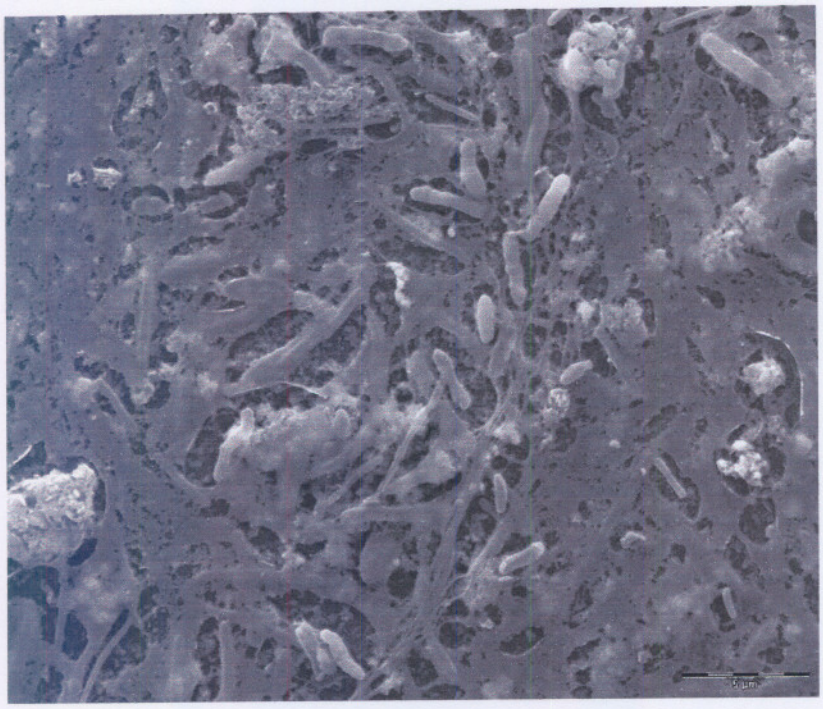

Figure 5.5: Scanning electron micrograph (magnification 8000x) of the microscope slide, representing the planktonic community from experiment 5.

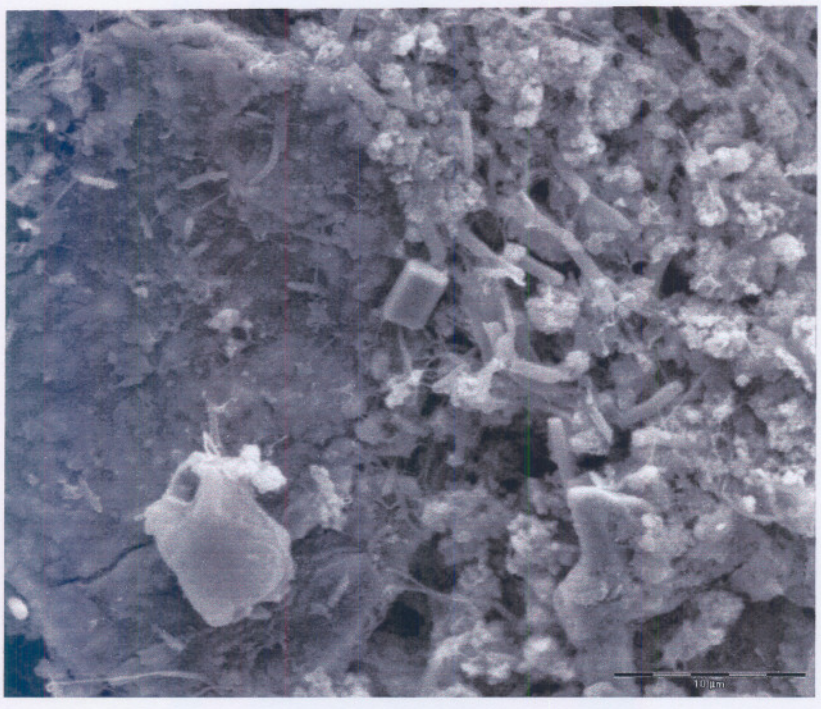

Figure 5.6: Scanning electron micrograph (magnification 6000x) of the biofilm from the biocells, representing the sessile community from experiment 1.

SEM examination of the biofilm in Figure 5.6 - Figure 5.8 show a multilayered biofilm, consisting of many bacterial cells within the EPS (extracellular polymeric substances) that covered the entire internal surface of the biocells. EPS was present between the cells and as a discontinuous layer covering the cells (Vickery *et al.*, 2004).

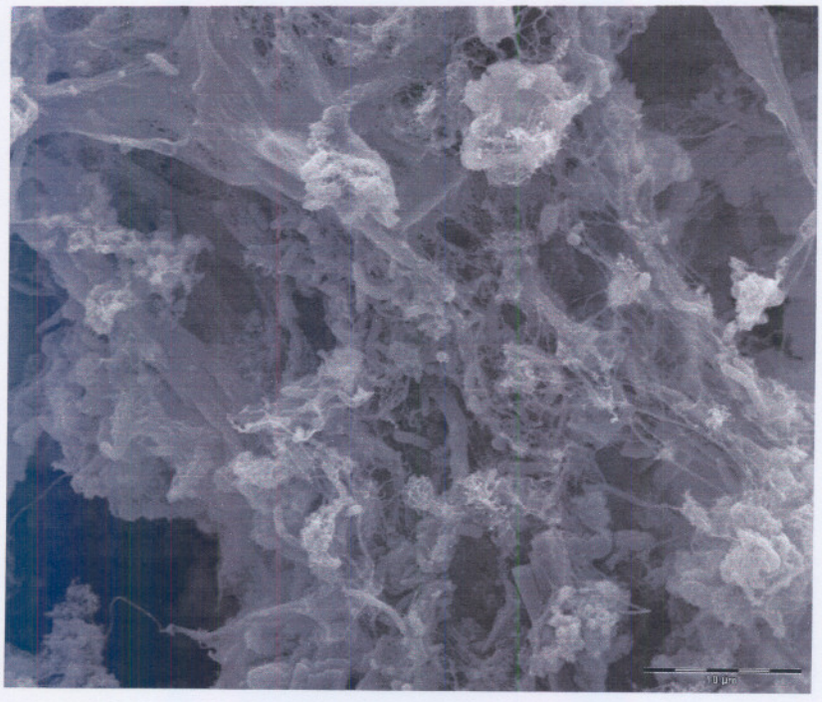

Figure 5.7: Scanning electron micrograph (magnification 5000x) of the biofilm from the biocells, representing the sessile community from experiment 4.

The biofilm cells were generally in large colonies although single cells were also observed (Figure 5.7). In Figure 5.7 and Figure 5.8 the EPS appears as a filamentous structure which could be the result of the drying process required for SEM preparation. This observation is due to binding sites within the EPS of the biofilm that interacts and leads to stronger cohesion (Flemming *et al.*, 2001b).

Figure 5.8: Scanning electron micrograph (magnification 8000x) of the biofilm from the biocells, representing the sessile community from experiment 5.

In general, the microbial numbers of the bacteria present within the planktonic and sessile phases differed. However, the SEM results illustrated that the planktonic and sessile microbial populations throughout the five experiments were similar, based on morphology.

5.3.3 Phospholipid fatty acid analysis results

Total normal unsaturated fatty acids (Total Nsats) are normally indicative of Gram-positive bacteria (O'Leary and Wilkinson, 1988). Monounsaturated fatty acids are considered to be indicative of Gram-negative bacteria (Wilkinson, 1988). Total Polys represents fungi within the community structure (Figure 5.9). Mid chain branched PLFA are likely from actinomycetes or from sulphate reducing bacteria (White *et al.*, 1996b). The total amount of PLFAs, ($PLFA_{tot}$) was used to indicate the total microbial biomass of the planktonic and sessile phase during each experiment (Figure 5.9). The bacterial biomass ($PLFA_{bact}$) and fungal biomass ($PLFA_{fung}$) ratio were used to indicate the relative amounts of fungal and bacterial biomasses (Figure 5.9). According to Figure 5.9 it is evident that Gram-positive bacteria (Total Nsats) dominated the overall

community structure, except for the planktonic samples of experiment 2, 3 and 4 were Gram-negative bacteria (Total Monos) were representative as the more dominant bacterial group. An interesting observation is that the planktonic phase of experiment 3 (Figure 5.9) had the highest percentage of Gram-negative bacteria (experiment 3) and the biofilm sample of this experiment attained the lowest percentage of Gram-negative bacteria. This could be due to the operational parameters of 2 cycles of concentration and a linear flow velocity of 1.2 m/s. Furthermore, the community structure within the planktonic and biofilm samples of experiments 1 and 5 were similar (Figure 5.9). The community structure composition of the planktonic and sessile phases in experiment 2 and 4 were also similar (Figure 5.9).

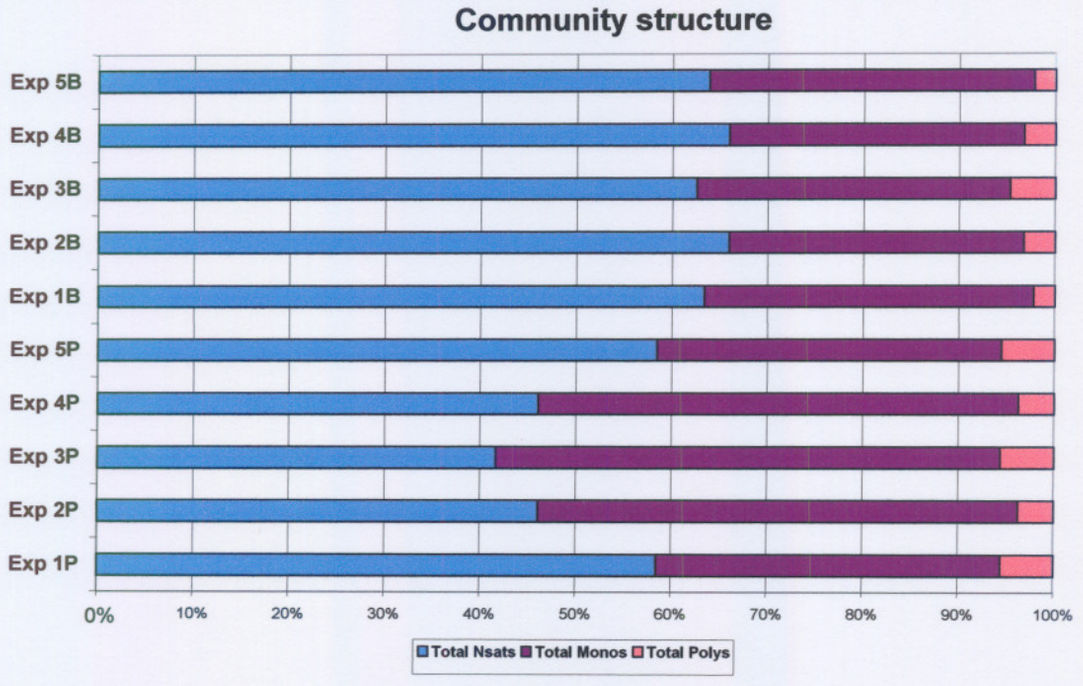

Total NSats = Total Normal unsaturated fatty acids, Total Monos = Total Monounsaturated fatty acids, Total Polys = Total Polyunsaturated fatty acids.

Figure 5.9: Microbial community structure on the basis of the mol percentage fraction of the major phospholipid fatty acid groups.

Experiment 1 and 5 were operated at a low linear flow velocity of 0.6 m/s. Although the linear flow velocity of experiment 2 and 4 differed, they were both operated at high cycles of concentration (3 and 4). Results of the PLFA analysis also demonstrated that

linear flow velocity and cycles of concentration as operating parameters, influence the resultant microbial community.

Similarities and relationships between the experiments were calculated using hierarchical cluster analysis (Ward's clustering algorithm and Euclidean distances) and represented in a dendrogram of similarities (Figure 5.10). This figure also illustrates the spatial differences between the lipid compositions of the microbial communites during the different experiments.

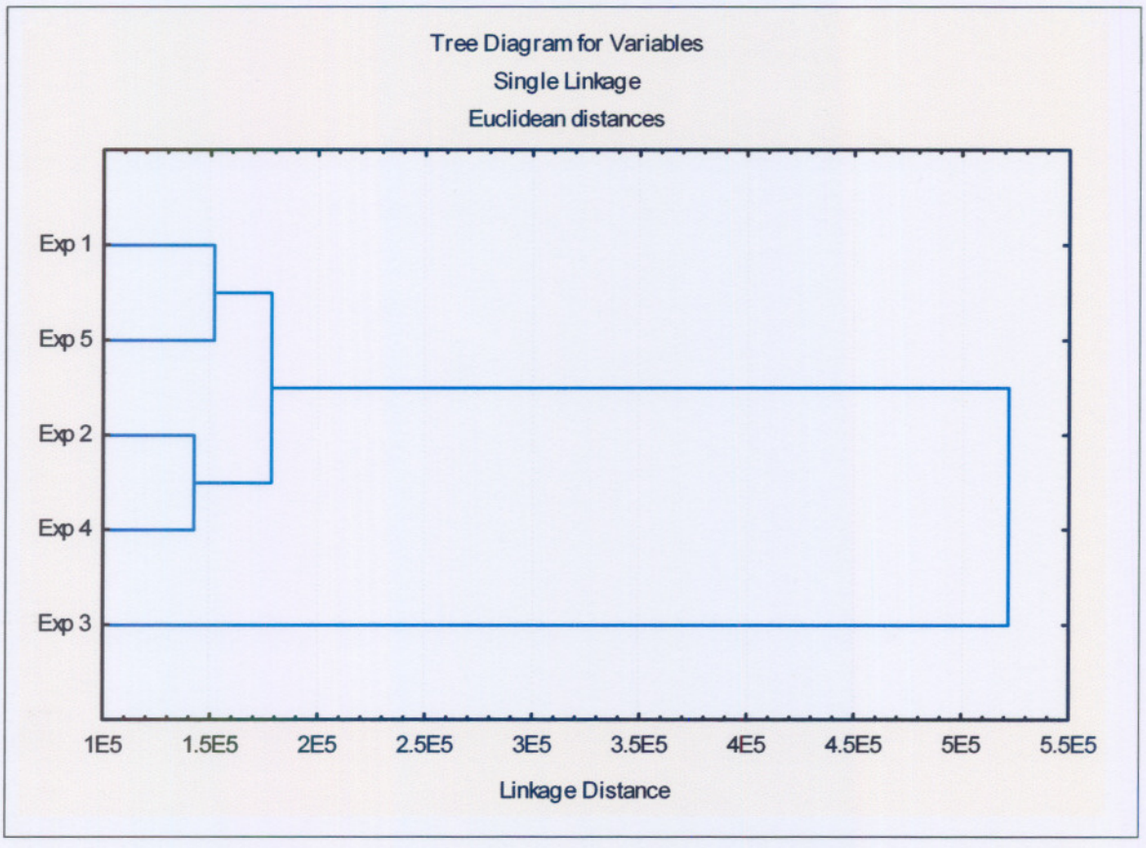

Figure 5.10: Dendrogram illustrating the clustering of the phospholipid fatty acid profiles from each experiment.

It is evident that the operating parameters (cycles of concentration and linear flow velocity) were the main differentiating factor during each experiment. The dendrogram in Figure 5.10 indicates the clustering of experiments 1 and 5 as well as experiment 2 and 4. Athough experiments 2 and 4 were operated at different flow rates, their cycles of concentration were both high (3 and 4). Thus, clustering of their phospholipid fatty

acid profiles are evident (Figure 5.10). Experiments 1 and 5 were both operated at a low linear flow velocity of 0.6 m/s. Position of experiment 3 (Figure 5.10) can be explained by the fact that this experiment had the highest estimated viable biomass (Figure 5.11).

The estimated viable biomass as pmol/g in the planktonic and sessile phases were determined and plotted in Figure 5.11. The biomass within the planktonic phase in all 5 experiments were higher than those from the sessile phase (Figue 5.11). Experiment 1 and 3 showed the highest cell numbers in both the planktonic and sessile phases (Figure 5.11). These high biomass values can be attributed to the fact that both experiment 1 and 3 were operated at 2 cycles of concentration. Experiment 4 which was operated at 4 cycles of concentration and a linear flow velocity of 1.2 m/s attained the lowest viable biomass (Figure 5.11). This implies that when a cooling system is operated at high cycles of concentration and a high linear flow velocity a low viable biomass wil be obtianed.

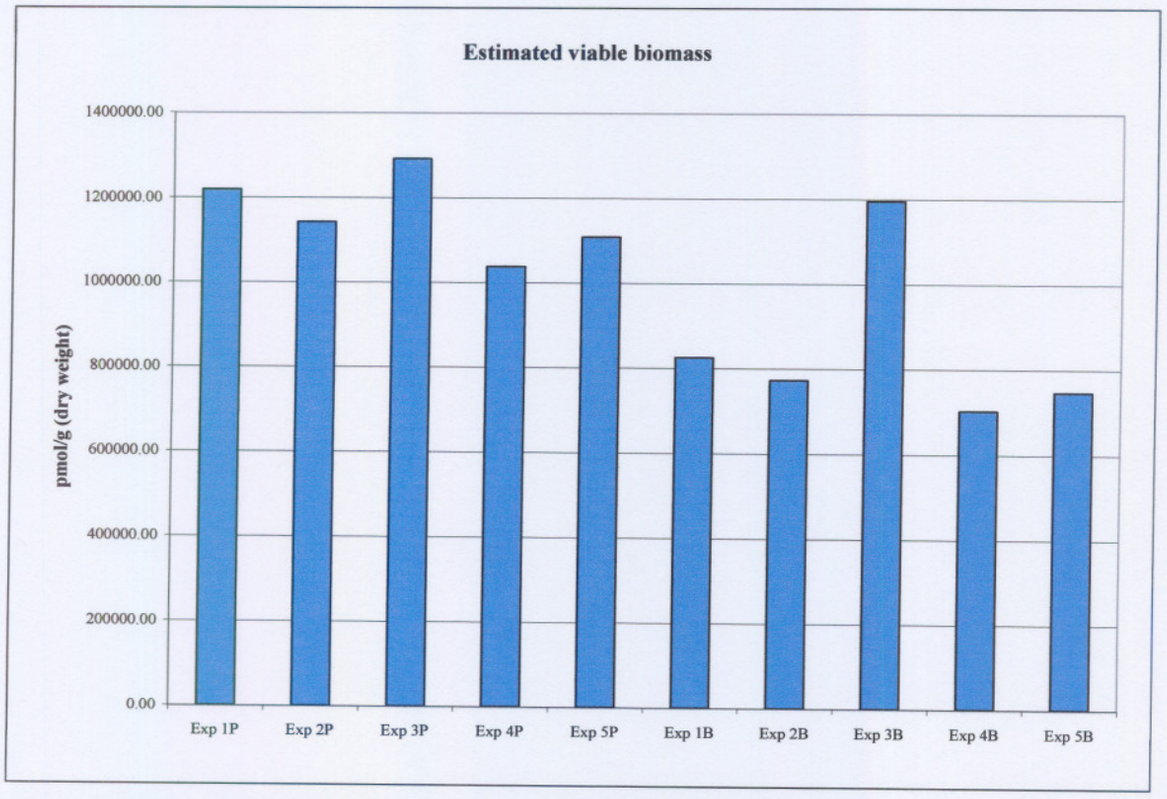

Figure 5.11: Estimated viable biomass pmol/g of the planktonic and biofilm (sessile) phases.

The RDA tri-plot (Figure 5.12) illustrates the variances in the major signature lipid biomarker groups of the planktonic and sessile phase in relation to fouling, scaling and corrosion rates. Fouling, scaling and corrosion of the corrosion coupons and heat exchanger tubes had a strong positive association with cycles of concentration. Further more fouling, scaling and corrsosion rates of the mild steel corrosion coupons had a strong positive association with cycles of concentration as well as linear flow velocity (Figure 5.12). Scaling and corrosion rates of the mild steel coupons had an effect on the biomass (fungi, Gram-positve and Gram-negative) in the sessile phase. Linear flow velocity had a positive association with the biomass within the sessile phase as well as the planktonic phase. This indicates that an increase in the biomass will result in an increase in the fouling, scaling and corrosion rates.

An interesting result is the negative association between the planktonic biomass and the cycles of concentration (Figure 5.12). This implies that the cycles of concentration did not have as a significant influence on the biomass of the planktonic phase, as the linear flow velocity. A negative association also exists between biomass (planktonic and sessile) and fouling of the coupons and heat exchanger tubes (Figure 5.12). This could be an indication that the fouling layer is not primarily microbial in nature. The fouling could possibly be caused by precipitation of inorganic and organic contaminants from the circulating water as well as corrosion products and not due to biological growth alone (You *et al.*, 1999). Biofilms promote the precipitation of minerals such as $CaCO_3$ which also lead to biological and non-biological deposits (Flemming *et al.*, 2001b).

According to the correlation summary of this RDA, the cycles of concentration and linear flow velocity are the environmental variables that correspond the most with the respective axes. The different groupings of the five experiments on the RDA graph can be clearly seen (Figure 5.12). These positions of the different experiments indicate that the x-axis represents the cycles of concentration and the y-axis represents the linear flow velocity. Experiment 2 which were operated at 3 cycles of concentration and linear flow velocity of 0.9 m/s are situated between experiments 4 and 5 which were operated at 4 cycles of concentration and linear flow velocities of 0.6 m/s and 1.2 m/s, respectively (Figure 5.12). According to the eigenvalues from the RDA log file, 48% of the variance was due to cycles of concentration and 24% due to linear flow velocity. The cumulative percentage variance of the species data was 72%. Thus meaning that

fouling, scaling and corrosion caused high variation in the data. According to the Monte Carlo test, the test of significance of the first canonical axis has a p-value of 0.002 and the test of significance of all canonical axes has a p-value of 0.002. This summarises that there is a statistical significance ($p \leq 0.05$) between the various data.

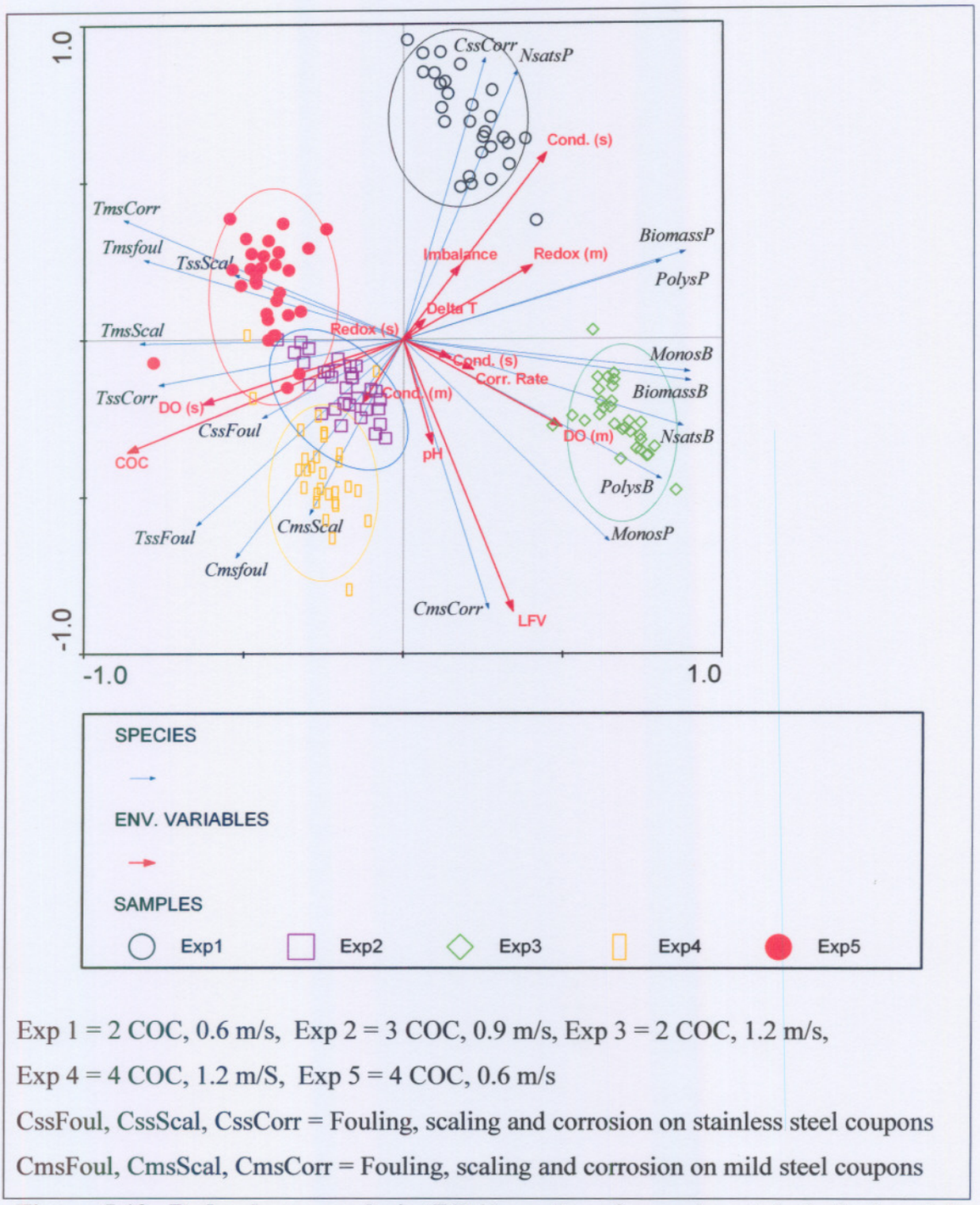

Exp 1 = 2 COC, 0.6 m/s, Exp 2 = 3 COC, 0.9 m/s, Exp 3 = 2 COC, 1.2 m/s,
Exp 4 = 4 COC, 1.2 m/S, Exp 5 = 4 COC, 0.6 m/s
CssFoul, CssScal, CssCorr = Fouling, scaling and corrosion on stainless steel coupons
CmsFoul, CmsScal, CmsCorr = Fouling, scaling and corrosion on mild steel coupons

Figure 5.12: Redundancy analysis (RDA) on the of experiment 1, 2, 3, 4 and 5 using the major phospholipid fatty acid groups

5.3.4 DGGE results

5.3.4.1 DNA concentrations

The average DNA concentration obtained from the planktonic phase samples was 325.99 ng/µl DNA (standard deviation 264.57). The average A_{260}/A_{280} from the planktonic phase samples was 1.48. The average DNA concentration obtained from the sessile phase samples was 668.07 ng/µl DNA (standard deviation 313.03). The average A_{260}/A_{280} from the sessile phase samples was 1,44. Table of DNA concentrations and DNA purity are listed in Appendix A (Table A2).

It is evident that the DNA concentrations obtained from the sessile phases were higher than those obtained from the planktonic phases (Appendix A Table A2). The DNA from the planktonic phase was purer than that obtained from the sessile phase. This could possibly be due to the presence of substances such as EPS which would be present in higher concentrations in the sessile phase

5.3.4.2 PCR and DGGE analyses

The DNA extracted from the planktonic and sessile phases were subjected to 16S rDNA PCR and electrophoresed on a 1% agarose gel (Figure 5.13) to determine if PCR was succesful and to confirm the sizes of the amplified fragments. Both the planktonic (P) and sessile (B) samples subjected to 16S rDNA PCR amplified successfully. From Figure 5.13 it is evident that the planktonic samples of experiment 2 (lane 2) did not amplify successfully.

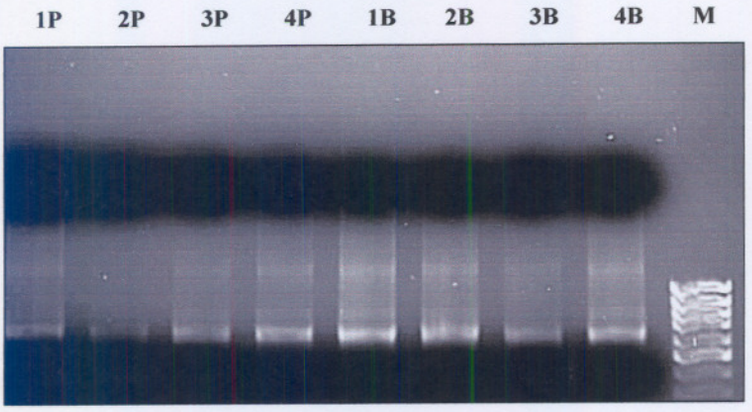

Figure 5.13: Example of agarose gel of the amplified microbial community 16S rDNA gene fragments.

Figure 5.13 shows the size of the amplified microbial community 16S rDNA gene fragments (± 550 base pair).

5.3.4.3 Community profile analysis – DGGE

Figure 5.14 is the community 16S rDNA PCR amplified DGGE fingerprints of the planktonic and sessile phases on a DGGE polyacrylamide gel. The community fingerprints in Figure 5.14 show several bands with varying intensities in the respective lanes. Each band represents a 16S rDNA fragment of 550 bp (Figure 5.14). For the DGGE interpretation, a single band may represent a single species (Kisand and Wikner, 2003). The differences in positions of the bands are functions of the melting domain and nucleotide composition differences (Low *et al*., 2000).

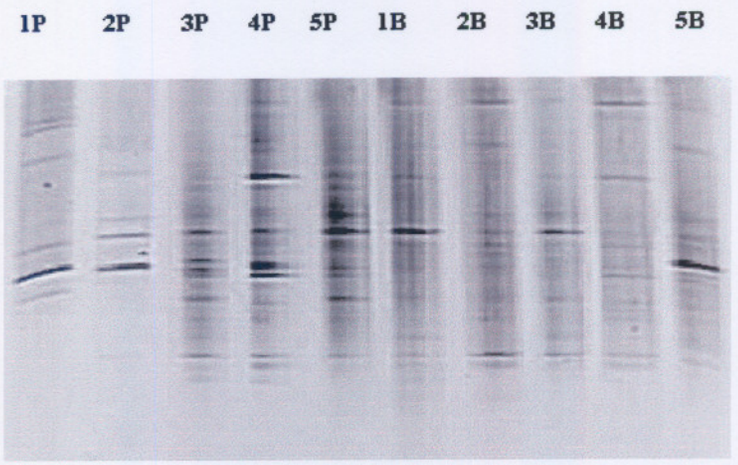

Figure 5.14: DGGE profile of PCR-amplified 16S ribosomal DNA sequence from planktonic and sessile samples.

Figure 5.15 illustrates the relative strain abundance in the planktonic (P) and biofilm samples (B) as determined by 16S rDNA DGGE analysis. The presence of the bands can be associated with the presence of bacterial strains. The percentages indicate the relative contribution of each species to the intensity of the profile (Figure 5.15). Band number 10 was present in all samples except in the biofilm sample of experiment 4. A disappearance of other strains and their reappearance later (e.g. strain numbered 7 and 16) can also be seen (Figure 5.15). Band 9 was present in all the plankonic samples except for sample 1P. Band 16 was present in all the plankonic samples except for sample 2P. Band 20 was present in both planktonic and sessile samples except sample 1P and 2P. Band 2 was present in all of the biofilm samples analysed by 16S rDNA DGGE analysis, except sample 1B.

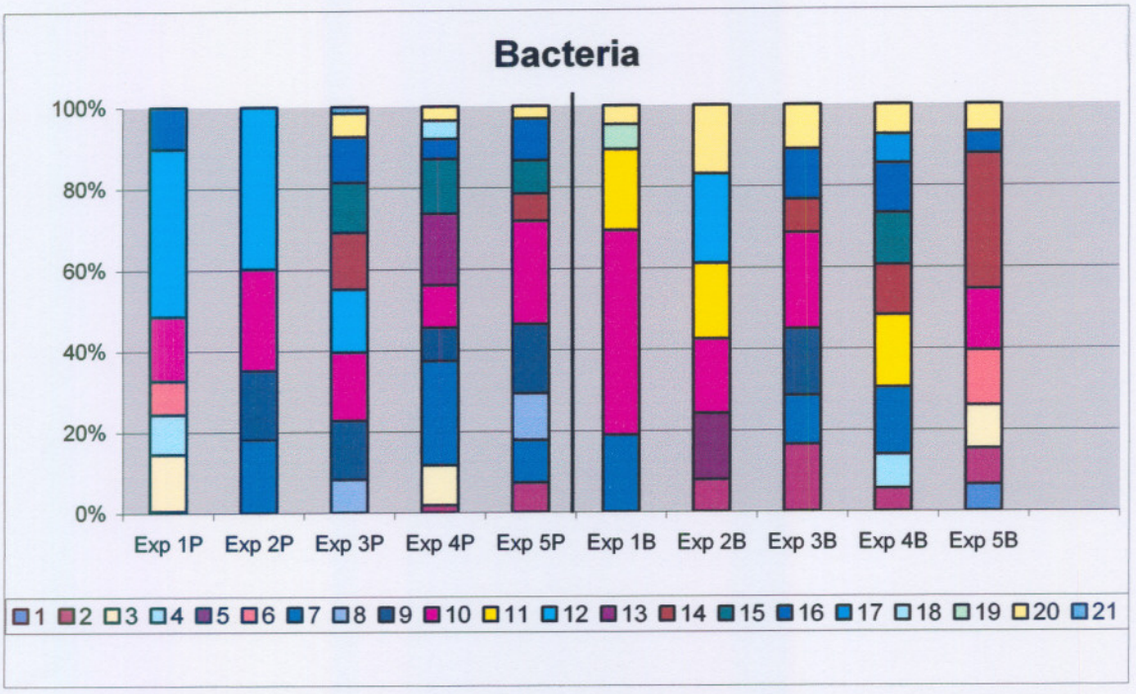

Figure 5.15: Numerical analysis of bacterial DGGE data showing relationship between different samples.

From Figure 5.14 and 5.15 it is also apparent that certain bands are present in the majority of the samples, though the intensities differ marking increases or decreases in species concentration due to the varying operation conditions of the cooling towers. The prominence of the bands indicated that the community was dominated by a relative small number of phylotypes. This was similar to observations by Leung and Topp, (2001) that also observed relative dominance by strain number of species. The planktonic samples were dominated by 3 bands and the sessile samples were dominated by 2 bands. Bands 9, 2 and 16 were more prominent in the planktonic phase, whereas bands 2 and 20 were more prominent in the sessile phase (Figure 5.15).

It can be assumed that the individual distinguishable bands represent distinct species. However, these results should be interpreted with some care because the possible occurance of of multiple copies of 16S genes in individual species may result in an increased number of phylotypes and therefore an overestimation of the microbial diversity (Ranjard *et al.*, 2000). Interpretation in terms of species richness and evenness may also be difficult to interpret, since one band may originate from different species and one cell may be represented by several bands (Ranjard *et al.*, 2000). Richness is the

genetic diversity in terms of the number of different genomes and evenness, the relative abundance of individual genomes (Ranjard *et al.*, 2000).

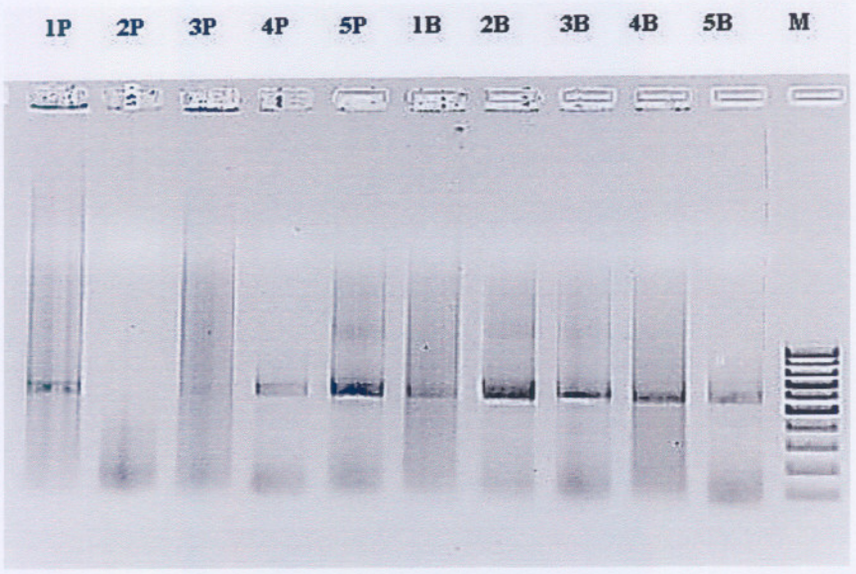

Figure 5.16: Agarose gel of the amplified microbial community 18S rDNA gene fragments from experiment 1, 2, 3, 4 and 5.

Both the planktonic and sessile phases extracted DNA was subjected to 18S rDNA PCR and electrophoresed on a 1% agarose gel. The planktonic and sessile samples that were subjected to 18S rDNA PCR amplified successfully except for the planktonic sample from experiment 2 and 3 (lane 2 and 3, Figure 5.16). This is most probably due to the presence of proteins and other aromatic constituents (phenol) that were present in the sample.

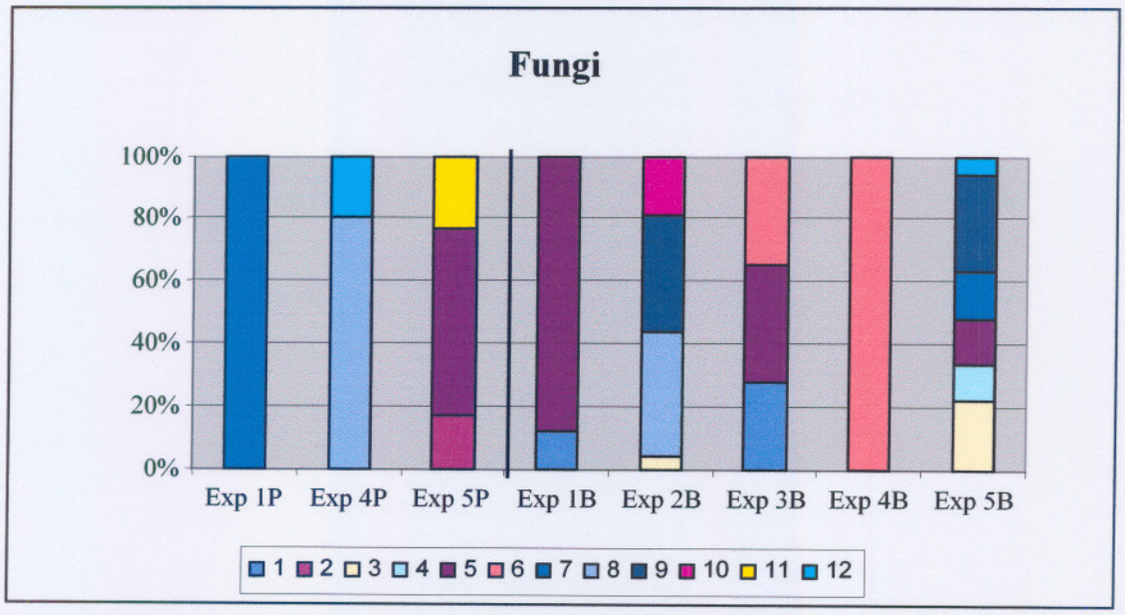

Figure 5.17: Numerical analysis of fungal DGGE data showing relationship between different samples.

Relative strain abundances in the planktonic (P) and biofilm samples (B) as determined by 18S rDNA DGGE analysis are shown in Figure 5.17. The planktonic samples of experiments 2 and 3 that were subjected to 18S rDNA PCR did not amplify successfully and is therefore not present in Figure 5.16. The presence of the bands can be associated with the presence of bacterial strains. The number and intensity of the bands also differed, the brightest bands corresponding to dominant organisms (Toffin *et al.*, 2004). The percentages indicate the relative contribution of each species to the intensity of the profile. It is evident from Figure 5.17 that the intensity of band 5 was the highest. In Figure 5.17 it can be seen that the planktonic and biofilm communities differed from each other since 10 of the 12 bands appeared in the biofilm samples and the planktonic phase was dominated by 3 bands only. Some bands were only found in certain lanes marking the appearance or disappearance of species due to the varying operation conditions of the cooling towers. Band 5 was present in the planktonic phase of experiment 5 and appeared also in the biofilm samples of experiment 1 and 3 (Figure 5.17). Experiment 1 and 5 were both operated at low linear flow velocities of 0.6 m/s.

5.3.4.4 Bacterial and fungal diversity

For the structural diversity of the bacterial (Figure 5.18) and fungal communities (Figure 5.19), the Shannon-Weaver index of diversity was calculated according to Luxmy *et al.* (2000).

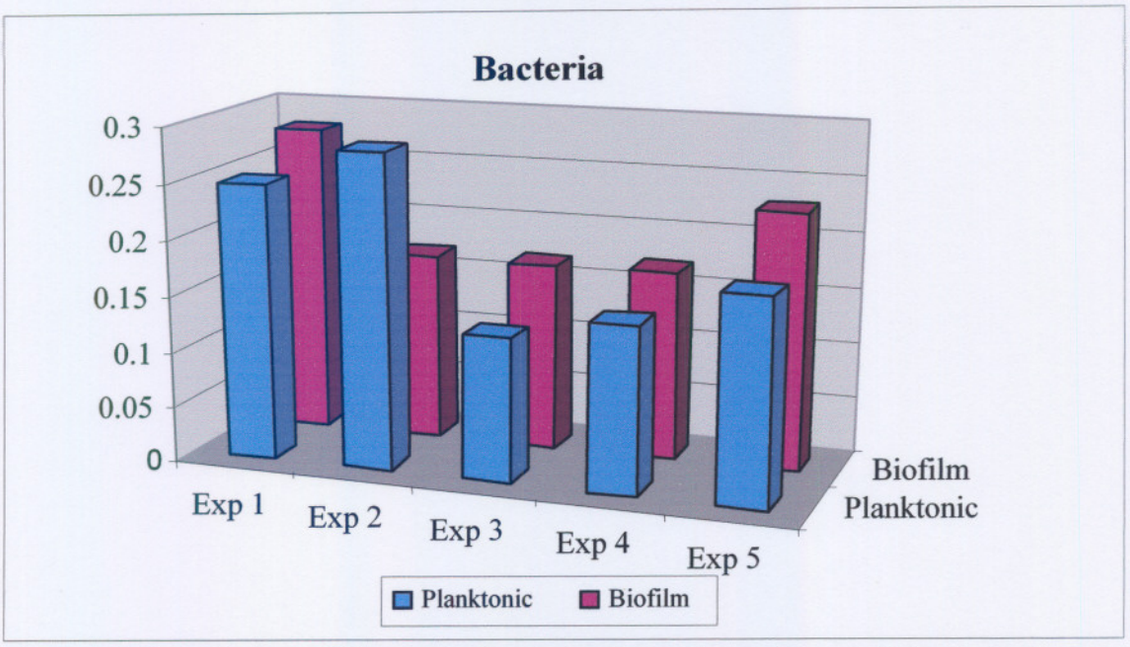

Figure 5.18: Shannon-Weaver index for comparison of bacterial species in the planktonic and biofilm samples.

According to the 16S Shannon-Weaver diversity index, the bacterial diversity of the planktonic samples were generally lower than the biofilm samples, except in experiment 2 (Figure 5.19). From Figure 5.18 it is also apparent that the planktonic bacterial diversity of experiment 1 and 2 were the highest, with a Shannon-Weaver index of almost 0.25. Experiment 1 and 2 were operated at a linear flow velocity of 0.6 and 0.9 m/s respectively, and also at 2 and 3 cycles of concentration. The biofilm samples that had the highest Shannon-Weaver diversity index were experiment 1 and 5. Experiment 5 was operated at 4 cycles of concentration and a linear flow velocity of 0.6 m/s. These high bacterial diversities (Figure 5.18) are possibly due to the operating conditions (low linear flow velocities) of experiments 1, 2 and 5.

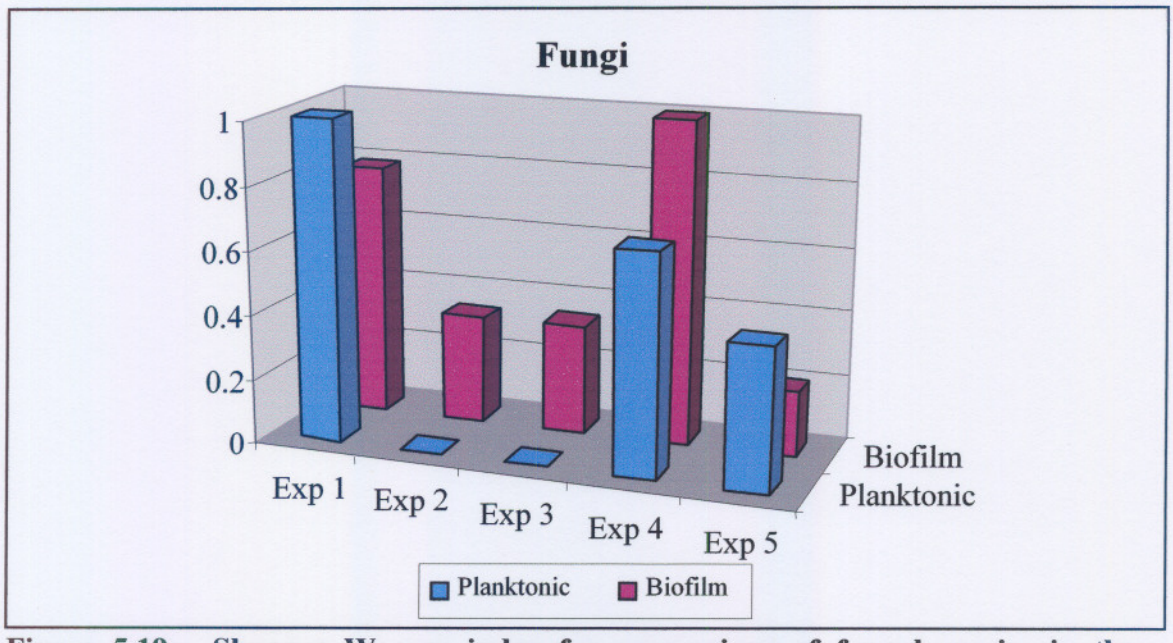

Figure 5.19: Shannon-Weaver index for comparison of fungal species in the planktonic and biofilm samples.

According to Figure 5.19 the fungal diversity of the biofilm phases were higher than the planktonic phases except in experiment 1 and 5, were fungal diversity in the planktonic phase were higher than in the biofilm. Experiment 1 showed the highest Shannon-Weaver diversity index in the planktonic phase Figure 5.19. This is probably due to the low linear flow velocity (0.6 m/s) at which this experiment was operated at. Fungal diversity within the biofilm was the highest in experiment 4, with a Shannon-Weaver indiex of almost 1. The planktonic samples of experiment 2 and 3 subjected to 18S rDNA PCR did not amplify successfully and therefore the diversity indices of these 2 experiments appear to be zero (Figure 5.19).

5.4 Conclusion

Total number of bacteria determined by plate counts, MPN as well as the relative composition of the bacterial community determined by DGGE and PLFA differed throughout this study as the operating parameters changed. Cell counts based on PLFA analysis and conventional culturing were similar, although the values obtained with PLFA analysis were considerably higher. This phenomenon is probably due to the underestimation of microbial numbers when using conventional culturing methods (Palojarvi *et al.*, 1997). The highest numbers of sulphate reducing bacteria were present

in experiment 5 which also resulted in the highest corrosion rate, no direct correlation between SRB numbers and the corrosion that one can predict from their presence exists (Jack *et al.*, 1992; Little *et al.*, 1998). It will therefore be unreasonable to conclude that the quantification of a single physiological group will provide a predictive tool for microbiological induced corrosion. However, the activity of the physiologically diverse microbial species within the biofilm is related to the numbers of bacteria present (Beech, 2004) and the specific combinations of microbes present in the biofilm is related to MIC (Jack *et al.*, 1992).

A negative association exists between the planktonic biomass and the cycles of concentration. This implies that the cycles of concentration did not have the same influence on the biomass of the planktonic phases, as the linear flow velocity had. From Figure 5.1 and 5.2 and also from previous studies, it is evident that no relationship exist between increase in numbers of aerobic bacteria and the cycles of concentration at which a cooling tower is operated at (Poulton *et al.*, 1995). A negative association also existed between biomass (planktonic and biofilm) and fouling of the coupons and heat exchanger tubes. This could be an indication that the fouling layer is not primarily microbial in nature. The fouling could possibly be caused by precipitation of inorganic and organic contaminants from the circulating water as well as corrosion products and not due to biological growth alone (You *et al.*, 1999; Sheikholeslami, 2004).

PLFA analysis also demonstrated that the highest estimated viable biomass was present when the cooling tower was operated at a low linear flow velocity of 0.6 m/s. Shannon-Weaver index of general structural diversity further indicated that bacterial diversity within the planktonic and biofilm samples were the highest at low linear flow velocities. Community structure within the planktonic and biofilm samples showed a similarity between experiment 1 and 5 and also between experiment 2 and 4 with the same percentages of Gram-positive bacteria, Gram-negative bacteria and fungi. This was supported by evidence from the DGGE Shannon-Weaver results that indicated highest species diversity (bacterial and fungal) in the case of experiments 1 and 5. Experiment 1 and 5 were operated at low linear flow velocities and experiment 2 and 4 were operated at high cycles of concentration. Experiment 3 that were operated at a high linear flow velocity and a low cycle of concentration had the smallest bacterial

diversity, low bacterial numbers and also resulted in minimal fouling, scaling and corrosion.

A general trend observed throughout this study was that as the operating parameters (cycles of concentration and linear flow velocity) of the cooling tower changed, fouling, scaling and corrosion rates changed. The rates at which these changed were influenced by the changes in chemistry and physical conditions but also by microbial population dynamics. Operation at low linear flow velocities resulted in high microbial numbers (plate counts and MPN) increased biomass (PLFA) as well as high structural diversity (DGGE). Not only did operation at these these low linear flow velocities result in increased fouling rates, but also high scaling and corrosion. Although, no relationship could be observed between cycles of concentration and increased microbial numbers (Poulton *et al.*, 1995), operating the cooling tower at high cycles of concentration resulted in high scaling and corrosion rates.

CHAPTER 6

Final discussion and recommendations

6.1 Discussion

The aim of this study was to evaluate the suitability of Fischer-Tropsch gas-to-liquid Primary Column Bottoms as process cooling water without first sending the effluent to a water treatment plant. Although this approach is technically feasible, the re-use of process water in the cooling systems is characterised by major problems (fouling, scaling and corrosion) due to the complicated chemistry of the process water and the increased nutrient loads within the system (Meesters *et al.*, 2003). Due to the corrosive nature of this process effluent, stabilisation of the water was essential. After stabilisation an accelerated corrosion test was conducted to determine whether efficient stabilisation was attained in order to minimise corrosion. Influence of the external operating parameters within the cooling tower on the rate of fouling, scaling and corrosion were also determined on mild steel and stainless corrosion coupons and heat exchanger tubes, in order to optimise cooling tower performance. Structural and functional diversity of planktonic and sessile communities were studied by making use of conventional microbiological techniques (plate counts, MPN technique) and molecular methods (PLFA, DGGE).

After chemical stabilisation and an accelerated corrosion test on mild steel and stainless steel (316L) corrosion coupons, it was evident that effective stabilisation was achieved. Stabilised Primary Column Bottoms was less corrosive than non-stabilised Primary Column Bottoms, confirmed through experimental data and also corresponded with the corrosive tendencies obtained from various scaling and corrosion indices. Structural and functional diversity of the planktonic and sessile community was determined through culture dependent methods (plate counts, most probable number) as well as culture independent methods (molecular methods). Compositional analysis of the fatty acid profiles distinguished between planktonic and sessile (biofilm) microbial populations and demonstrated the effect of different operating parameters (cycles of concentration and linear flow velocity). Cycles of concentration and linear flow velocity changed the microbial PLFA pattern. A similarity between the community

structures of experiments 1 and 5 as well as experiments 2 and 4 were evident. Experiments 1 and 5 were both operated at a low linear flow velocity of 0.6 m/s. Experiments 2 and 4 were operated at different flow rates but their cycles of concentration were both high (3 and 4). Dissimilarities were observed in terms of microbial intensities, biofilm thickness as well as crystal formations. These differences are due to the different operating parameters, especially flow rate at which each experiment was operated at (Bondonno *et al.*, 1999). From the 16S rDNA and 18S rDNA sequences, although certain bands (representing a single species) were present in the majority of the planktonic and biofilm samples, their intensities differed. These intensities mark increases or decreases in species concentration, also due to varying operation conditions of the cooling tower. The SEM results illustrated that the planktonic and sessile microbial populations throughout the five experiments were similar, based on morphology.

Variation in cycles of concentration and linear flow velocity had a significant effect ($p>0.05$) on the fouling, scaling and corrosion rates on the mild steel corrosion coupons and heat exchanger tubes. Low linear flow velocities resulted in high fouling rates, increased bacterial numbers as well as high bacterial and fungal diversities. High cycles of concentration resulted in high scaling and corrosion rates and also had the result of similar community structure profiles. Limiting the cycles of concentration in the circulated water resulted in reduced scaling. Scale build-up depends on the flow rate of the circulating water, low linear flow velocities enhance the formation of deposits, increase corrosion rates and also increases microbial activity (Anon, 1994; You *et al.*, 1999). Experiments 1, 2 and 5 that were operated at low flow rates of 0.6m/s and 0.9 m/s resulted in relative high scaling and corrosion rates.

Although growth of the microbes are more rapid in recirculating systems with concentrated nutrients bacterial numbers will not necessarily increase (Abd El Aleem *et al.*, 1998; Ludensky, 2003). Through the elements found on the corrosion products it can be concluded that $FeCO_3$ contributes to corrosion as well as the amount of S observed, related to SRB activity. High sulphate concentrations due to the presence of SRB have shown higher corrosion rates of steel coupons than those in a low sulphate concentration (Peng and Park, 1994).

6.2 Conclusion

A clearly noticeable difference could be seen in the response of the cooling tower to the different linear flow velocities based on fouling, scaling and corrosion results as well as microbial numbers and diversity. However, a similar trend was observed at low linear flow velocities where high microbial numbers, increased biomass as well as high structural diversity was attained. All three microbiological methods provided complementary information and each approach can substantiate the results obtained from the other (e.g. biomass). Operation at 3 and 4 cycles of concentration resulted in worst operating problems (fouling, scaling and corrosion) than when operated at 2 cycles of concentration. In order to minimise fouling, scaling and corrosion the cooling tower should be operated at low cycles of concentration and high linear flow velocities (You *et al.*, 1999).

6.3 Recommendations:

(i) It will be more useful to model the scaling and corrosion indices before the experimental run is completed in order to predict the scaling and corrosive tendencies of the water.

(ii) DGGE band excision and sequence determination would be necessary for full interpretation of DGGE patterns (Perkiömäki *et al.*, 2003).

(iii) In terms of biofilm formation: it is necessary to study the gene expression and the identification of gene products (Stephens, 2002), contribution that the microbial communities within the biofilm have on biofouling and MIC corrosion should be evaluated in more detail (Lutey and Steyn, 2001).

(iv) The biofilm structure of EPS (extracellular polymeric substances) can be used to determine the biological and physico-chemical properties of biofilms, since they are responsible for the structural and functional integrity of biofilms (Flemming and Wingender, 2001a; Sutherland, 2001).

(v) In terms with fouling: identification of the biological reactions as well as the rate-limiting steps and substrates responsible for the fouling-related problem should be evaluated.

(vi) The high fouling rates that were obtained should be further queried. To determine whether the fouling was caused due to organic compositions or biological deposits, the amount of volatile solids and fixed solids should

also be calculated by igniting the total dissolved and suspended solids at 550°C (Viessman and Hammer, 1998).

(vii) Another recommendation could be to calculate the biofouling rate by weight difference of the biocell with and without the attached biomass (Nikolov *et al.*, 2002; Palazzo and Allison, 2004).

(viii) Future work may also include the use of water treatment programmes when evaluating Primary Column Bottoms as cooling medium.

In conclusion, the selection of optimised operational parameters in the utilisation of stabilised Primary Column Bottoms effluent as cooling tower water, in order to minimise fouling, scaling and corrosion were achieved. This research approach could facilitate the selection of optimised operational parameters for the re-use of industrial process water as cooling water to minimise fouling, scaling and corrosion.

REFERENCES

Aasberg-Petersen, K., Christensen, T.S., Nielsen, C.S. and Dybkjaer, I. (2003) Recent developments in autothermal reforming and pre-reforming for synthesis gas production in GTL applications. *Fuel Processing Technology.* **83**, 253-261.

Abd El Aleem, F.A., Al-Sugair, K.A. and Alahmad, M.I. (1998) Biofouling problems in membrane processes for water desalination and reuse in Saudi Arabia. *Internation Biodeterioration and Biodegradation.* **41**, 19-23.

Abdul Azis, P.K., Al-Tisan, I. and Sasikumar, N. (2001) Biofouling potential and environmental factors of seawater at a desalination plant intake. *Desalination.* **135**, 69-82.

Abedi, S.S., Abdolmaleki, A. and Adibi, N. (2006) Failure analysis of SCC and SRB induced cracking of a transmission oil products pipeline. *Engineering Failure Analysis.***14**, 250-261.

Aguilar, A., Casas, C. and Lema, J.M. (1995) Degradation of volatile fatty acids by differently enriched metanogenic cultures: kinetics and inhibition. *Water Research.* **29**, 505-509.

Al-Ahmad, M., Abdul Aleem, F.A., Mutiri, A. and Ubaisy, A. (2000) Biofouling in RO membrane systems, part 1: Fundamentals and control. *Desalination.* **132**,173-179.

Allain, E.J., McCoy, W.F., Yang, S. and Dallmier, A.W. (1998) Strategies used in nature for microbial fouling control: applications for industrial water treatment. *Corrosion 98.* **520**, 1-10.

Alva-Argáez, A., Kokossis, A.C. and Smith, R. (1998) Wastewater minimisation of industrial systems using an integrated approach. *Computers and Chemical Engineering.* **22**, 741-744.

Amann, R.I., Ludwig, W., Schleifer, K.H. (1995) Phylogenetic identification and *in situ* detection of individual microbial cells without cultivation. *Microbiology Review*. **59**, 143 – 169.

Ampe, F. and Miambi, E. (2000) Cluster analysis, richness and biodiversity indexes derived from denaturing gradient gel electrophoresis fingerprints of bacterial communities demonstrate that traditional maize fermentations are driven by the transformation process. *International Journal of Food Microbiology*. **60**, 91–97.

Andijani, I. and Turgoose, S. (2004) Prediction of oxygen induced corrosion in Industrial waters. *In* Water science and technology. *Scaling and Corrosion*. IWA publishing. **49**, 115-120.

Angell, P. (1999) Understanding microbially influenced corrosion as biofilm mediated changes in surface chemistry. *Current Opinion in Biotechnology*. **10**, 269-272.

Angell, P. and Urbanic, K. (2000) Sulphate-reducing bacterial activity as a parameter to predict localized corrosion of stainless alloys. *Corrosion Science*. **42**, 897-912.

Anon, (1994) The industrial water society (IWS). Cooling water treatment: A code of practise. Tamworth. 85 p.

Anon, (2004a) Langelier Saturation Index.
[Web:] http://www.corrosiondoctors.org/NaturalWaters/Langelier.htm
[date of access 29 August 2006]

Anon, (2004b) Larson-Skold Index.
[Web:] http://www.corrosion-doctors.org/NaturalWaters/Larson-Skold.htm
[date of access: 29 August 2006]

Anon, (2004c) Puckorius Scaling Index.
[Web:] http://www.corrosion-doctors.org/NaturalWaters/Puckorius.htm
[date of access: 29 August 2006]

Anon, (2004d) Ryznar Stability Index.
[Web:] http://www.corrosiondoctors.org/NaturalWaters/Ryznar.htm
[date of access: 29 August 2006]

Anon, (2005) The water page.
[Web:] http://www.thewaterpage.com/drghtwater.htm#_Toc390163828
[date of access: 24 Mei 2005]

Anon, (2006a) Corrosion doctors
[Web:]
http://www.corrosionsource.com/technicallibrary/corrdoctor/corrosivity.htm
[date of access: 29 August 2006]

Anon, (2006b) Nalco
[Web:] http://www.nalco.com/asp/service/applied/trasar/trasar.asp.htm
[date of access: 5 July 2006]

Anon, (2006c) Energy research centre.
[Web:] http://www.erc.uct.ac.za
[date of access: 29 August 2006]

Anon, (2006d) Rand Water.
[Web:] http://www.randwater.co.za.
[date of access: 29 August 2006]

APHA, (American Public Health Association), AWWA (American Water Works Association), WPCF (Water Pollution Control Federation) (1985) Standard methods for the examination of water and wastewater. 16th. Ed. APHA. USA.1268 p.

Araya, R., Tani, K., Takagi, T., Yamaguchi, N. and Nasu, M. (2003) Bacterial activity and community composition in stream water and biofilm from and urban river determined by fluorescent in situ hybridization and DGGE analysis. *FEMS Microbiology Ecology*. **24**, 279-285.

Ascolese, C.H. and Douglas, I.B. (1998) Take advantage of effective cooling water treatment programs. *Chemical Engineering. Materials*. March, p49-54.

ASTM, (American Society for Testing and Materials) (1999a) Standard practice for laboratory immersion corrosion testing of metals. G31-72, p101-108.

ASTM, (American Society for Testing and Materials) (1999b) Standard guide for examination and evaluation of pitting corrosion. G46-94, p178-182.

ASTM, (American Society for Testing and Materials) (1999c) Standard practise forpreparing, cleaning and evaluating corrosion test specimens. G1-90, p15-22.

Bagajewicz, M. (2000) A review of recent design procedures for water networks in refineries and process plants. *Computers and Chemical Engineering*. **24**, 2093–2113.

Basson, M.S., Van Niekerk, P.H. and Van Rooyen, J.A. (1997) Overview of water resources availability and utilisation in South Africa. Department of Water Affairs and Forestry. South Africa. (RP No 01/97).

Basini, L. (2005) Issues in H_2 and synthesis gas technologies for refinery, GTL and small and distributed industrial needs. *Catalysis Today*. **104**, 34-40.

Beech, I.B. (2004) Corrosion of technical materials in the presence of biofilms – current understanding and state-of-the art methods of study. *International Biodeterioration and Biodegradation*. **53**, 177-183.

Benzaoui, A. and Bouabdallah, A. (2004) Desalination and biological wastewater treatment process. *Desalination*. **165**, 105-110.

Berdelle-Hilge, P. (1995) Biocorrosion in pumps and pumping systems. *World Pumps*. 50-56.

Beyer, A.H. (1993) Choose the right cooling tower fill. *Chemical Engineering Progress. Energy Transfer / Conversion.* July, p42-46.

Bishop, P.L., Zhang, T.C. and Fu, Y.C. (1995) Effects of biofilm structure, microbial distributions and mass transport on biodegradation processes. *Water Science and Technology.* **31**, 143-152.

Blenkinsopp, S.A. and Costerton, J.W. (1991) Understanding bacterial biofilms. *Tibtech.* **9**, 138-143.

Bligh, E.G. and Dyer, W.J. (1959) A rapid method of total lipid extraction and purification. *Canadian Journal of Biochemistry and Physiology* **37**, 911-917.

Bondonno, A., Prinsloo, C., Ramotlhola, J. and Ringas, C. (1999) Microbial corrosion of common piping materials in the PWV area. Water Research Commission. South Africa. (RP No. 432/1/99).

Botha, J.J., Myburgh, I.S. and Schaberg, P.W. (1998) Sasol's synthetic fuel development - meeting the clean air challenge. Proceedings of the 11th world clean air congress.

Brandt, K.K., Jørgensen, N.O.G., Nielsen, T.H. and Winding, A. (2004) Microbial community-level toxicity testing of linear alkylbenzene sulfonates in aquatic microcosms. *FEMS Microbiology Ecology.*
[Web:] http://www.sciencedirect.com
[date of access: 6 November 2006]

Brás Pereira, I.M., Socorro de Almeida, L.F. and De Matos Beleza, V. (1997) Contribution of air pollution to the fouling of heat exchangers in cooling water circuits. *Experimental Thermal and Fluid Science.***14**, 438-441.

Brink, H., Slaats, P.G.G. and Van Eekeren, M.W.M. (2004) Scaling in domestic heating equipment: getting to know a complex phenomenon. *In* Water Science and Tehnology. Scaling and Corrosion. IWA publishing. **49**, 129-136.

Brözel, V.S., Dawood, Z. and McLeod, E. (1997) An investigation into the role played by *Shewanella* and other sulphide-producing bacteria in metallic corrosion in industrial water systems. Water Research Commission. South Africa. (*RP* No.661/1/97).

Buecker, B. and Post, R. (1998) Control biofouling in evaporative cooling systems. *Chemical Engineering Progress. Energy Transfer / Conversion.* September, p45-50.

Buhrmann, F., Van der Walt, M., Hanekom, D. and Finlayson, F. (1999) Treatment of industrial wastewater for reuse. *Desalination.* **124**, 263-269.

Camper, A., Burr, M., Ellis, B., Butterfield, P. and Abernathy, C. (1999) Development and structure of drinking water biofilms and techniques for their study. *In* Aquatic microbiology: Journal of Applied Microbiology Symposium Supplement, Volume 85. Dennis, P.J., Godfree, A.F. and Stewart- Tull, D.E.S. Blackwell science. London. 271 p.

Casademont, C., Araya-Farias, M., Pourcelly, G. and Bazinet, L. (2006) Effect of Mg/Ca ratio in treated solutions on membrane fouling during electrodialysis. *Desalination.* **200**, 618-619.

Chen, C.- I., Griebe, T. and Characklis, W.G. (1993) Biocide action of monocloramine on biofilm systems of *Pseudomonas areuginosa. Biofouling.* **7**.

Choi, D., You, S. and Kim, J. (2002) Development of an environmentally safe corrosion, scale and microorganism inhibitor for open recirculating cooling systems. *Materials Science and Engineering.* **A335**, 228-236.

Choudhary, S.G. (1998) Emerging microbial control issues in cooling water systems. *Hydrocarbon Processing.* 77, 91-102.

Cocolin, L., Lopez, I., Marshall, M., Mills, D.A., Orr, E., Phister, T., Ruiz-Larrea, F.and Van der Gheynst, J. (2003) Design and evaluation of PCR primers for analysis of bacterial populations in wine by denaturing gradient gel electrophoresis. *Applied and Environmental Microbiology.* **69**, 6801-6807.

Collins, J.P., Font Freide, J.J.H.M. and Nay, B. (2006) A History of Fischer-Tropsch wax upgrading at BP from catalyst screening studies to full scale demonstration in Alaska. *Journal of Natural Gas Chemistry.* **15**, 1-10.

Cord-Ruwisch, R. (2000) Microbially influenced corrosion of steel. *In* Environmental microbe-metal interactions. Lovley, D.R. ASM Press. Washington, D.C. 395 p.

Costerton, J.W. (1984) Influence of biofilm on efficacy of biocides on corrosion-causing bacteria. *National Association of Corrosion Engineers. Materials Performance.* February, p13-17.

Csuros, M. and Csuros, C. (1999) Microbiological examination of water and wastewater. Lewis publishers. USA. 324p.

Demirbas, A. (2006) Progress and recent trends in biofuels. *Progres in Energy and Combustion Science.*
[Web:] http://www.sciencedirect.com
[date of access 29: August 2006]

Dry, M.E. (1999) Fischer-Tropsch reactions and the environment. *Applied Catalysis A: General.* **189**, 185-190.

DWAF, (Department of Water Affairs and Forestry). (2002) National Water Resource Strategy. Proposed first edition. 37 p.
[Web:] http://www.dwaf.gov.za.
[date of access 29: August 2006]

DWAF, (Department of Water Affairs and Forestry), (2003) The management of complex industrial wastewater discharges. Introducing the Direct Estimation of Ecological Effect Potential (DEEEP). Institute of water quality studies, DWAF. January, 2003. Pretoria, South Africa. 37p.

Echols, J.T. and Mayne, S.T. (1990) Cooling tower management using ozone instead of multichemicals. *Ashrae Journal. Ozone in Cooling Towers.* June, p34-38.

EPRI, (Electric Power Research Institute) (2003) Use of degraded water sources as cooling water in power plants. Final report - October 2003. 168 p.
[Web:] http://www.epri.com
[date of access: 29 August 2006]

Flemming, H.C. (1997) Reverse osmosis membrane biofouling. *Experimental Thermal and Fluid Science.* **14**, 382-391.

Flemming, H.C. and Wingender, J. (2001a) Relevance of microbial extracellular polymeric substances (EPSs) – part I: Structural and ecological aspects. *In* Water Science and Technology. Extracellular polymeric substances. IWA publishing. **43**, 1-8.

Flemming, H.C. and Wingender, J. (2001b) Relevance of microbial extracellular polymeric substances (EPSs) – part II: Technical aspects. *In* Water Science and Technology. Extracellular polymeric substances. IWA publishing. **43**, 9-16.

Gebbie, P. (2000) Water stability – what does it mean and do you measure it? 63rd Annual water industry engineers and operators' conference. 6-7 September. Fisher Stewart Pty Ltd. Warrnambool. p50-58.

Hall, K.R. (2005) A new gas to liquids (GTL) or gas to ethylene (GTE) technology. *Catalysis Today.* **106**, 243–246.

Hamilton, A. (1994) Metabolic interactions and environmental microniches: implication for the modelling of biofilm processes. *In* Biofouling and biocorrosion in industrial water systems. Geesey, G.G., Lewandowski, Z., Flemming, H.C. Lewis publishers. USA. 297 p.

Hamrouni, B. and Dhahbi, M. (2002) Calco-carbonic equilibrium calculation. *Desalination.* **152**, 167-174.

Hargreaves, D.G., Pajkos, A., Deva, A.K., Vickery, K., Filan, S.L. and Tonkin, M.A. (2002) The role of biofilm formation in percutaneous kirschner-wire fixation of radial fractures. *Journal of Hand Surgery.* **27B**, 365-368.

Hey, G.W. and Hollingshad, W.R. (1988) Corrosion control in cooling tower systems. *Ashrae Journal. Corrosion Control.* August, p33-36.

Hidalgo, M.D. and García-Encina, P.A. (2002) Biofilm development and bed segregation in a methanogenic fluidized bed reactor. *Water Research.* **36**, 3083-3091.

Hilbert, L.R., Bagge-Ravn, D., Kold, J. and Gram, L. (2003) Influence of surface roughness of stainless steel on microbial adhesion and corrosion resistance. *International Biodeterioration and Biodegradation.* **52**, 175-185.

Hillis, D.M., Moritz, C. (1990) *Molecular Systematics*. Sinauer Associates: Massachusetts. p.502 – 515.

Hodgkiess, T. (2004) Inter-relationships between corrosion and mineral-scale deposition in aqueous systems. *In* Water Science and Technology. Scaling and Corrosion. IWA publishing. **49**, 121-128.

Hugenholtz, P., Goebbel, B.M., Pace, N.R. (1998) Impact of culture-independent studies on the emerging phylogenetic view of bacterial diversity. *Journal of Bacteriology.* **180**, 4765 - 4774.

Ibekwe, A.M., Kennedy, A.C., Frohne, P.S., Papiernik, S.K., Yang, C.H. and Crowley, D.E (2002) Microbial diversity along a transect of agronomic zones. *FEMS Microbiology Ecology*. **39**, 183-191.

Iojoiu, E.E., Landrivon, E., Raeder, H., Torp, E.G., Miachon, S. and Dalmon, J. (2006) The "Watercatox" process: Wet air oxidation of industrial effluents in a catalytic membrane reactor. First report on contactor CMR up-scaling to pilot unit. *Catalysis Today*.
[Web:] http://www.sciencedirect.com
[date of access 29: August 2006]

Iverson, W.P. (1987) Advances in applied microbiology. Volume 32. Academic Press. New Jersey. p1-37

Jack, R.F., Ringelberg, D.B. and White, D.C. (1992) Differential corrosion rates of carbon steel by combinations of *Bacillus* sp., *Hafnia Alvei* and *Desulfovibrio gigas* established by phospholipids analysis of electrode biofilm. *Corrosion Science*. **33**, 1843-1853.

Jain, D.K. (1995) Evaluation of the semisolid Postgate's B medium for enumerating sulphate-reducing bacteria. *Journal of Microbiological Methods*. **22**, 27-38.

Jefferson, K.K. (2004) What drives bacteria to produce a biofilm? *FEMS Microbiology Letters*. **236**, 163-173.

Johansson, L. and Saastomoinen, T. (1999) Investigating early stages of biocorrosion with XPS: AISI 304 stainless steel exposed to *Burkholderia* species. *Applied Surface Science*. **114**, 244-248.

Kajdasz, R., Einstman, R.V. and Young-Bandala, L. (1984) Biocide efficacy with respect to sessile and planktonic organisms. IWC-84-60. p85-92.

Karlberg, L. and Penning de Vries, F.W.T. (2004) Exploring potentials and constraints of low-cost drip irrigation with saline water in sub-Saharan Africa.

Physics and Chemistry of the Earth. **29**, 1035–1042.

Keevil, C.W. (2004) The physico-chemistry of biofilm-mediated pitting corrosion of copper pipe supplying potable water. *In* Water Science and Technology. Scaling and Corrosion. IWA publishing. **49**, 91-98.

Kehrmeyer, S.R., Applegate, B.M., Pinkart, H.C., Hedrick, D.B., White, D.C. and Sayler, G.S. (1996) Combined lipid / DNA extraction method for environmental samples. *Journal of Microbiological Methods.* **25**, 153-163.

Kemmer, F.N. and McCallion. J. (1979) The NALCO Water handbook. McGraw-Hill. New York. 750 p.

Keresztes, Z., Felhösi, I. and Kálmán, E. (2001) Role of redox properties of biofilms in corrosion processes. *Electrochimica Acta.* **46**, 3841-3849.

Kim, J., Savulescu, L. and Smith, R. (2001) Design of cooling systems for effluent temperature reduction. *Chemical Engineering Science.* **56**, 1811-1830.

Kisand, V. and Wikner, J. (2003) Limited resolution of 16S rDNA DGGE caused by melting properties and closely related DNA sequences. *Journal of Microbiological Methods.* **54**, 183-191.

Knottenbelt, C. (2002) Mossgas "gas-to-liquid" diesel fuels-an environmentally Friendly option. *Catalysis Today.* **71**, 437-445.

Koenig, A., Zhang, T., Liu, L. and Fang, H.H.P. (2005) Microbial community and biochemistry process in autosulfurotrophic denitrifying biofilm. *Chemosphere.* **58**, 1041-1047.

Kolb, F.R. and Wilderer, P.A. (1995) Activated carbon membrane biofilm reactor for the degradation of volatile organic pollutants. *Water Science and Technology.* **31**, 205- 213.

Kozdrój, J. and Van Elsas, J.D. (2001) Structural diversity of microorganisms in chemically perturbed soil assessed by molecular and cytochemical approaches. *Journal of Microbiological Methods*. **43**, 197-212.

LeChevallier, M.W., Lowry, C.D., and Lee, R.G. (1988) Factors promoting survival of bacteria in chlorinated water supplies. *Applied and Environmental. Microbiology*. **54**, 649 p.

Lens, P.N., De Poorter, M.P., Cronenberg, C.C. and Verstraete, W.H. (1995) *Water Research*. **29**, 871-880.

Leung, K. and Topp, E. (2001) Bacterial community dynamics in liquid swine manure during storage: molecular analysis using DGGE/PCR of 16S rDNA. *FEMS Microbiology Ecology*. **38**, 169-177.

Li, H., Ma, W., Wang, L., Liu, R., Wei, L. and Wang, Q. (2006) Inhibition of calcium and magnesium-containing scale by a new antiscalant polymer in laboratory tests and a field trial. *Desalination*. **196**, 237-247.

Little, B.J., Ray, R.I. and Wagner, P.A. (1998) Tame microbiologically influenced corrosion. *Chemical Engineering Progress*. September. p. 51-60.

Low, E.W., Chase, H.A., Milner, M.G. and Curtis, T.P. (2000) Uncoupling of metabolism to reduce Biomass Production in the Activated Sludge Process. *Water Research* **34**, 3204 – 3212.

Ludensky, M. (2003) Control and monitoring of biofilms in industrial applications. *International Biodeterioration and Biodegradation*. **51**, 255-263.

Lutey, R.W. (1996) Applied industrial microbiological control. Buckman Laboratories International. Memphis: USA. 23 p.

Lutey, R.W. and Stein, A. (2001) A review and comparison of MIC indices (models). 62nd International Water Conference. Paper 4 (IWC-01-04). October 21-25.

Pittsburg: USA.

Lutterbach, M.T.S. and De França, F.P. (1997) Biofilm formation monitoring in an industrial open water cooling system. *Revista de Microbiologia.* **28**, 106-109.

Luxmy, B.S., Nakajima, F., Kamamoto, K. (2000) Analysis of bacterial community in membrane-separation bioreactors by fluorescent *in situ* hybridization (FISH) and denaturing gradient gel electrophoresis (DGGE) techniques. *Water Science and Technology* **41**, 259-268.

Macadam, J. and Parsons, S.A. (2004) Calcium carbonate scale control, effect of material and inhibitors. *In* Water Science and Technology. Scaling and Corrosion. IWA publishing. **49**, 153-159.

MacKay, W.G., Leanord, A.T. and Williams, C.L. (2002) Water, water everywhere nor any a sterile drop to rinse your endoscope. *Journal of Hospital Infection.* **51**, 256-261.

Mackintosh, G.S., De Villiers, H.A., Du Plessis, G.J., Loewenthal, R.E. and Kornmüller, U. (1998) Stabilisation of soft acidic waters with limestone. Water Research Commission. South Africa. (RP No 613/1/98).

Maguire, J.J. (1980) Handbook of industrial water conditioning. 8th ed. Betz Laboratories. Pennsylvania. 437 p.

Makkinejad, N. (2001) Temperature profile in countercurrent / cocurrent spray towers. *International Journal of Mass and Heat Transfer.* **44**, 429-442.

Maniatis, T., Fritsch, E.F., Sambrook, J. (1989) *Molecular Cloning: A Laboratory Manual.* Cold Spring Harbour laboratory, New York, USA.

Marcucci, M. and Tognotti, L. (2002) Reuse of wastewater for industrial needs: the Pontedera case. *Resources, conservation and recycling.* **34**, 249–259.

Martínez, S.S., Gallegos, A.A. and Martínez, E. (2004) Electrolytically generated silver and copper ions to treat cooling water: environmentally friendly novel alternative. *International Journal of Hydroenergy*. **29**, 921-932.

McLaughlan, R.G. and Stuetz, R.M. (2004) A field based study of ferrous metal corrosion in groundwater. *In* Water Science and Technology. Scaling and corrosion. IWA publishing. **49**, 41-47.

Meesters, K.P.H., Van Groenestjin, J.W. and Gerritse, J. (2003) Biofouling reduction in cooling systems through biofiltration of process water. *Water Research*. **37**, 525-532.

Meroney, R.N. (2006) CFD prediction of cooling tower drift. *Journal of Wind Engineering and Industrial Aerodynamics*. **94**, 463-490.

Meyer, B. (2003) Approaches to prevention, removal and killing of biofilms. *International Biodeterioration and Biodegradation*. **51**, 249-253.

Mohsen, S. (2004) Treatment and reuse of industrial effluents: case study of a thermal power plant. *Desalination*. **167**, 75-86.

Mohsen, M.S. and Jaber, J.O. (2002) Potential of industrial wastewater reuse. *Desalination*. **152**, 281-289.

Mueller, R.F. (1994) Biofilm formation in water systems and their industrial relevance. *Biological Sciences Symposium*. p195-201.

Muyzer, G. (1999) DGGE/TGGE a method for identifying genes from natural ecosystems. *Current Opinion in Microbiology*. **2**, 317-322

Muyzer, G., Brinkhoff, T.,Nübel, U., Santegoeds, C., Schäfer, H. and Wawer, C. (1997) Denaturing gradient gel electrophoresis (DGGE) in microbial ecology, p.1 – 27. *In* A.D.L.Akkermans, J.D. van Elsas, and F.J. de Bruijn (ed.), *Molecular Microbial Ecology Manual*, vol. 3.4.4. Kluwer, Dordrecht, De Nederlande.

Muyzer, G., De Waal E.C., Utterlinden, A.G. (1993) Profiling of complex microbial populations by denaturing gradient gel electrophoresis analysis of polymerase chain reaction-amplified genes coding for 16S rRNA. *Applied and Environmental Microbiology.* **59**, p. 695 – 700.

Muyzer, G., Macheret, V. Laguerre, G., Rigaud, A. Soulas, G., Topp, E. and Vallaeys, T. (1997) Evaluation of denaturing gradient gel electrophoresis in the detection of 16S rDNA sequence variation in rhizobia and methanotrophs. *FEMS Microbiology Ecology.* **24**, 279-285

Nakagawa, T., Fukui, M., Sato, S. and Yamamoto, Y. (2002) Successive changes in community structure of an ethylbenzene-degrading sulfate-reducing consortium. *Water Research.* **36**, 2813–2823.

Natarajan, S, and Kumaresh Babu, S.P. (2006) Corrosion and its inhibition in SA213 - T22 TIG weldments used in power plants under neutral and alkaline environments. *Materials Science and Engineering A.* **432**, 47-51.
[Web:] http://www.sciencedirect.com
[date of access: 29 August 2006]

Negaresh, E., Le-Clech, P. and Chen, V. (2006) Fouling mechanisms of model extracellular polymeric substances in submerged membrane reactor. *Desalination.* **200**, 715–717.

Nikolov, L., Karamanev, D., Mamatarkova, V., Mehochev, D. and Dimitrov, D. (2002) Properties of the biofilm of *Thiobacillus ferrooxidans* formed in rotating biological contractor. *Biochemical Engineering Journal.* **12**, 43-48.

Nordell, E. (1961) Water treatment. 2nd ed. Reinhold Publishing. New York. 598 p.

O'Leary, W.M. and Wilkinson, S.G. (1988) Gram-positive bacteria. *In* Microbial lipids. Ratledge, C. and Wilkinson, S.G. Academic Press Ltd. London. p117-201.

Olesen, B.H., Lorenzen, J., Kjellerup, B.V., Ødum, S., Nielsen, P.H. and Frølund, B. (2004) MIC mitigation in a 100 MW district heating peak load unit. *In* Water Science and Technology. Scaling and Corrosion. IWA publishing. **49**, 99-105.

Olsen, S. and Gobina, E. (2004) GTL synthesis gas generation membrane for monetizing stranded gas. *Membrane Technology*. June 2004, p5-10.

Palojarvi, A., Sharma, S., Rangger, A., Von Lutzow, M. and Insam, H. (1997) Comparison of Biolog and phospholipid fatty acid patterns to detect changes in microbial communities . *In.* Microbial communities - Functional versus structural approaches. Springer verlag, New York. p. 37-48.

Parsons, S.A. and Doyle, J.D. (2004) Struvite scale formation and control. *In* Water Science and Technology. Scaling and Corrosion. IWA publishing. **49**, 177-182.

Peng, C. and Park, J.K. (1994) Electrochemical mechanisms of corrosion influenced by sulphate-reducing bacteria in aquatic systems. *Water Research.* **28**, 1681-1692.

Perkiömäki, J.,Tom-Petersen, A., Nybroe, O. and Fritze, H. (2003) Boreal forest microbial community after lorng-term field exposure to acid and metal pollution and its potential remediation by using wood ash. *Soil Biology and Biochemistry.* **35**, 1517-1526.

Petrucci, G. and Rosellini, M. (2005) Chlorine dioxide in seawater for fouling control and post-disinfection in potable waterworks. *Desalination.* **182**, 283-291.

Picón-Núnez, M., Nila-Gasca, C. and Morales-Fuentes, A. (2006) Simplified model for the determination of the steady state response of cooling systems. *Applied Thermal Engineering.*
[Web:] http://www.sciencedirect.com
[date of access 29 August 2006]

Poulton, W.I.J., Cloete, T.E. and Von Holy, A. (1995) Microbiological survey of open recirculating cooling water systems and their raw water supplies at twelve fossil-fired power stations. *Water S.A.* **21**, 357-364.

Qi, X., Liu, Z. and Li, D. (2006) Performance characteristics of a shower cooling tower. *Energy Conversion and Management.*
[Web:] http://www.sciencedirect.com
[date of access: 29 August 2006]

Qureshi, B.A. and Zubair, S.M. *(2006) A complete model of wet cooling towers with* fouling in fills. *Applied Thermal Engineering.* **26,** 1982-1989.

Rafferty, K. (2000) Scaling in geothermal heat pump systems. *GHC Bulletin.* March 2000. p11-15.

Ramotlhola, J.S. and Ringas, C. (2000) Corrosion: brochure for local authorities. Water Research Commission. South Africa. (RP TT 112/99).

Ranjard, L., Poly, F. and Nazaret, S. (2000) Monitoring complex bacterial communities using culture-independent molecular techniques: application to soil environment. *Res. Microbiol.* **151**, 167-177.

Rao, T.S., Sairam, T.N., Viswanathan, B. and Nair, K.V.K. (2000) Carbon steel corrosion by iron oxidising and sulphate reducing bacteria in a freshwater cooling system. *Corrosion Science.* **42**, 1417-1431.

Ray, R. and Little, B. (2003) Environmental electron microscopy applied to biofilms. *In* Biofilms in medicine, industry and environmental biotechnology: characteristics, analysis and control. Lens, P., Moran, A.P., Mahony, T., Stoodley, P. and O'Flaherty, V. IWA Publishing. London. 610 p.

Rostrup-Nielsen, J.R. (2002) Syngas in perspective. *Catalysis Today.* **71**, 243-247.

Salgot, M., Huertas, E., Weber, S., Dott, W. and Hollender, J. (2006) Wastewater reuse and risk: definition of key objectives. *Desalination.* **187**, 29–40.

Sampson, I. (2001) Introduction to a legal framework to pollution management in South Africa. Water Research Commission. South Africa (RP TT 149/01).

Sartory, D.P. and Watkins, J. (1999) Conventional culture for water quality assessment: is there a future? *In* Aquatic microbiology: Journal of Applied Microbiology Symposium Supplement, Volume 85. Stewart-Tull, D.E.S., Dennis, P.J. and Godfree, A.F. Blackwell science. London. 271p.

Schröder, E.W. and De Haast, J. (1988) Anaerobic digestion in effluent treatment. Part 2: microbiology and process control. *South African Journal of Dairy science.* **20**.

Semmens, M.J., Dahm, K., Shanahan, J. and Christianson, A. (2003) COD and nitrogen removal by biofilms growing in gas permeable membranes. *Water Research.* **37**, 4343-4350.

Sheikholeslami, R. (2004) Scaling of process equipment by saline streams - challenges ahead. *In* Water Science and Technology. Scaling and Corrosion. IWA publishing. **49**, 201-210.

Slaats, P.G.G., Mesman, G.A.M., Rosenthal, L.P.M. and Brink, H. (2004) Tools to monitor corrosion of cement-containing water mains. *In* Water Science and Technology. Scaling and Corrosion. IWA publishing. **49**, 33-39.

Slatter, N.P. and Alborough, H. (1992) Chemical oxygen demand using microwave digestion: a tentative new method. *Water* S.A. **18**, 145-147.

Sousa-Aquiar, E.F., Appel, L.G. and Motu, C. (2005) Natural gas chemical transformations: the path of refining in the future. *Catalysis Today.* **101**, 3-7.

Stephens, C. (2002) Microbiology: Breaking down biofilms. *Current Biology*. **12**, 132-134.

Stams, A.J.M., Oude Elferink, S.J.W.H. (1997) Understanding and advancing wastewater treatment. *Current Opinion in Biotechnology*. **8**, 328-334.

Stilinovic, B. and Hrenovic, J. (2004) Rapid detection of sulphide-producing bacteria from sulphate and thiosulfate. *Folia Microbiology*. **49**, 513-518.

Sutherland, I.W. Exopolysaccharides in biofilms, flocs and related structures. *Water Science and Technology*. **43**, 77-86.

Teske, A., Wawer, C., Muyzer, G., Ramsing, N.B. (1996) Distribution of sulfate-reducing bacteria in a Stratified Fjord (Mariager Fjord, Denmark) as evaluated by most probable number counts and denaturing gradient gel electrophoresis of PCR-amplified ribosomal DNA fragments. *Applied and Environmental Microbiology* **62**, 1405-1415.

Thomas, S. and Dawe, R.A. (2003) Review of ways to transport natural gas energy from Countries which do not need the gas for domestic use. *Energy*. **28**, 1461-1477.

Tiedt, L.R. and Pretorius, W.E. (2006) An introduction to electron microscopy and x-ray analysis. Laboratory for electron microscopy. North West University, Potchefstroom, South Africa.

Tijmensen, M.J.A., Faaij, A.P.C., Hamelinck, C.N. and Van Hardeveld, M.R.M. (2002) Exploration of the possibilities for production of Fischer-Tropsch liquids and power via biomass gasification. *Biomass and Bioenergy*. **23**, 129-152.

Toffin, L., Webster, G., Weightman, A.J., Fry, J.C. and Prieur, D. (2004) Molecular monitoring of culturable bacteria from deep-sea sediment of the Nankai Trough, Leg 190 Ocean Drilling Program. *FEMS Microbiology Ecology*. [Web:] http://www.sciencedirect.com

[date of access 29 August 2006]

Van der Kooij, D., Vrouwenvelder, H.S. and Veenendal, H.R. (2003) Elucidation and control of biofilm formation processes in water treatment and distribution using the unified biofilm approach. *In* Water Science and Technology. Biofilm monitoring. IWA publishing. **47**, 83-90.

Van der Merwe, T., Riedel, K-H. and Wolfaardt, F. (2002) Analysis of the structural diversity of the microbial community in a paper-mill water system. *Water S.A.* **28**, 407-411.

Van Dyk, J.C., Keyser, M.J. and Coertzen, M. (2006) Syngas production from South African coal sources using Sasol-Lurgi gasifiers. *International Journal of Coal Geology*. **65**, 243-253.

Vickery, K., Pajkos, A. and Cossart, Y. (2004) Removal of biofilm from endoscopes: evaluation of detergent efficiency. *American Journal of Infection Control*. **32**, 170-176.

Videla, H.A. (1994) Biocorrosion of nonferrous metal surfaces. *In* Biofouling and biocorrosion in industrial water systems. Geesey, G.G., Lewandowski, Z., Flemming, H.C. Lewis publishers. USA. 297 p.

Videla, H.A. (2002) Prevention and control of biocorrosion. *International Biodererioration and Biodegradation*. **49**, 259-270.

Viessman, W. and Hammer, M.J. (1998) Water supply and pollution control. 6th ed. Addison Wesley Longman. California. 827p.

Von Mũnch, E. and Pollard, P.C. (1997) Measuring bacterial biomass-COD in wastewater containing particulate matter. *Water Research*. **31**, 2550-2556.

Vrouwenvelder, J.S., Kappelhof, J.W.N.M, Heijman, S.G.J., Schippers, J.C. and Van der Kooij, D. (2003) Tools for fouling diagnosis of NF and RO membranes

and assessment of the fouling potential of feed water. *Desalination.* **157**, 361-365.

Ward, D.M, Ferris, M.J., Nold, D.C., Bateson, M.M. (1990) A natural view of microbial biodiversity within hot spring cyanobacterial mat communities. *Molecular Biology Review* **62**, 1353 – 1370.

Webb, R.L. and Wei, L. (2000) Fouling in enhanced tubes using cooling tower water Part 1: long-term fouling data. *International Journal of Heat and Mass Transfer.* **43**, 3567-3578.

White, D.C., Arrage, A.A., Nivens, D.E., Palmer, R.J., Rice, J.F. and Sayler, G.S. (1996a) Biofilm ecology: on-line methods bring new insights into MIC and microbial biofouling. *Biofouling.* **10**, 3-16.

White, D.C., Stair, J.O. and Ringelberg, D.B. (1996b) Quantitative comparisons of *in situ* microbial biodiversity by signature biomarker analysis. *Journal of Industrial Microbiology.* **17**, 185-196.

White, D.C., Kirkegaard, R.D., Palmer, R.J., Flemming, C.A., Chen, G., Leung, K.T., Phiefer, C.B. and Arrage, A.A. (1999) The biofilm ecology of microbial biofouling, biocide resistance and corrosion. *In* Biofilms in the Aquatic Environment. The Royal Society of chemistry. UK. 130 p.

White D.C. and Ringelberg, D.B. (1998) Signature Lipid Biomarker Analysis. In: Burlage, R.S., Atlas, R., Stahl, D., Greesey, G., Sayler, G. (Eds.), *Techniques in microbial ecology*, Oxford University Press, New York. p. 255 - 272.

Wilkinson, S.G. (1988) Gram-negative bacteria. *In* Microbial Lipids. Ratledge, C. and Wilkinson, S.G. Academic Press Ltd. London. p. 299-488.

Wobus, A., Kloep, F., Röske, K. and Röske, K. (2003) Influence of population structure on the performance of biofilm reactors. *In* Biofilms in Wastewater Treatment. Wuertz, S., Bishop, P.L. and Wilderer, P.A. IWA publishing. New York. 359 p.

Wuertz, S., Bishop, P.L. and Wilderer, P.A. (2003) Biofilms in wastewater treatment: an interdisciplinary approach. IWA publishing. New York. 359 p.

Yang, J., Peng, J., Shen, Z., Jia, Z. and Zhang, F. (2006) Corrosion protection of iron in water by activated carbon fiber (ACF). *Carbon*. **44**, 19-26.

You, S., Tseng, D., Guo, G. and Yang, J. (1999) The potential for recovery and reuse of cooling water in Taiwan. *Resources, Conservation and Recycling*. **26**, 53-70.

APPENDIX

A1: Calculation of the total suspended solids and total dissolved solids.

$$TSS(mg/L) = \frac{(m_1 - m_2) \times 10^6}{V_1}$$

Calculate the total dissolved solids as follows:

$$TDS(mg/L) = \frac{(m_3 - m_4) \times 10^6}{V_2}$$

Where:
- m_1 = Mass of GF/A filter paper with residue (g)
- m_2 = Mass of GF/A filter paper before use (g)
- m_3 = Mass of evaporating dish with residue (g)
- m_4 = Mass of empty evaporating dish (g)
- V_1 = Volume of sample used for filtration (ml)
- V_2 = Volume of sample evaporated (ml)

Table A1: EDS elemental analysis of the crystals on the microscope slides from experiment 2 and 3.

Elements present	Weight %	
	Exp 2	Exp 3
C	13.99	16.98
Na	0.44	-
Mg	0.38	-
Si	0.43	0.35
S	11.18	-
Ca	13.35	29.68
O	60.22	52.98
Total:	**100**	**100**

Table A2: DNA concentrations obtained form the respective samples.

Sample	DNA Concentration (ng/µl)	DNA Purity (260nm/280nm)
Experiment 1 Planktonic	476.93	1.64
Experiment 1 Sessile	585.51	1.39
Experiment 2 Planktonic	166.73	1.33
Experiment 2 Sessile	746.37	1.46
Experiment 3 Planktonic	739.46	1.65
Experiment 3 Sessile	828.45	1.49
Experiment 4 Planktonic	204.38	1.33
Experiment 4 Sessile	1031.21	1.38
Experiment 5 Planktonic	42.44	1.46
Experiment 5 Sessile	148.80	1.51

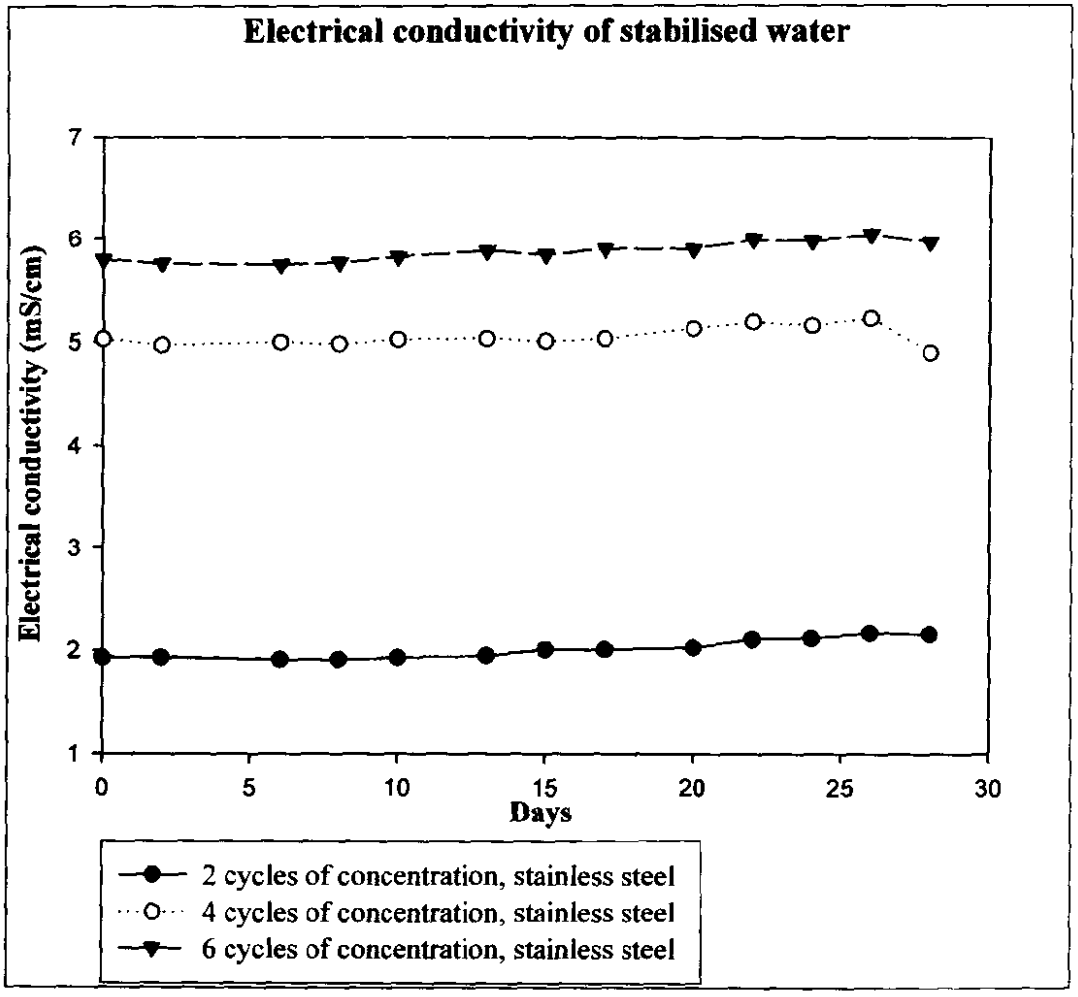

Figure A1: Electrical conductivity of the stabilised water, stainless steel coupons.

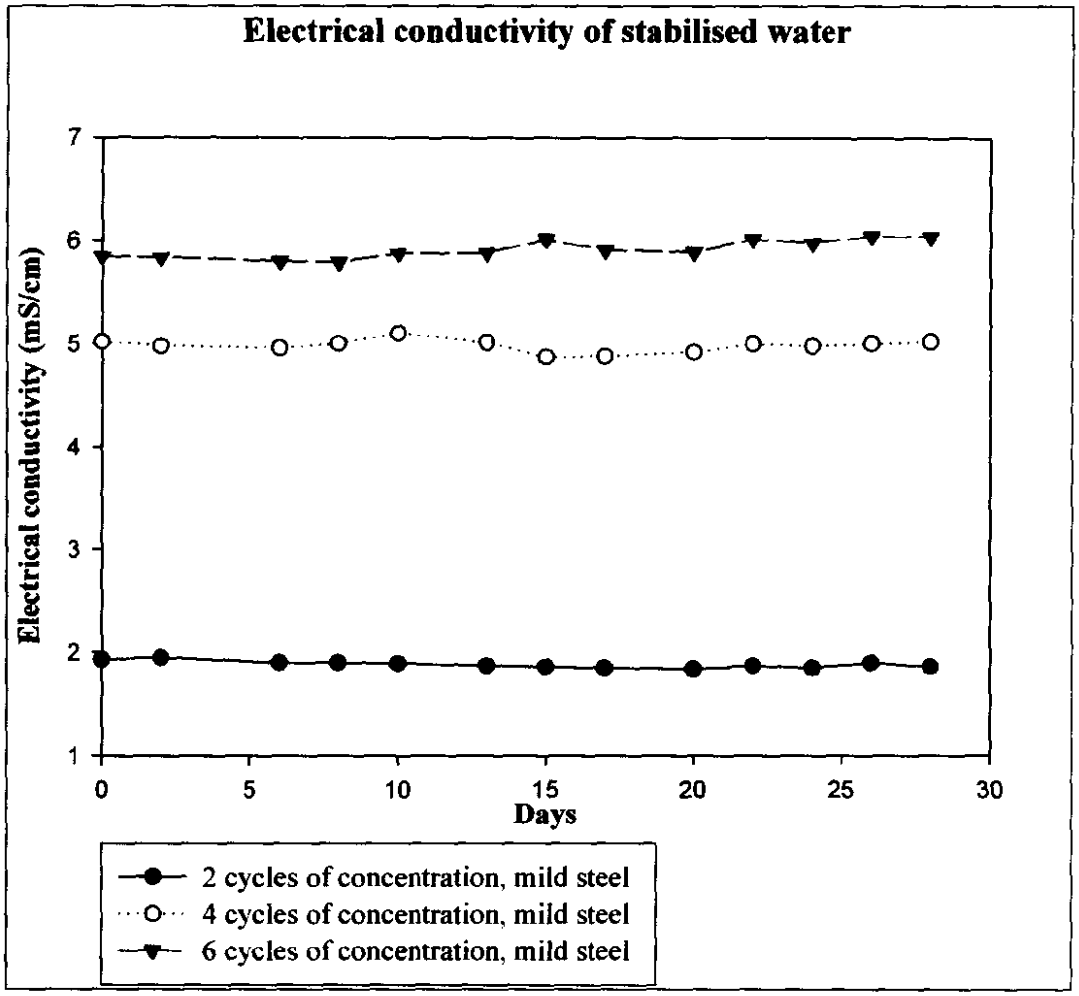

Figure A2: Electrical conductivity of the stabilised water, mild steel coupons.

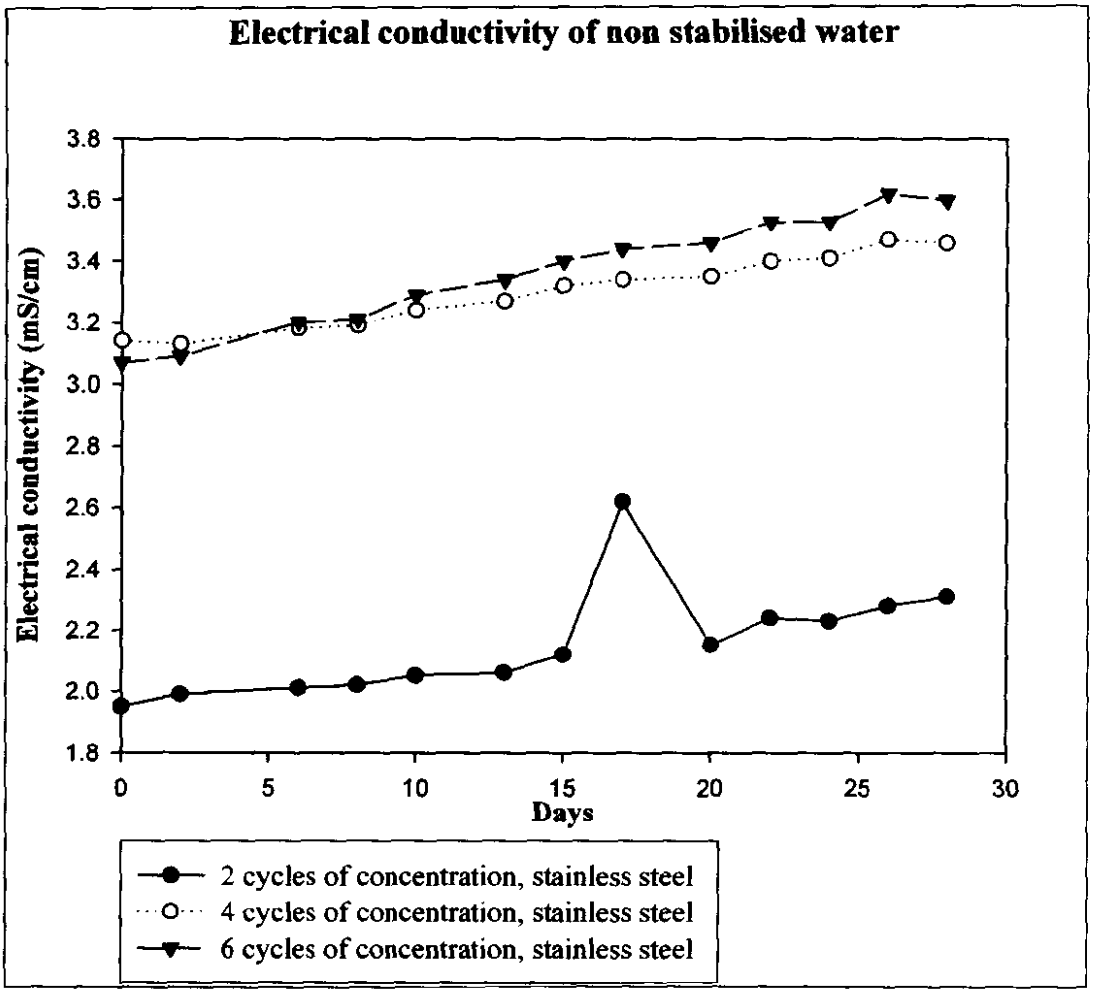

Figure A3: Electrical conductivity of the non-stabilised water, stainless steel coupons.

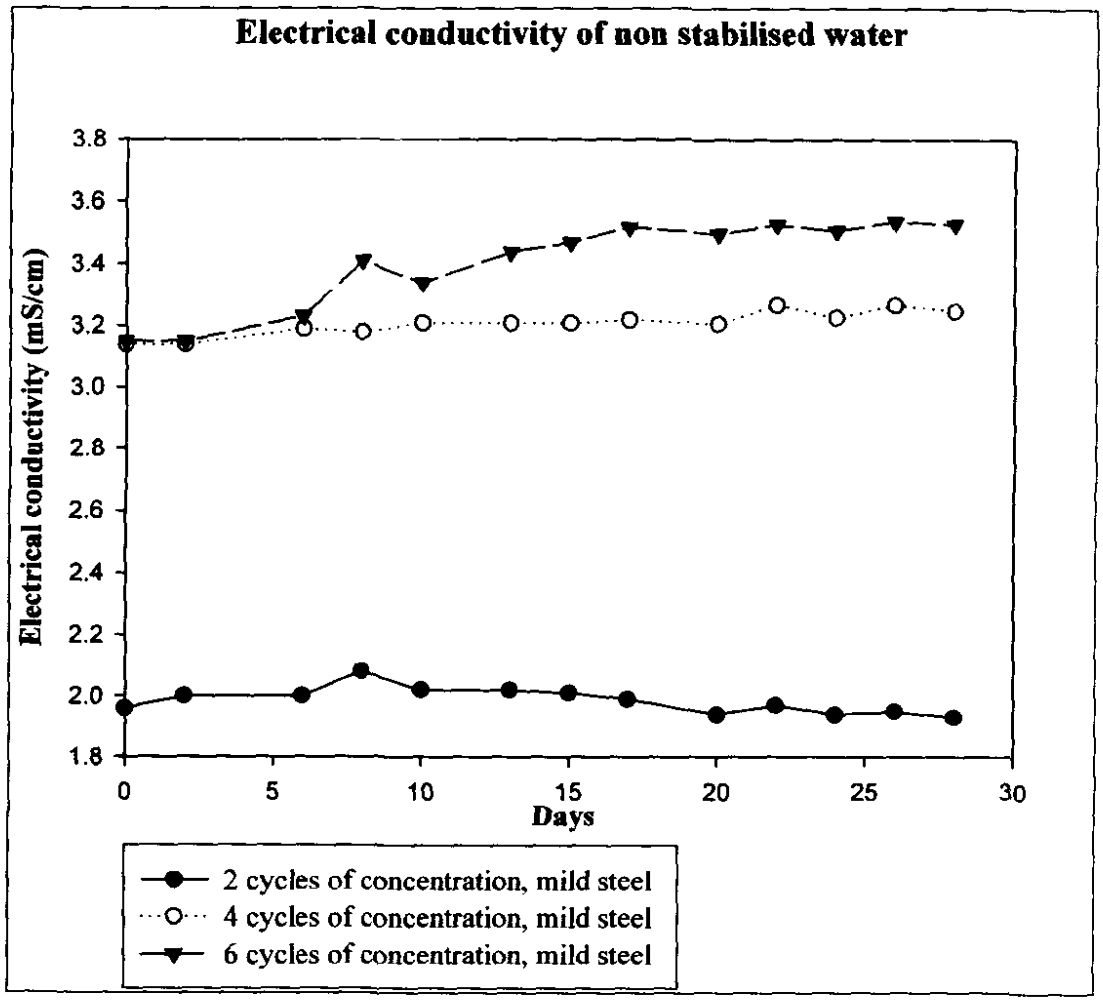

Figure A4: Electrical conductivity of the non-stabilised water, mild steel coupons.

APPENDIX B

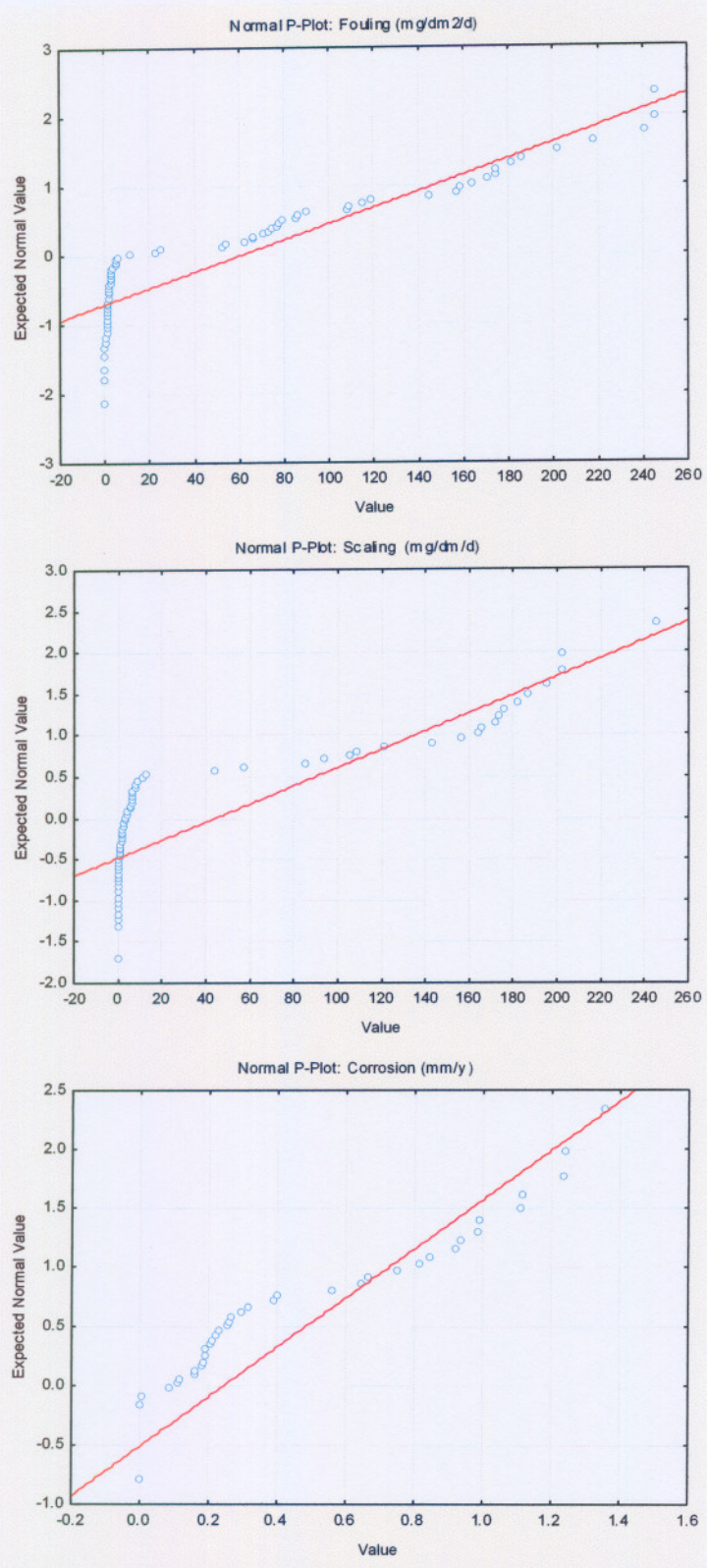

Figure B1: Normal probality plots on fouling, scaling and corrosion rates.

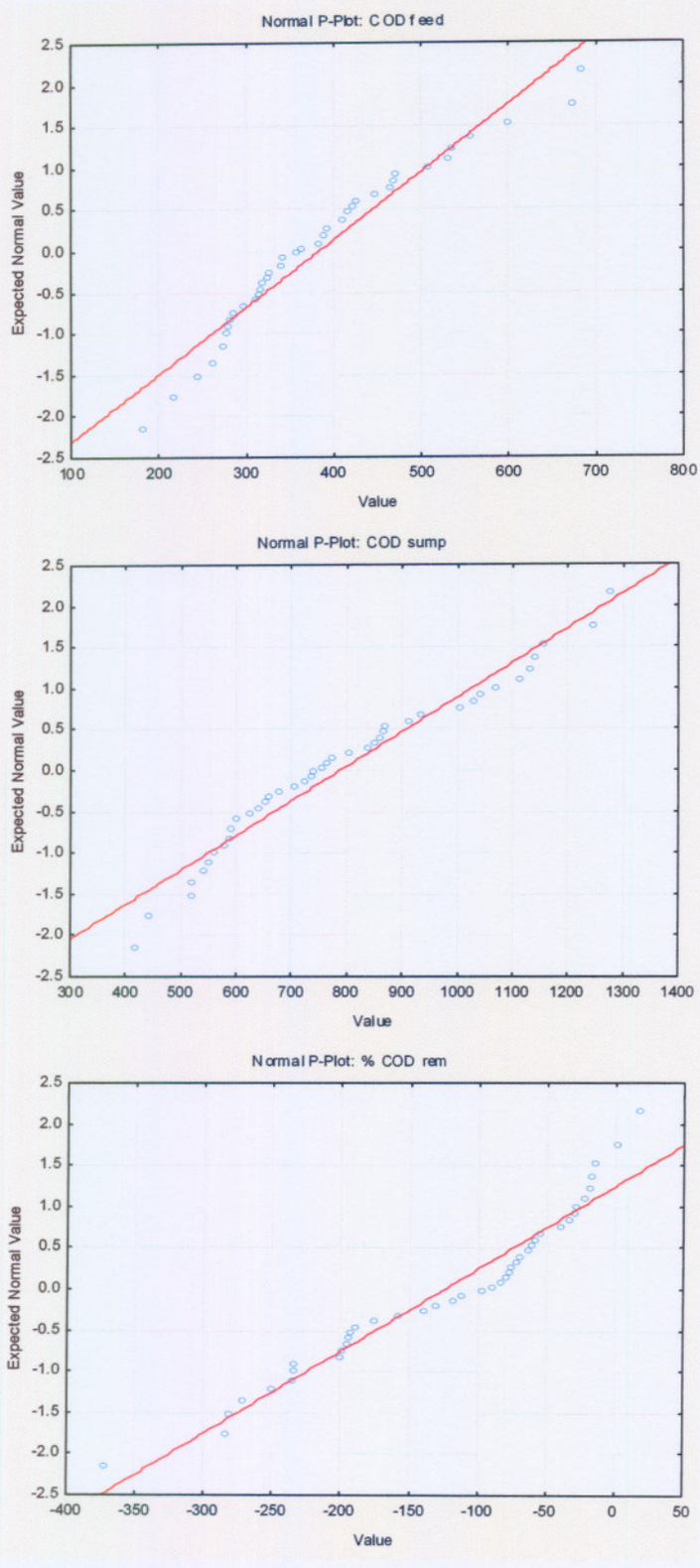

Figure B2: Normal probality plots on COD in the make-up, sump water as well as the percentage COD removal.

APPENDIX C

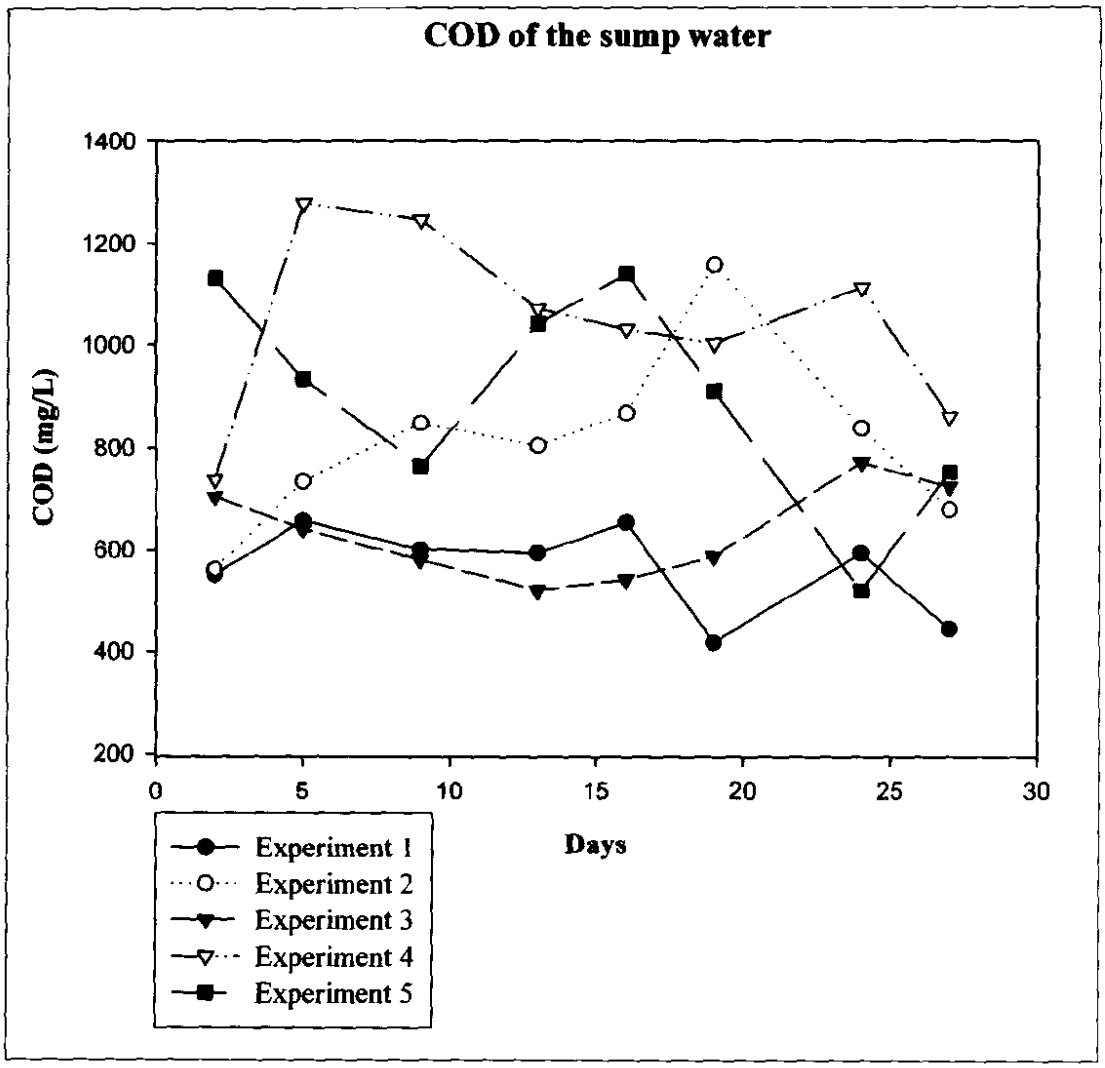

Figure C1: COD values of the sump water against time.

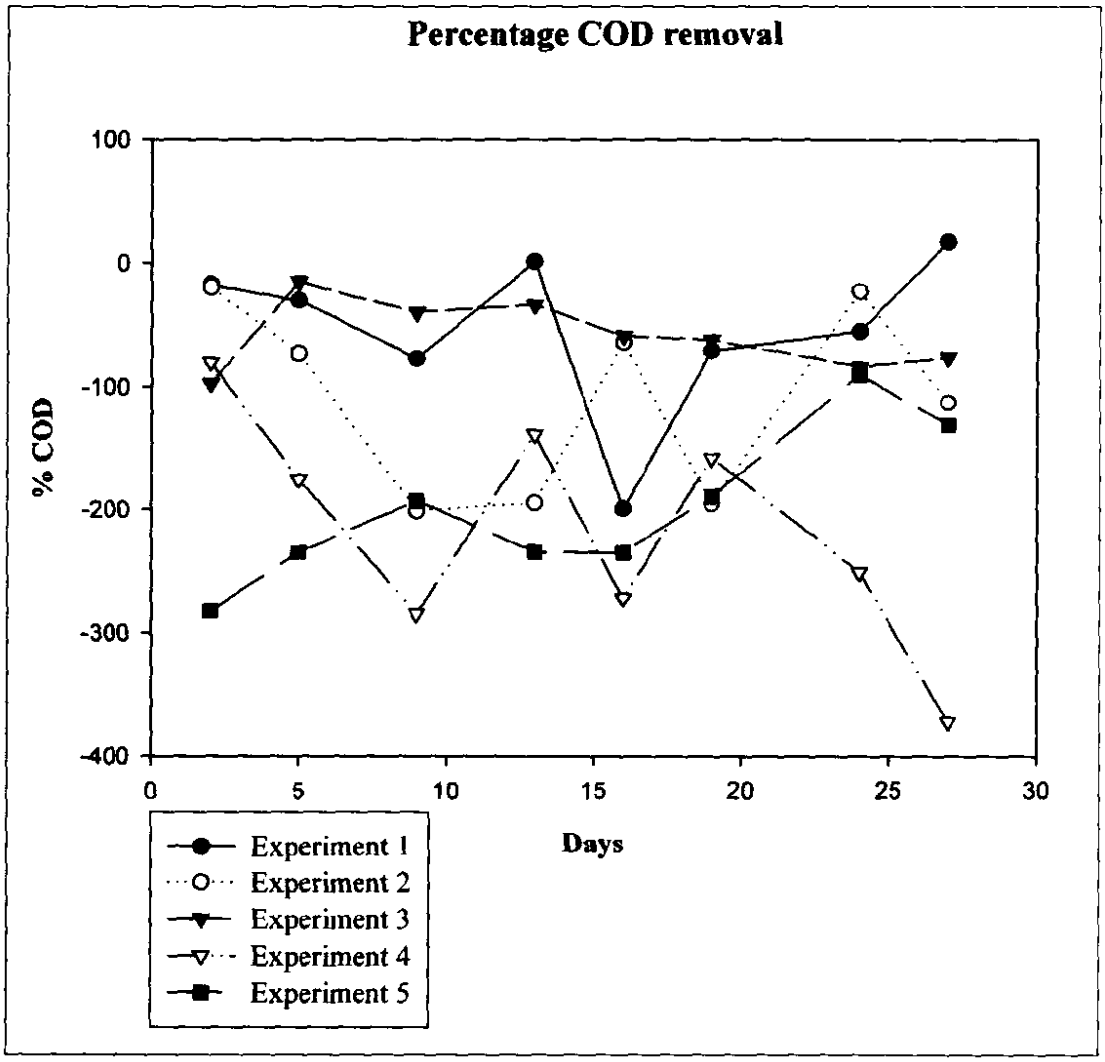

Figure C2: Percentage COD removal during all 5 experiments.

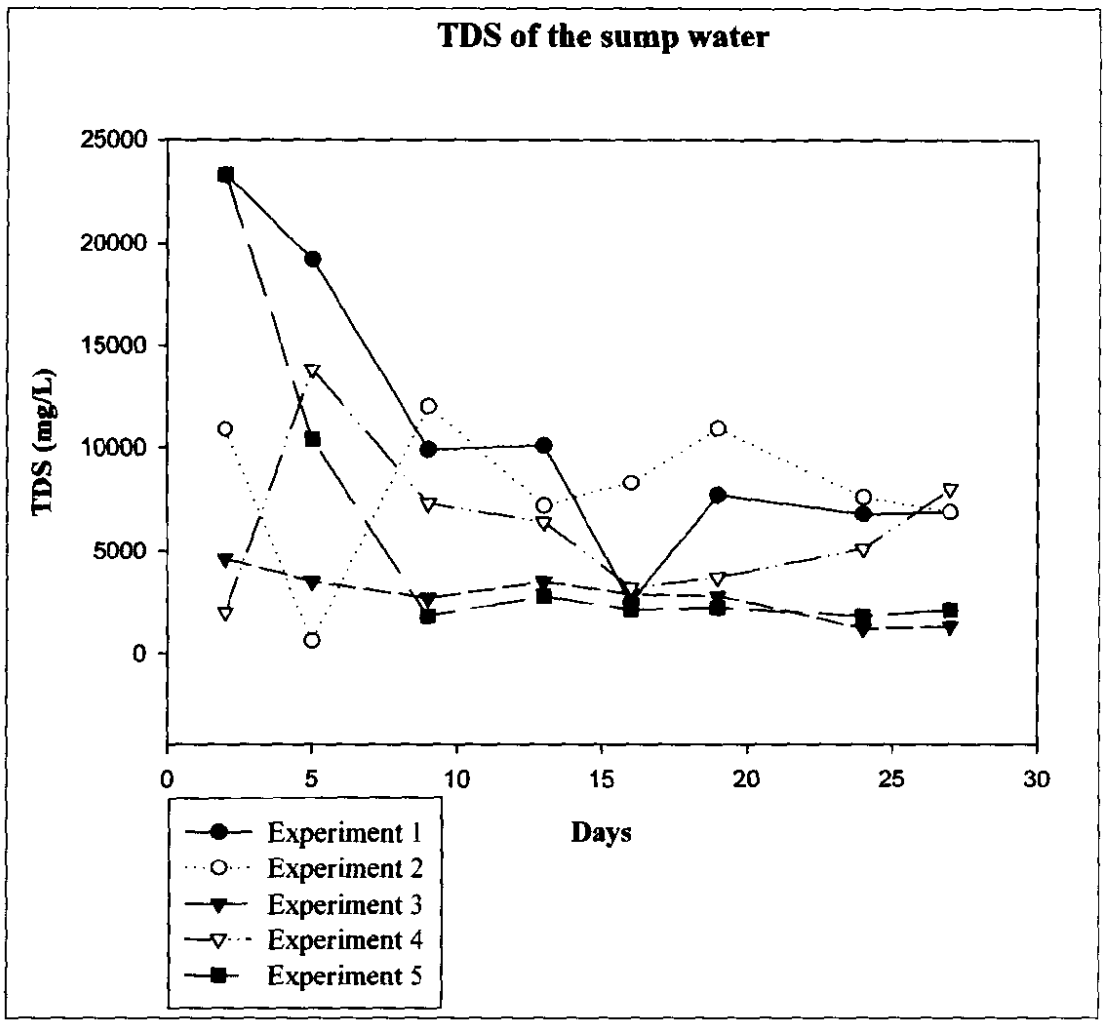

Figure C3: TDS of the sump against time.

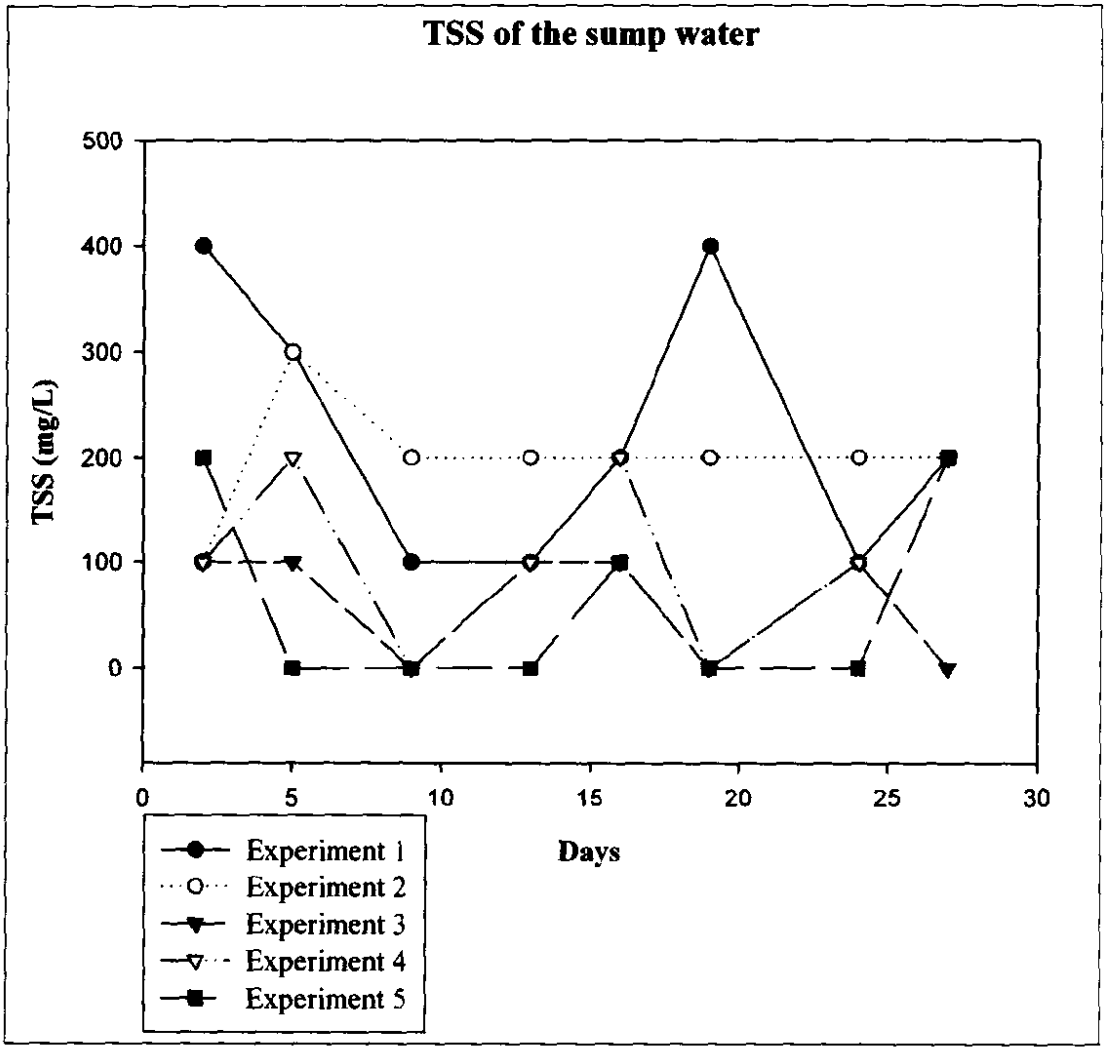

Figure C4: TSS of the sump against time.